

Geometric Deep Learning: Quo Vadimus?

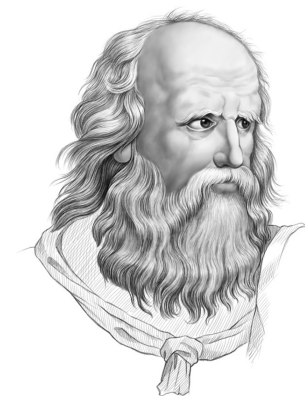
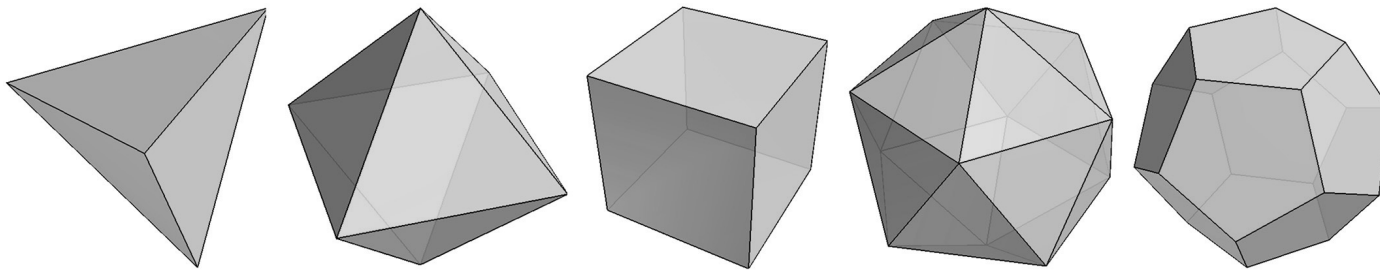
Michael Bronstein

University of Oxford & AITHYRA

“Symmetry, as wide or as narrow as you may define its meaning, is one idea by which man through the ages has tried to comprehend and create order, beauty, and perfection”



H. Weyl



Plato

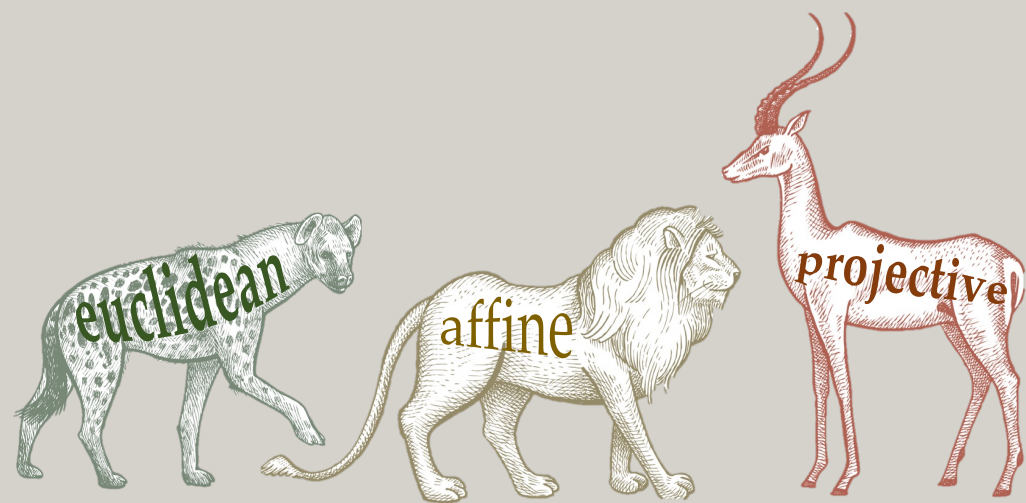
~370 BC

Portrait: Ihor Gorskyi

ΑΓΕΩΜΕΤΡΗΤΟΣ
ΜΗΔΕΙΣ ΕΙΣΙΤΩ

XIX century

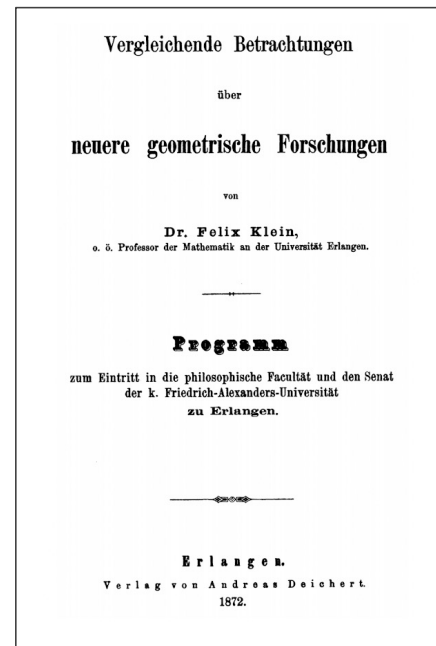




The Erlangen Programme



Geometry = space + transformation group



F. Klein

1872

Euclidean geometry



$E(3)$

A horizontal arrow pointing from the original cat to the three transformed cats.

Translation



Rotation



Reflection



H. Poincaré

1904



H. Minkowski

1907



E. Noether

1918



H. Weyl

1929

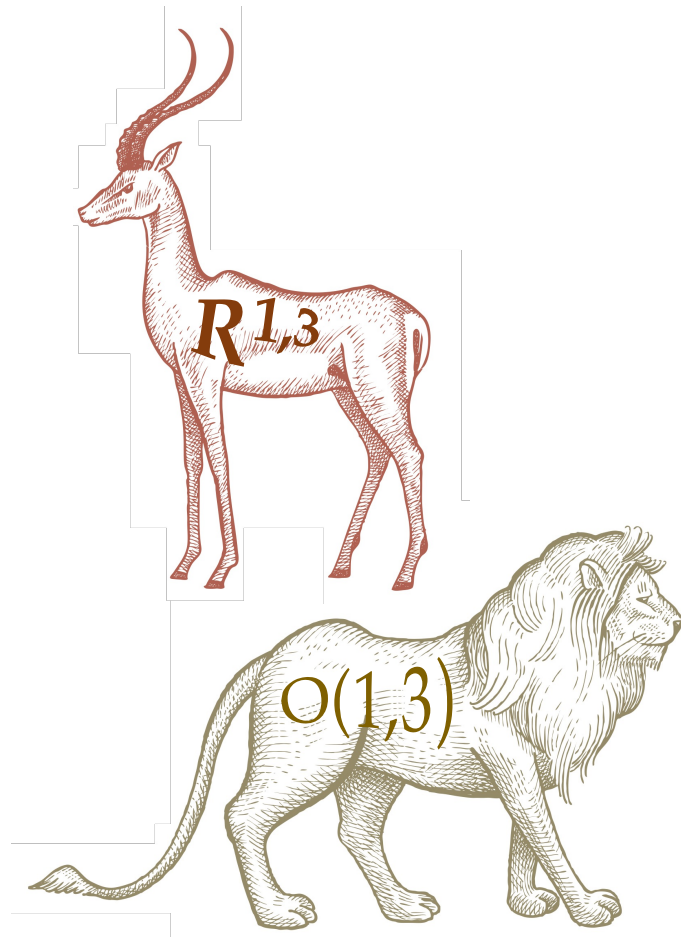


C. N. Yang

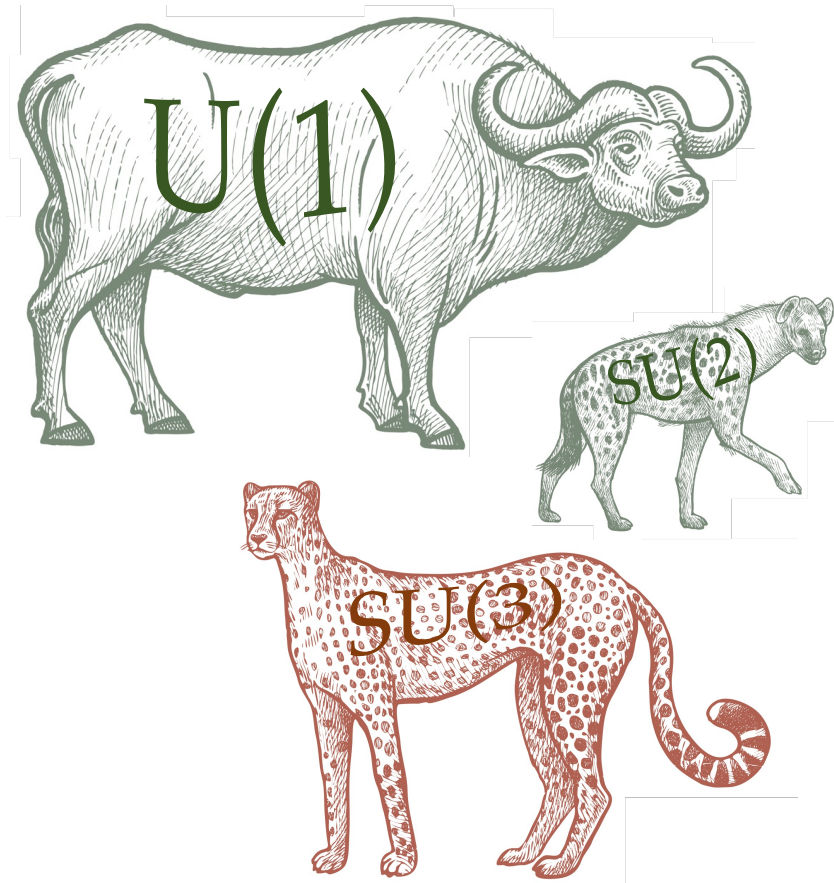
1954



R. L. Mills



External symmetry



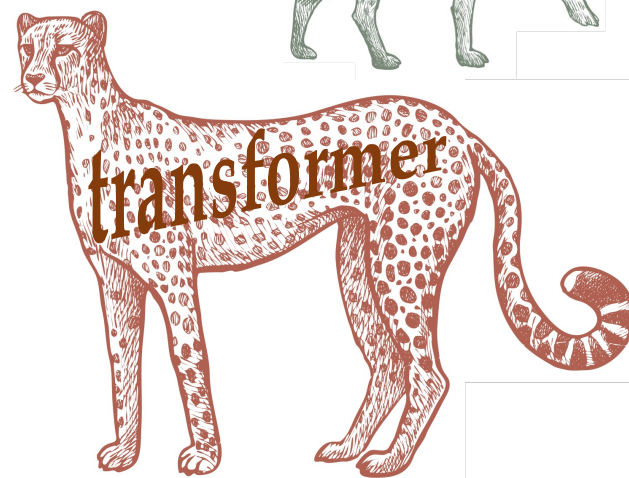
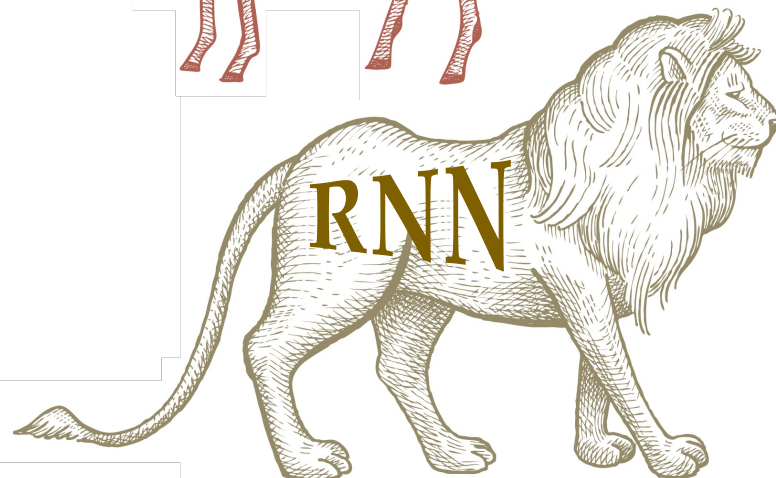
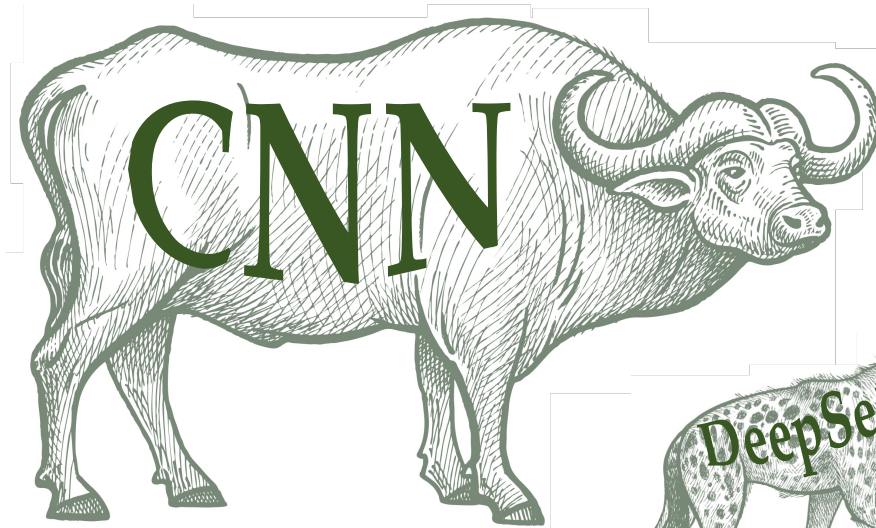
Internal symmetry

“It is only slightly overstating the case to say that Physics is the study of symmetry”

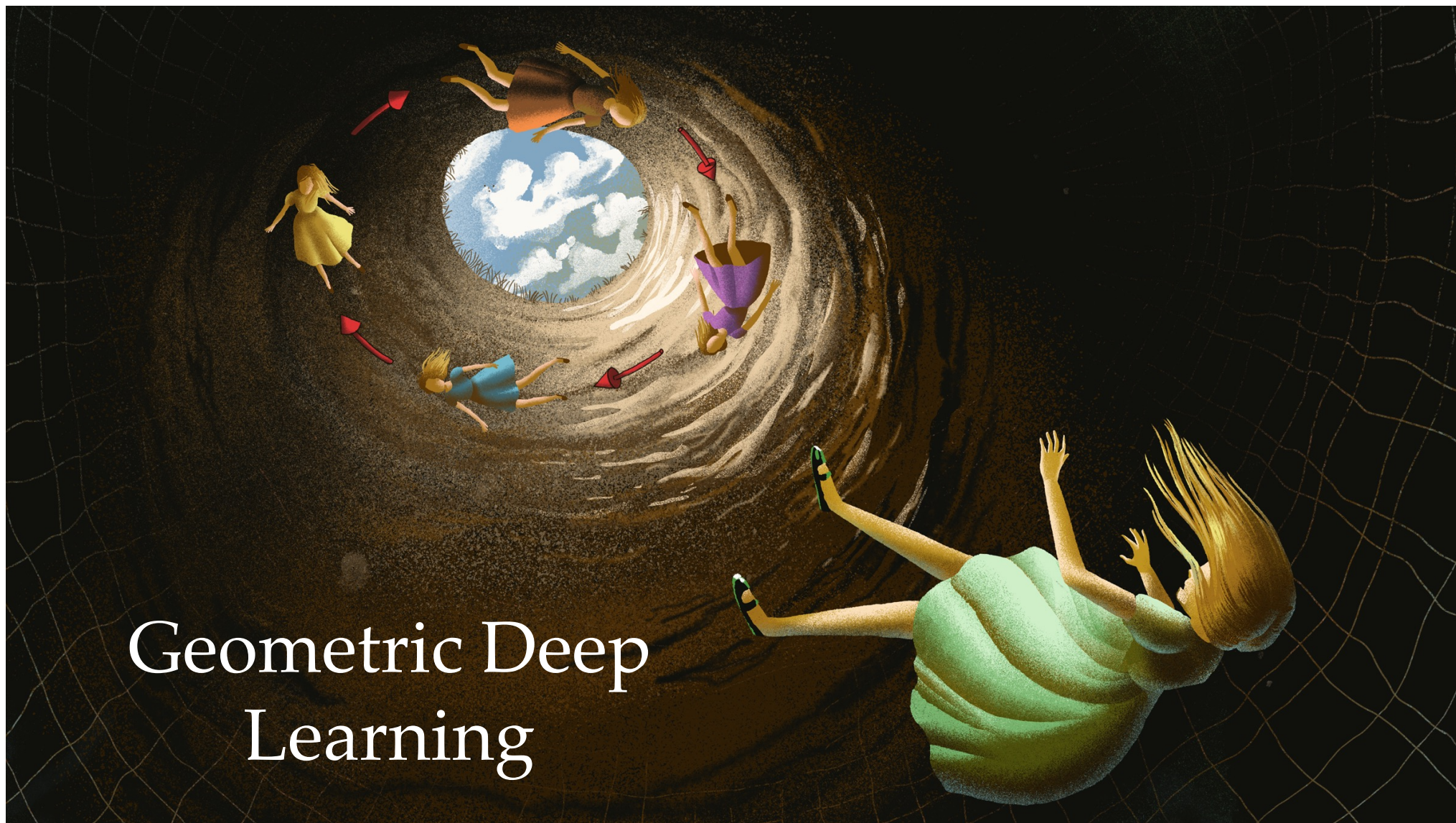
— *More is different*



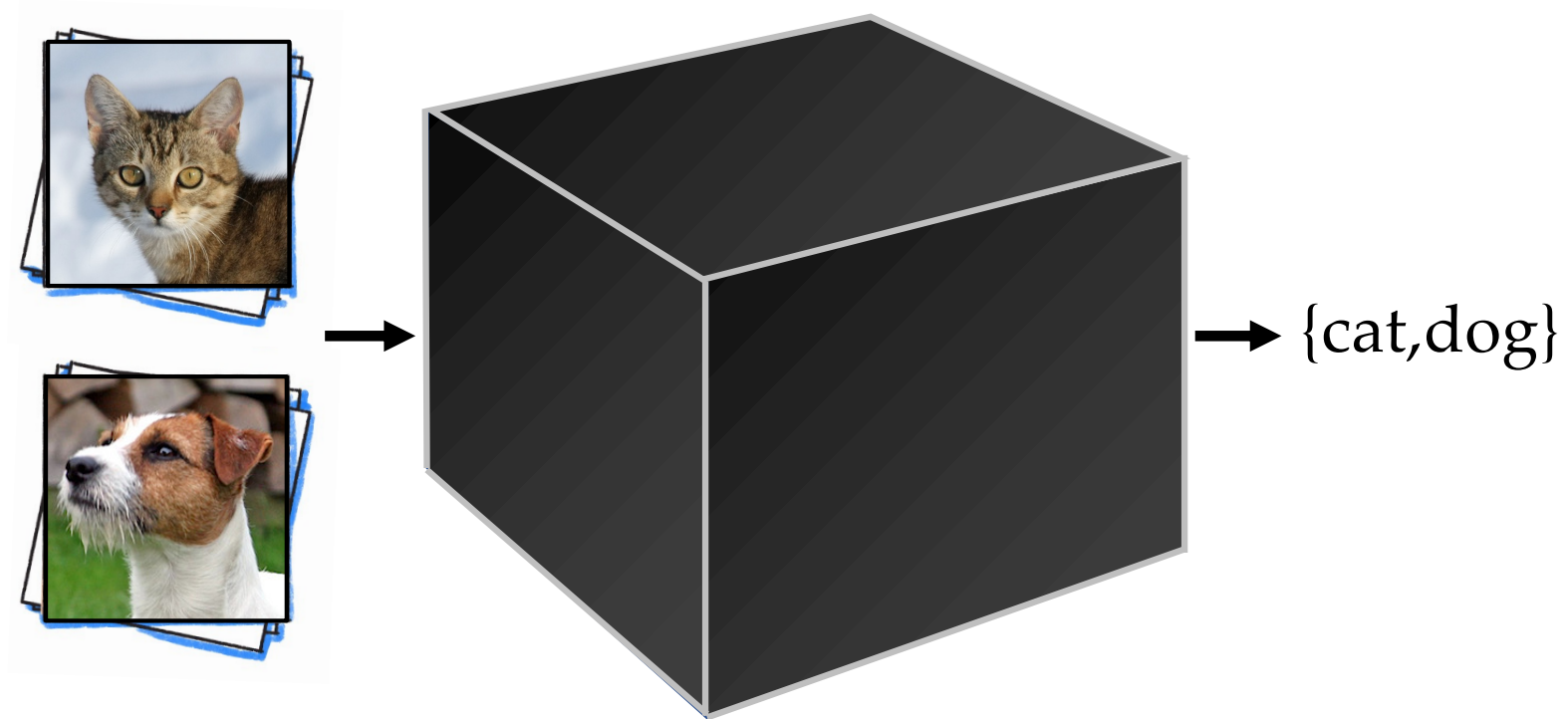
P. Anderson



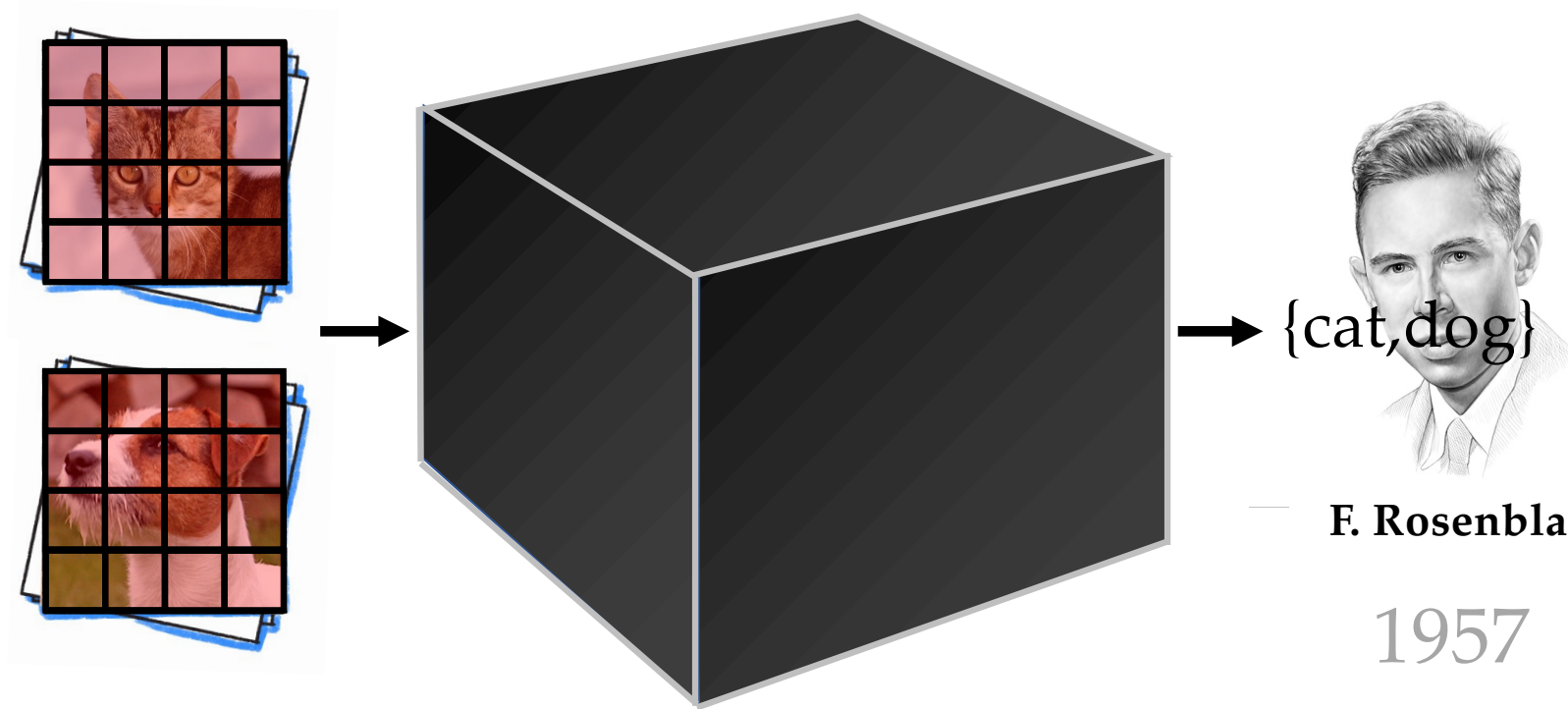
Geometric Deep Learning



Supervised ML = Function Approximation

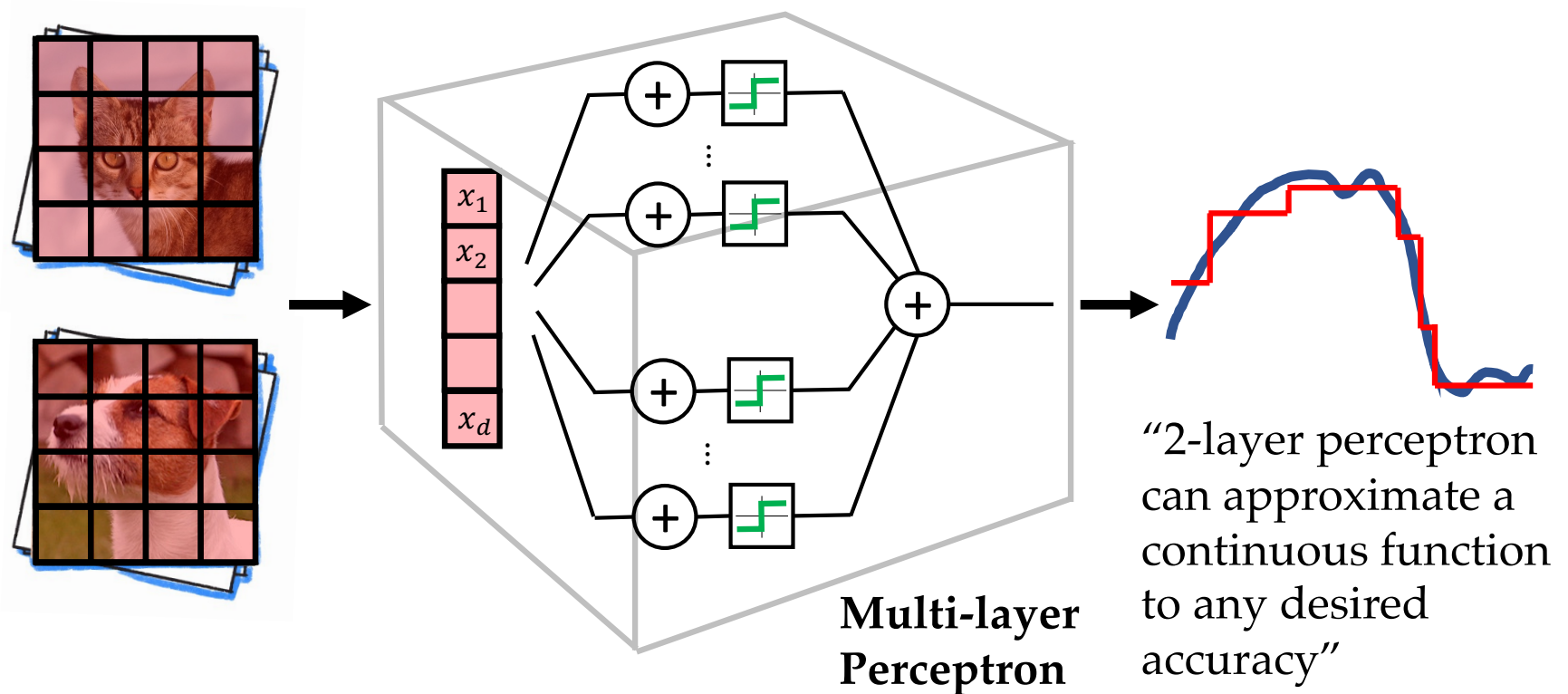


Supervised ML = Function Approximation

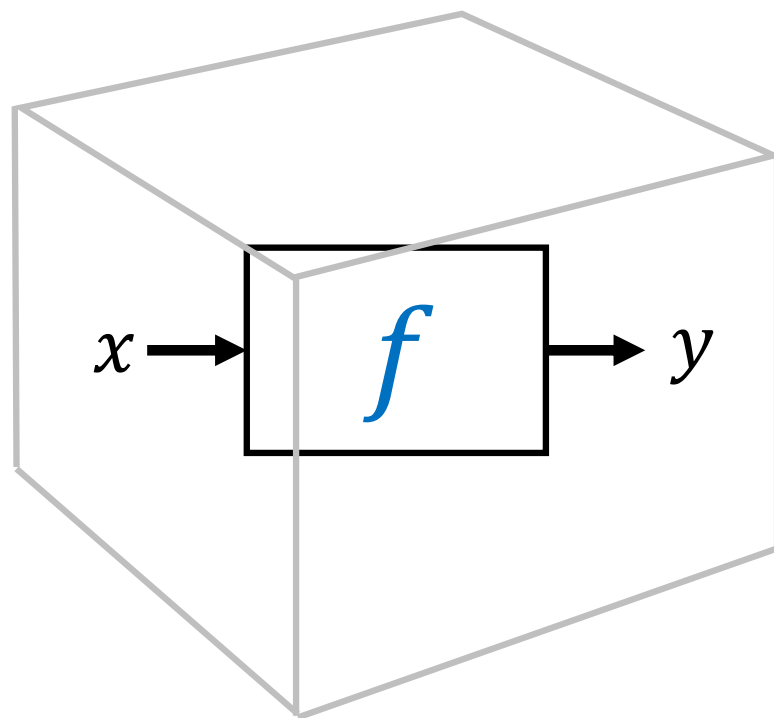


Rosenblatt 1957; Portrait: Ihor Gorskyi

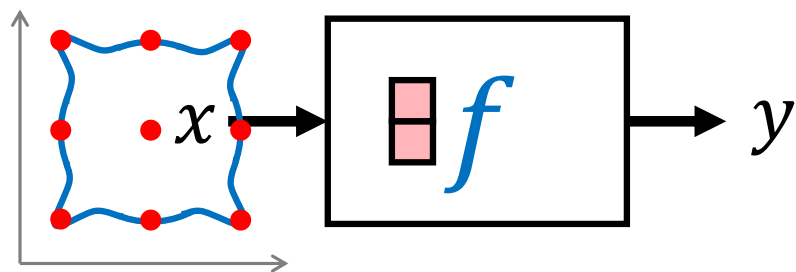
Universal Approximation



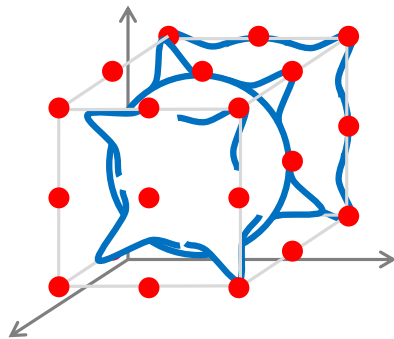
Universal Approximation: Hilbert's 13th problem 1900; Kolmogorov 1956; Arnold 1957; Cybenko 1989; Hornik 1991; Barron 1993; Leshno et al 1993; Maiorov 1999; Pinkus 1999



2-dimensional



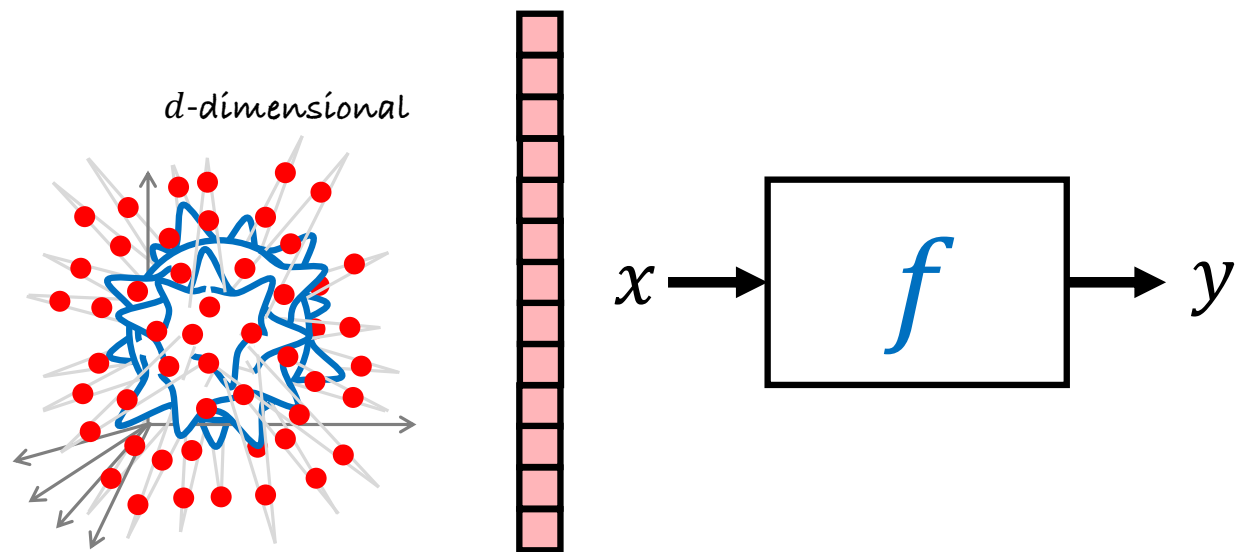
3-dimensional



x



y

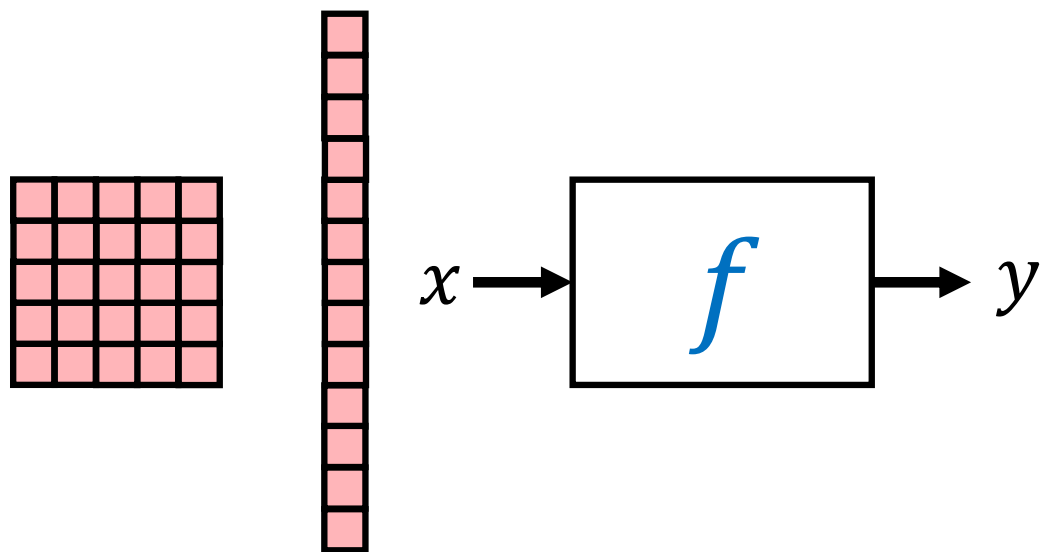


$O(\varepsilon^{-d})$ samples

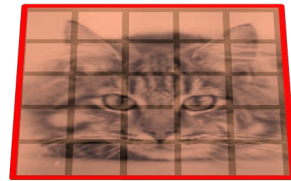
A still from the Harry Potter film series showing Lord Voldemort, played by Alan Rickman, in his dark, flowing robes. He is bald and has a pale, snake-like face. He is pointing his right hand forward, from which a powerful, bright green lightning bolt spell (the Avada Kedavra curse) is being cast. The spell travels horizontally across the frame towards the right. The background is a courtyard with stone walls and pillars, and some green magical sparks are visible in the air and on the ground.

Curse of dimensionality

Geometric priors

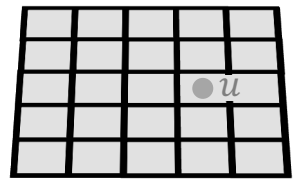


Geometric priors

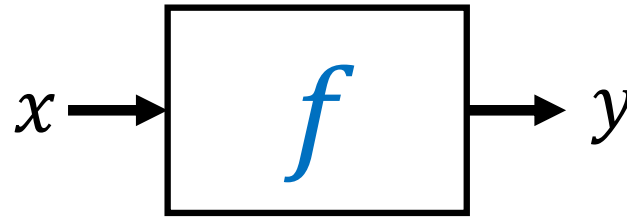


Geometric priors

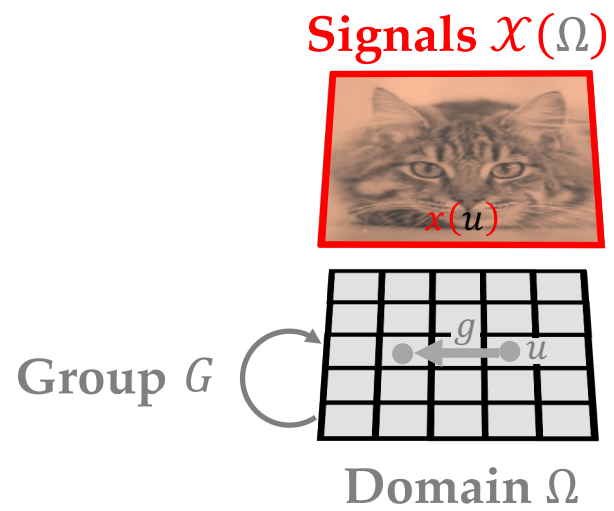
Signals $\mathcal{X}(\Omega)$



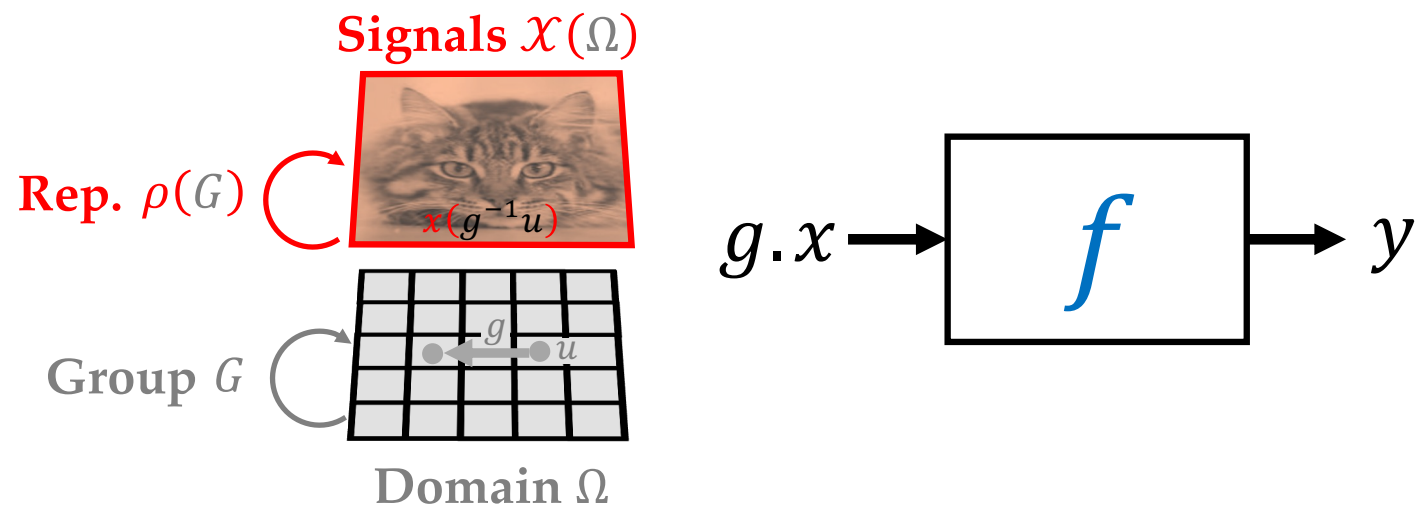
Domain Ω



Geometric priors

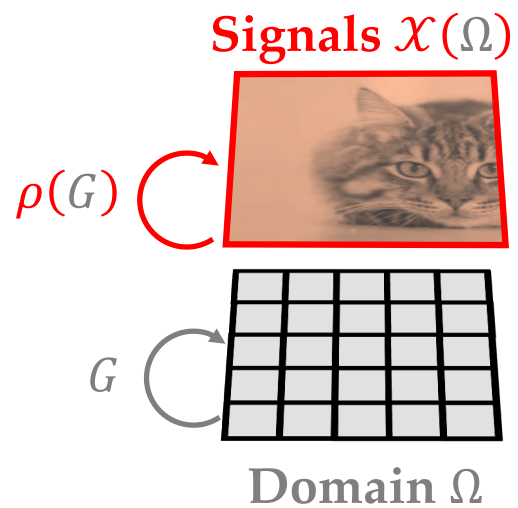


Geometric priors



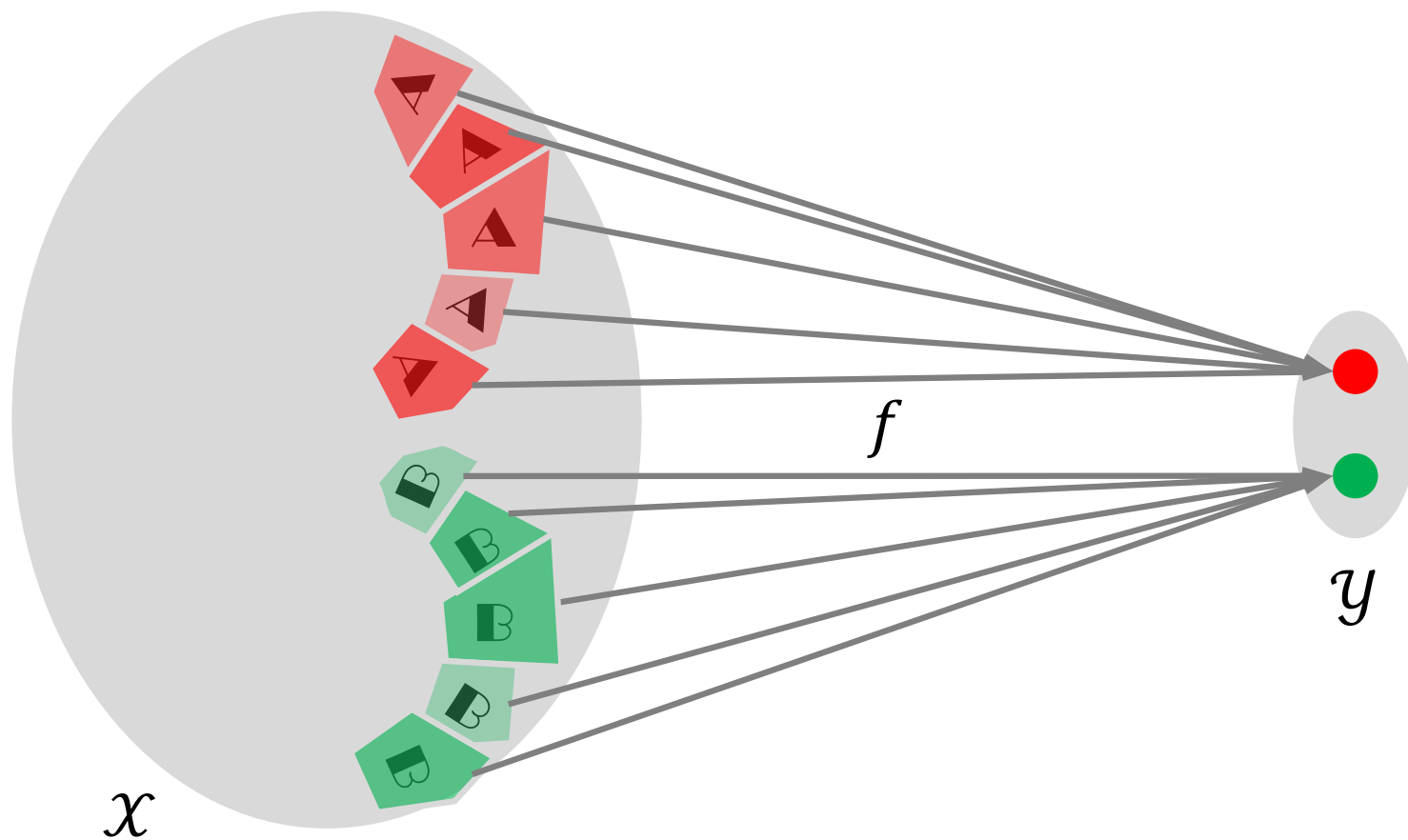
“How f interacts with the group G ?”

Geometric priors: Invariance

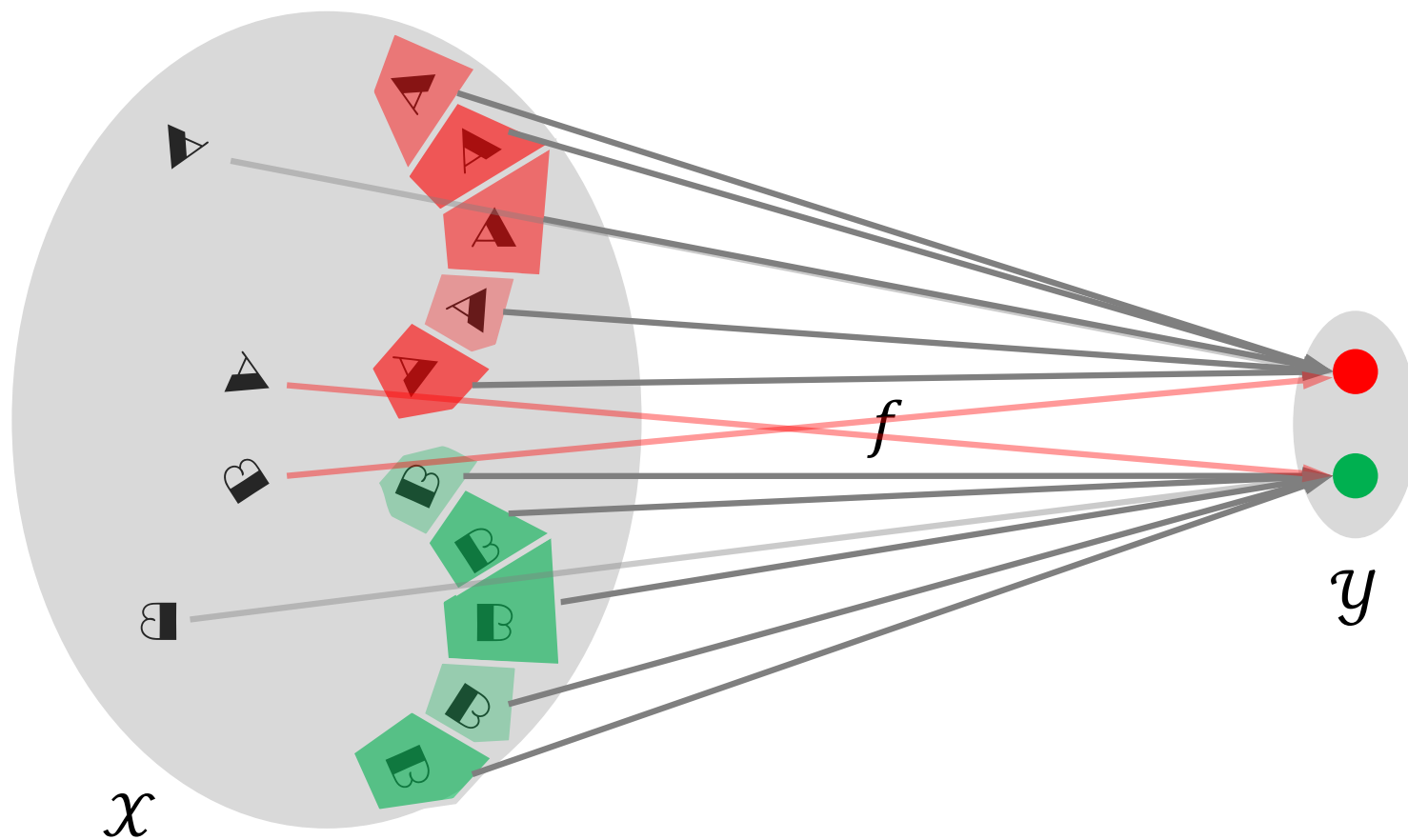


$$f(\rho(g)x) = f(x) \quad \forall g \in G$$

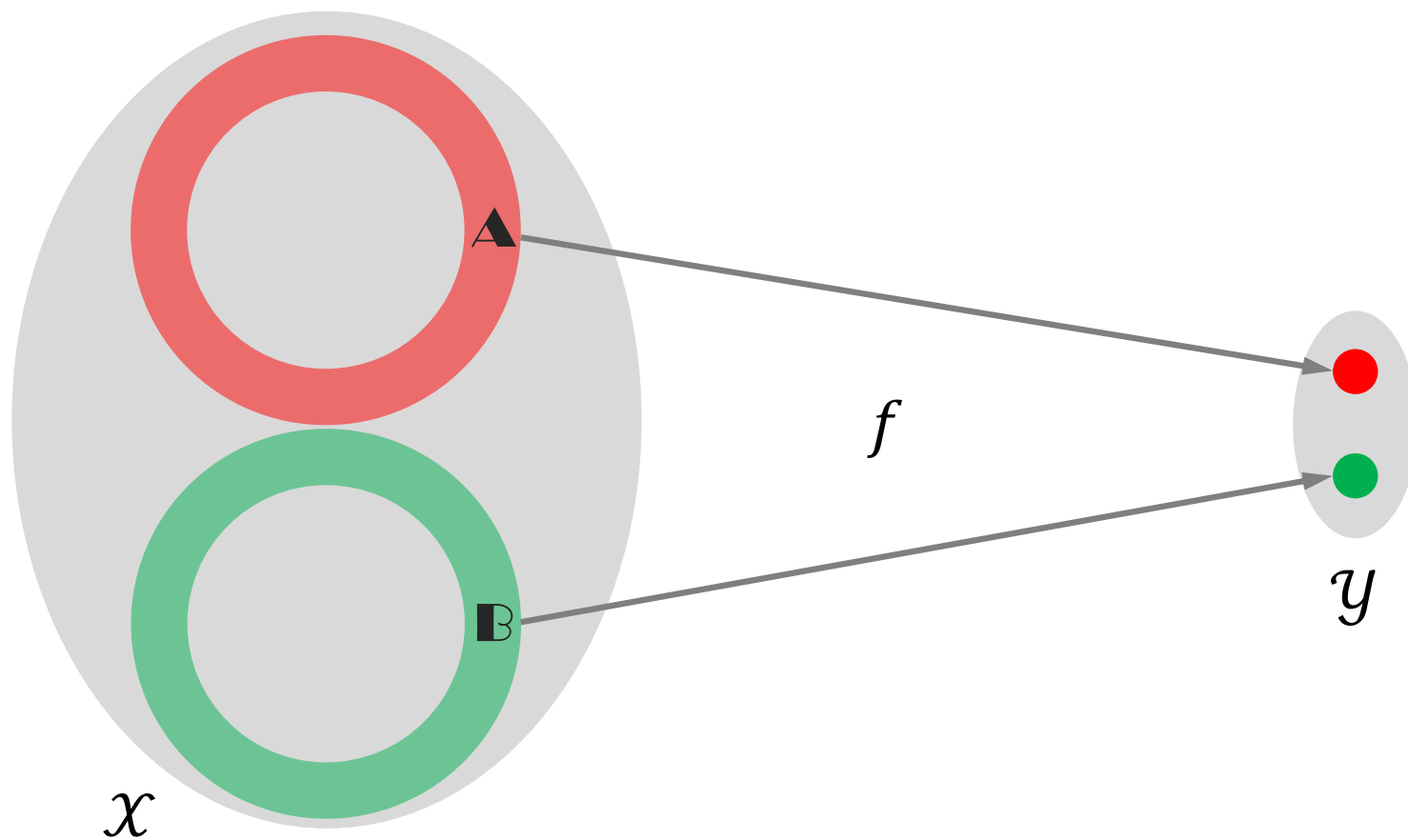
Symmetries of the Label Function



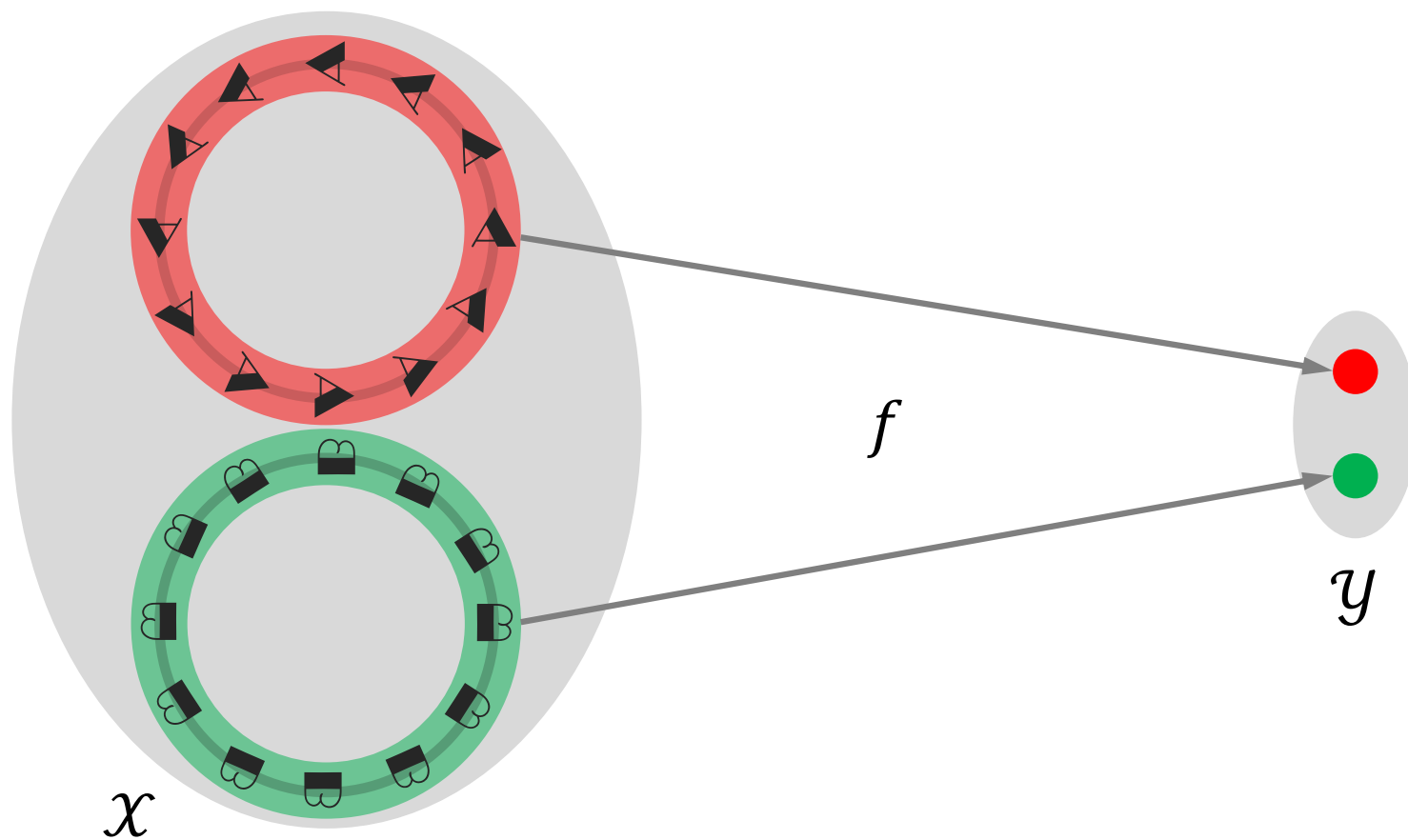
Symmetries of the Label Function



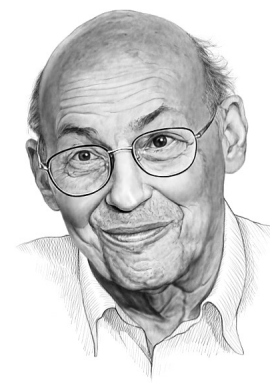
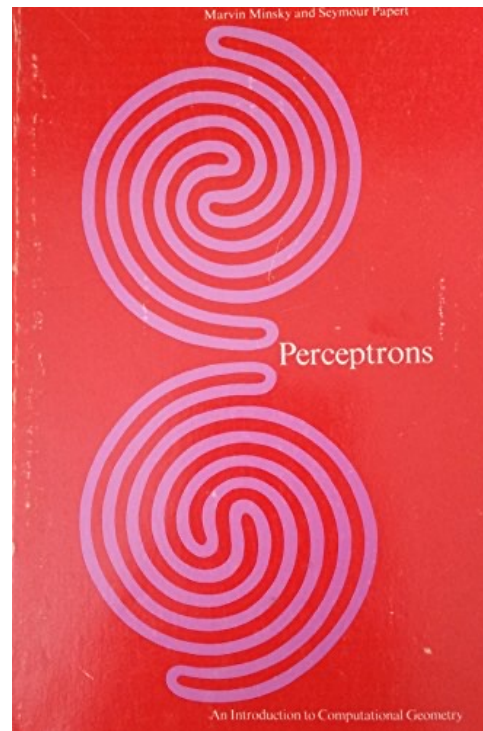
Symmetries of the Label Function



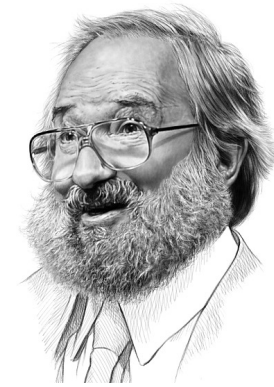
Symmetries of the Label Function



First “geometric” machine learning



M. Minsky

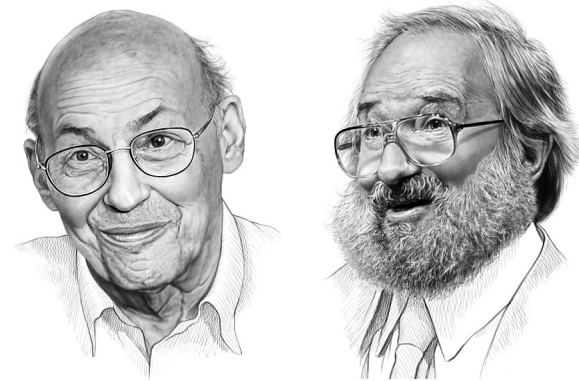


S. Papert

1969

First “geometric” machine learning

Group Invariance Theorem: “if a neural network is invariant to a group, then its output can be expressed as functions of the orbits of the group”

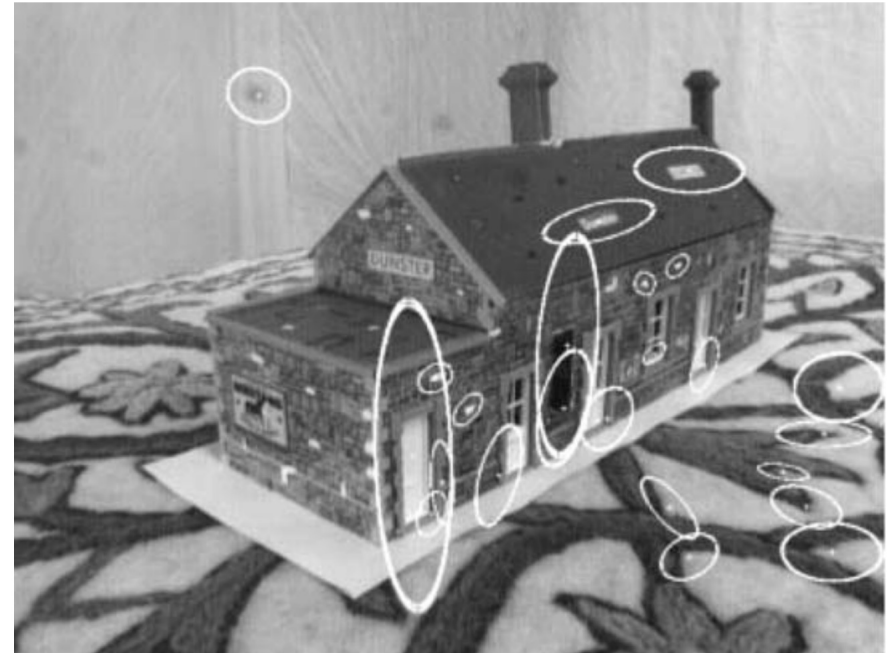
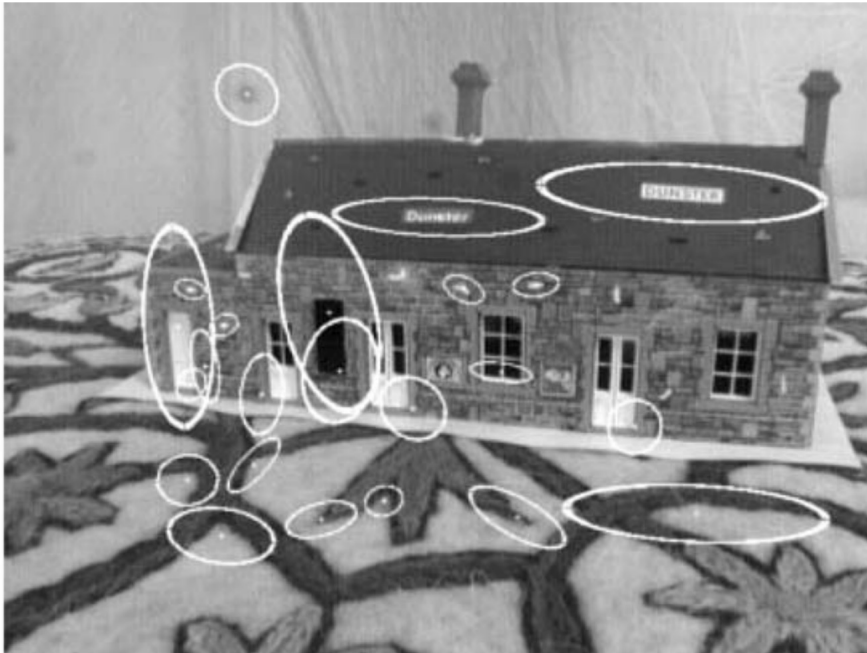


M. Minsky

S. Papert

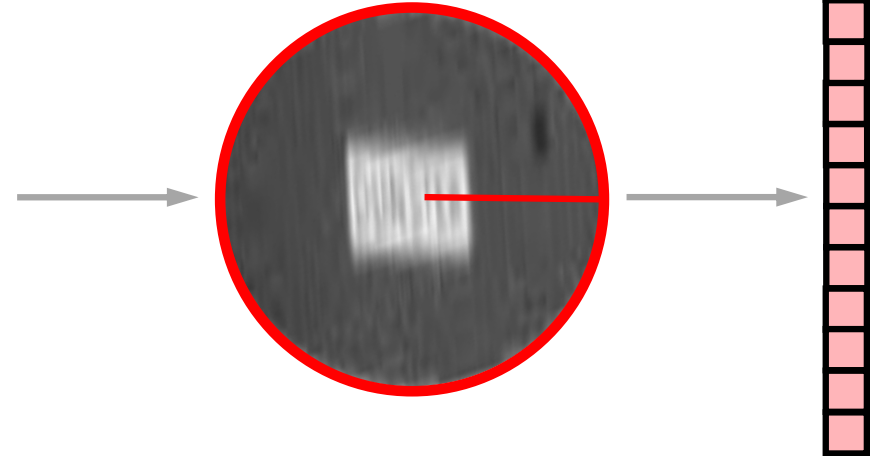
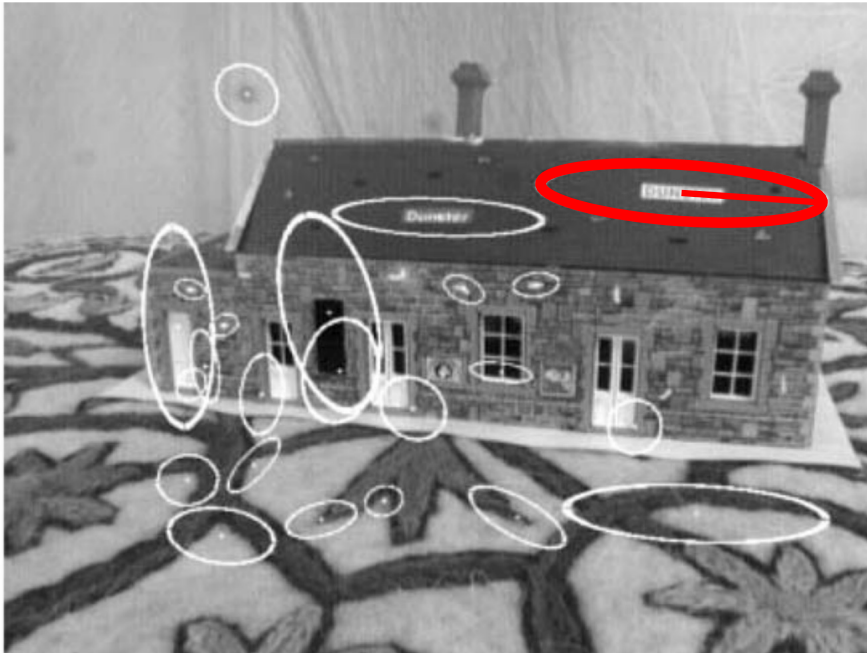
1969

Canonisation



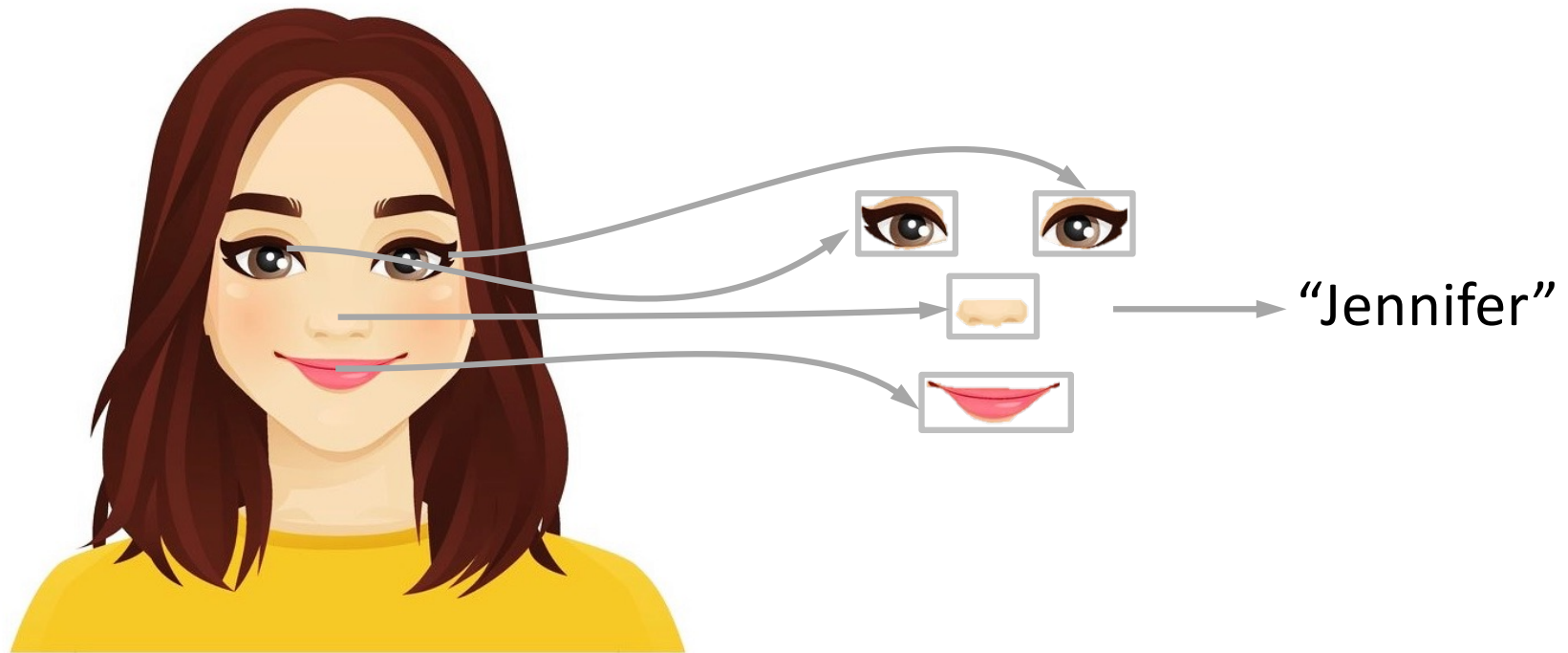
Mikolajczyk, Schmid 2004

Canonisation

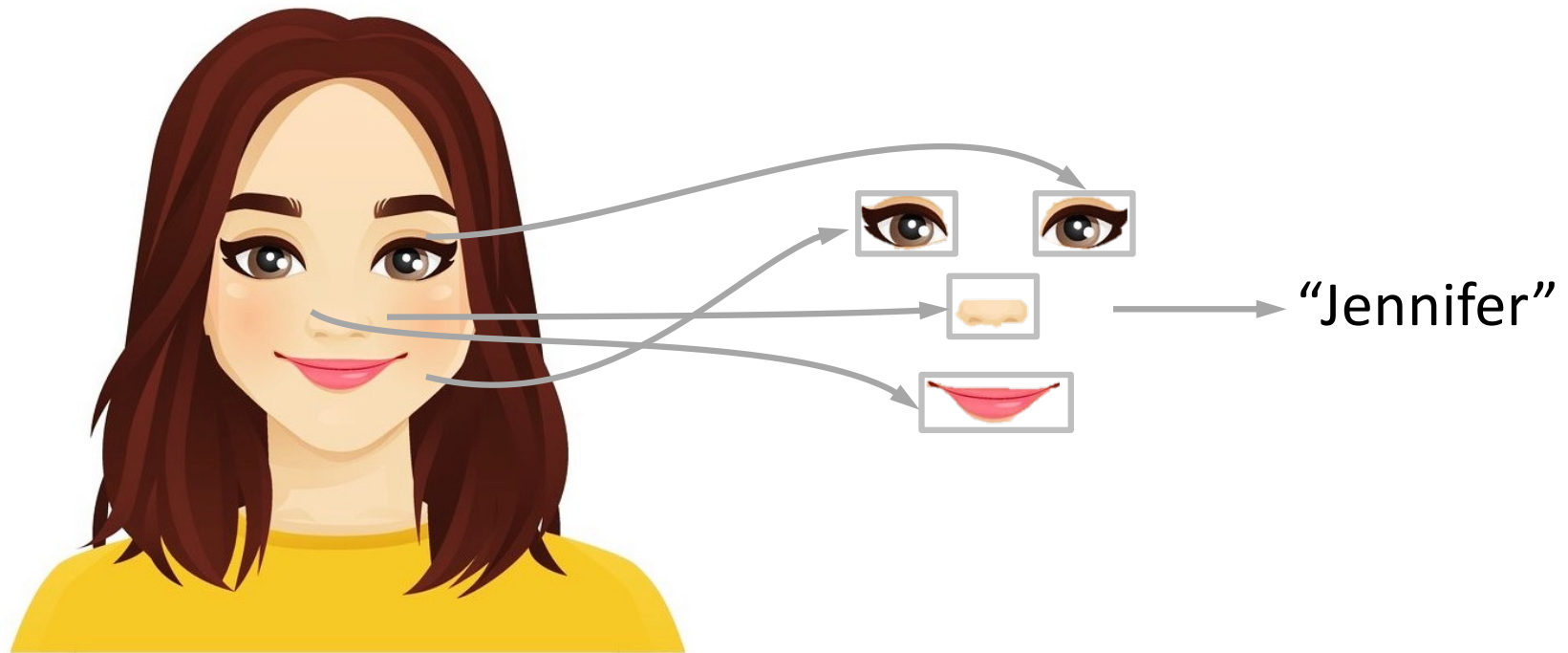


canonisation

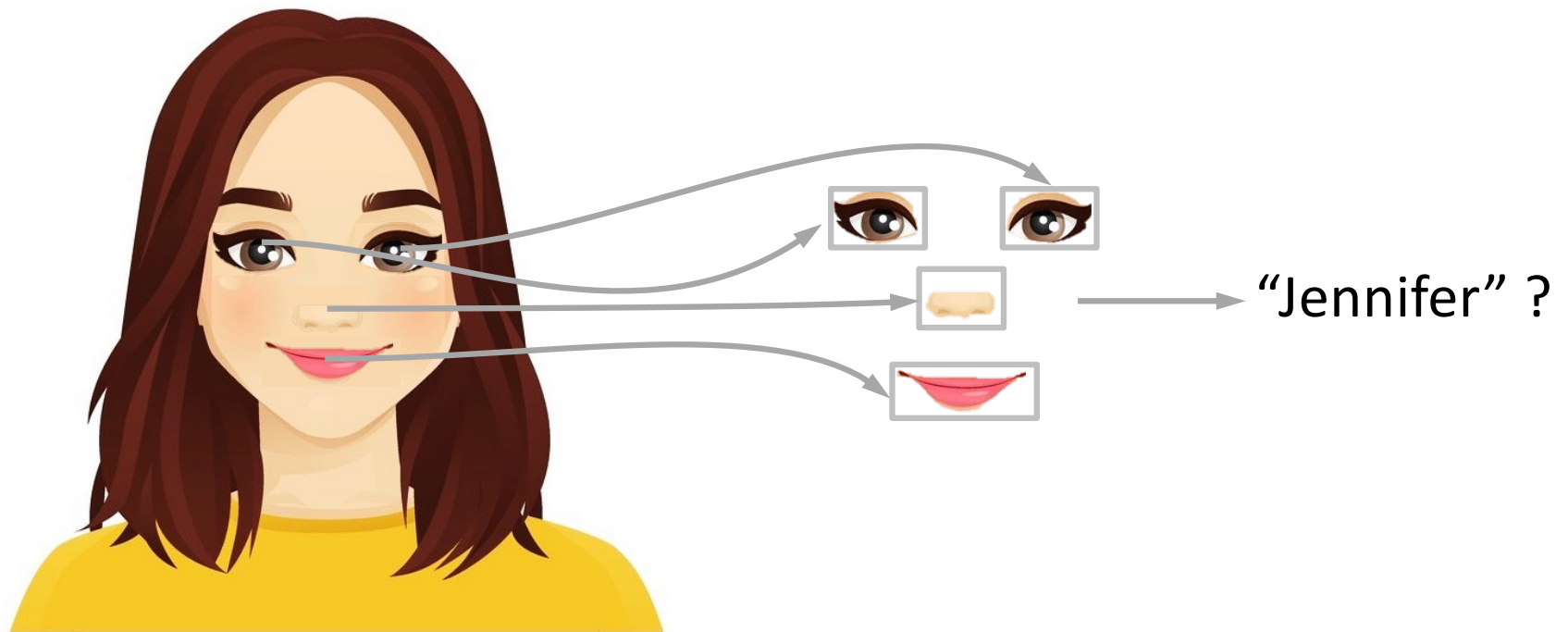
Canonisation

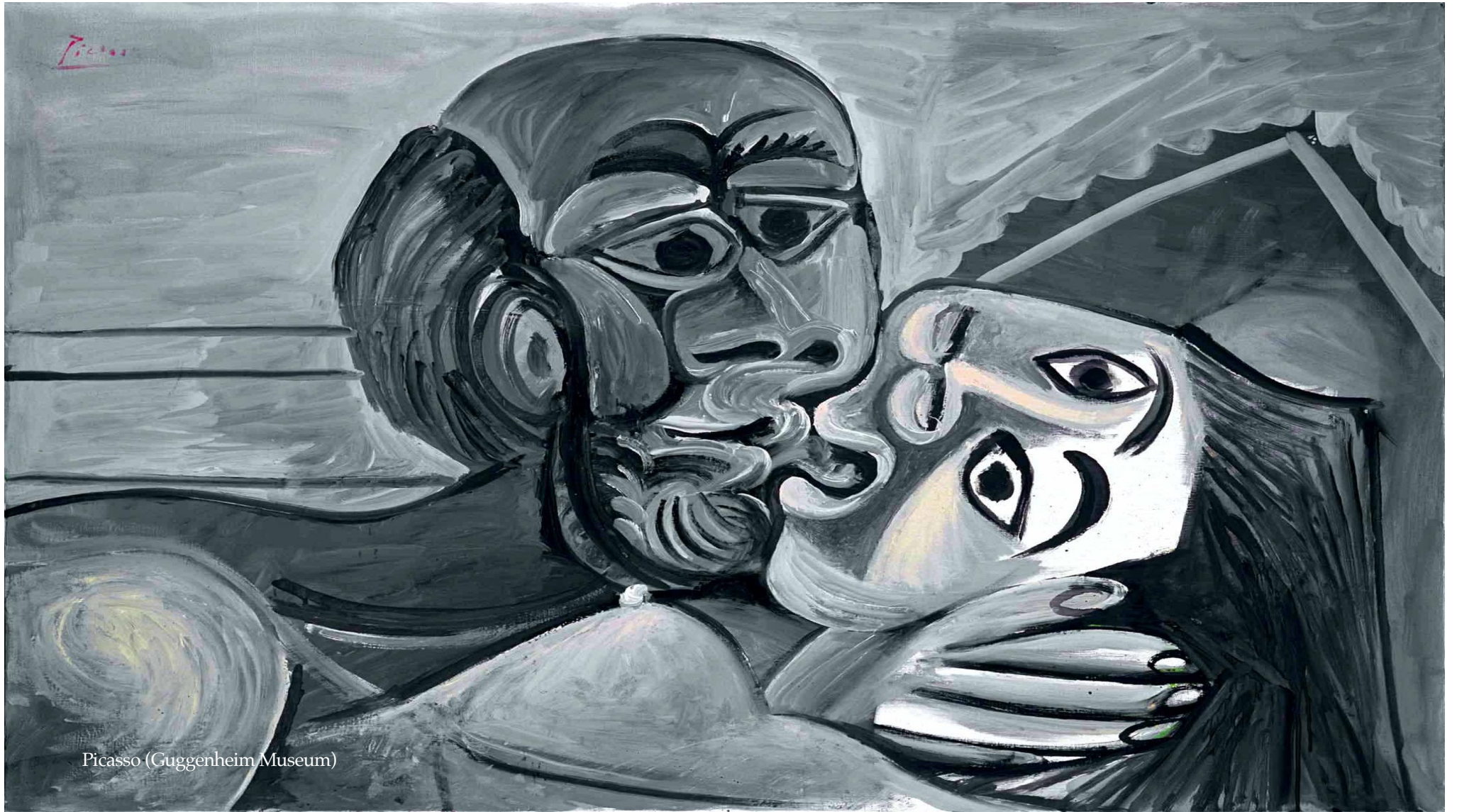


Canonisation



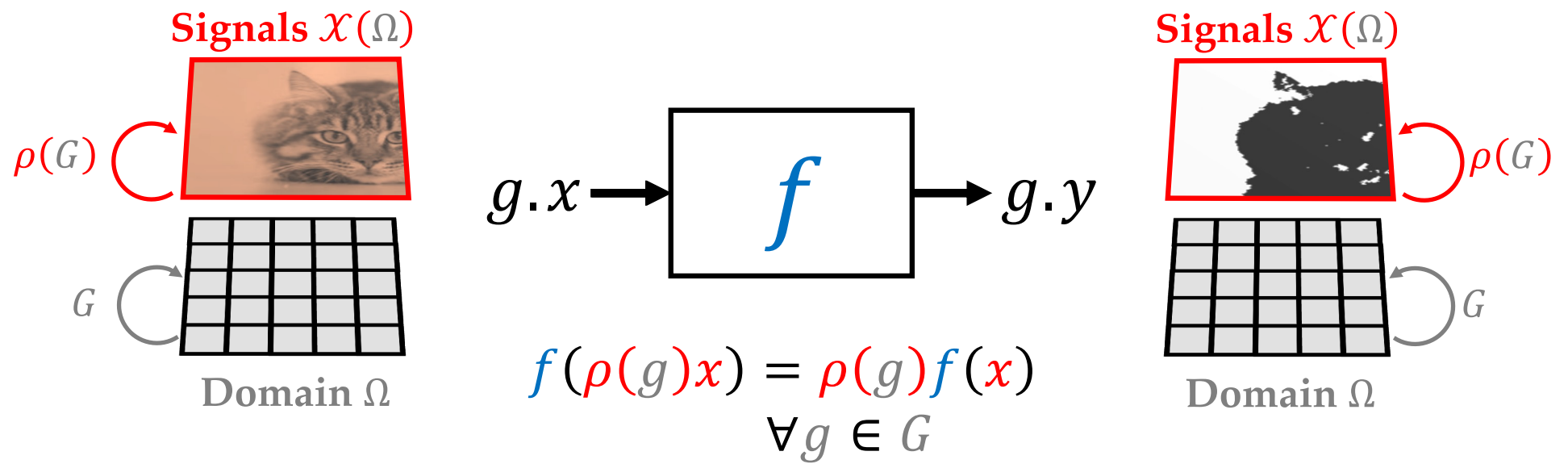
Canonisation



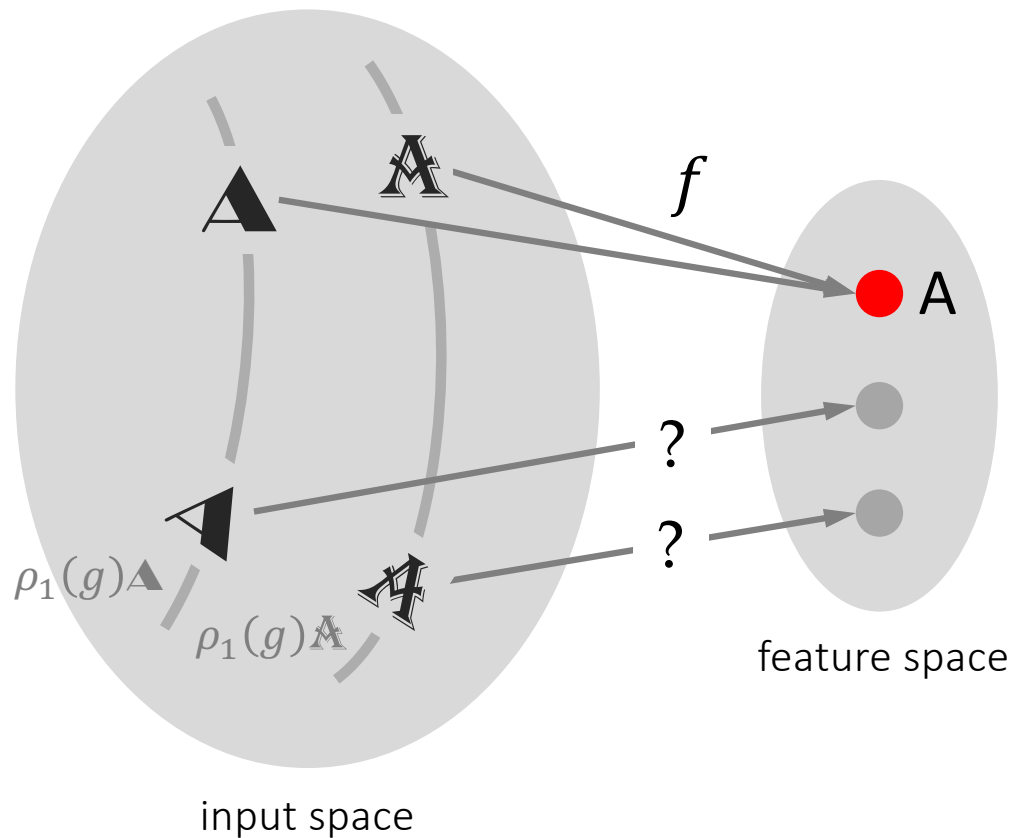


Picasso (Guggenheim Museum)

Geometric priors: Equivariance



Equivariance = Symmetry-consistent generalisation

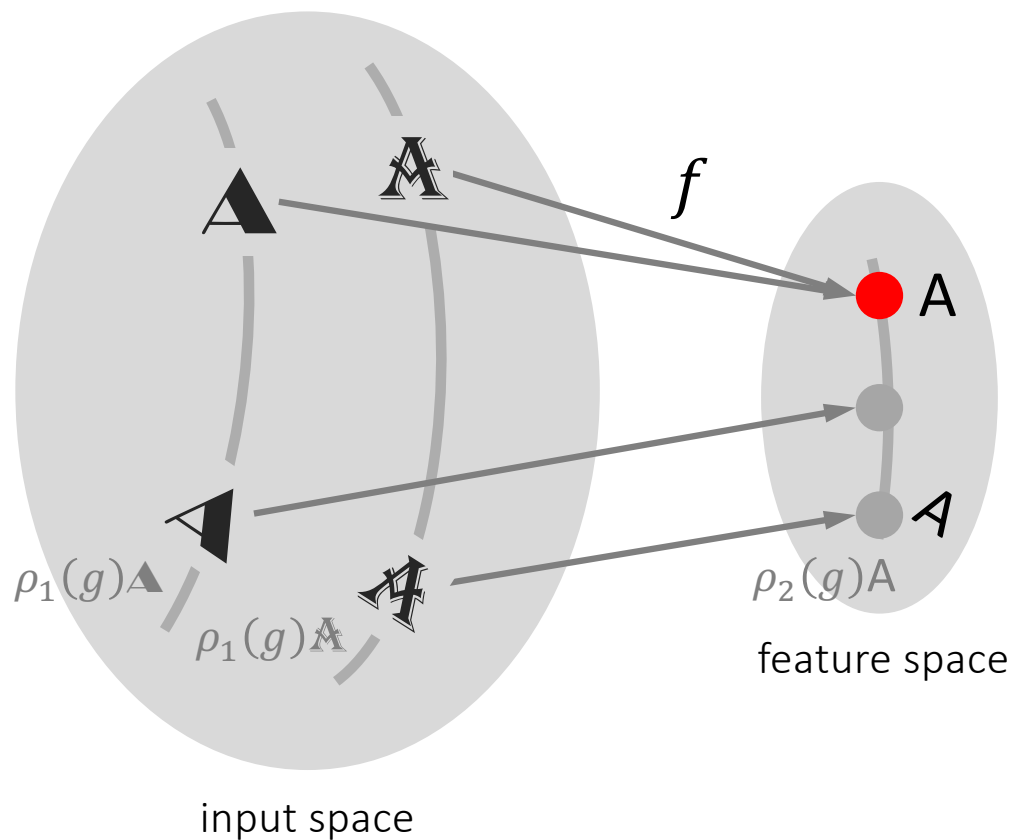


$$f(\rho_1(g)\blacktriangle) = \rho_2(g) \color{red}{f(\blacktriangle)}$$

$$\parallel$$

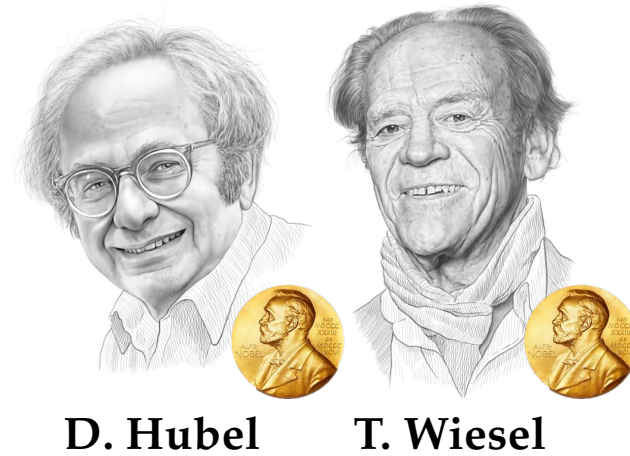
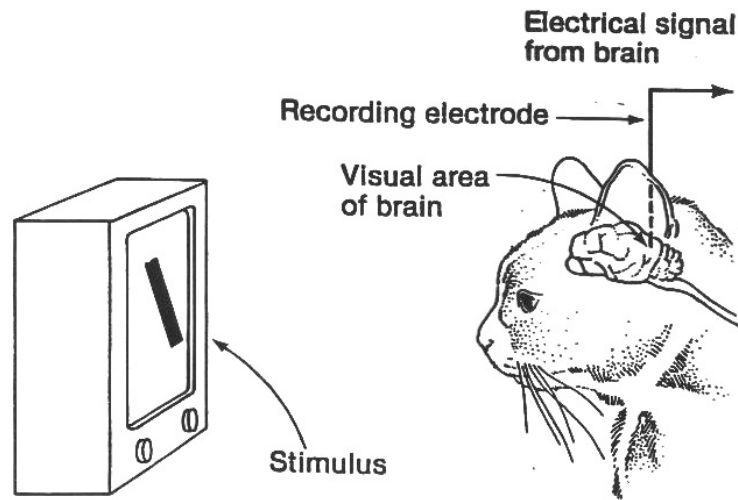
$$f(\rho_1(g)\mathbb{A}) = \rho_2(g) \color{red}{f(\mathbb{A})}$$

Equivariance = Symmetry-consistent generalisation



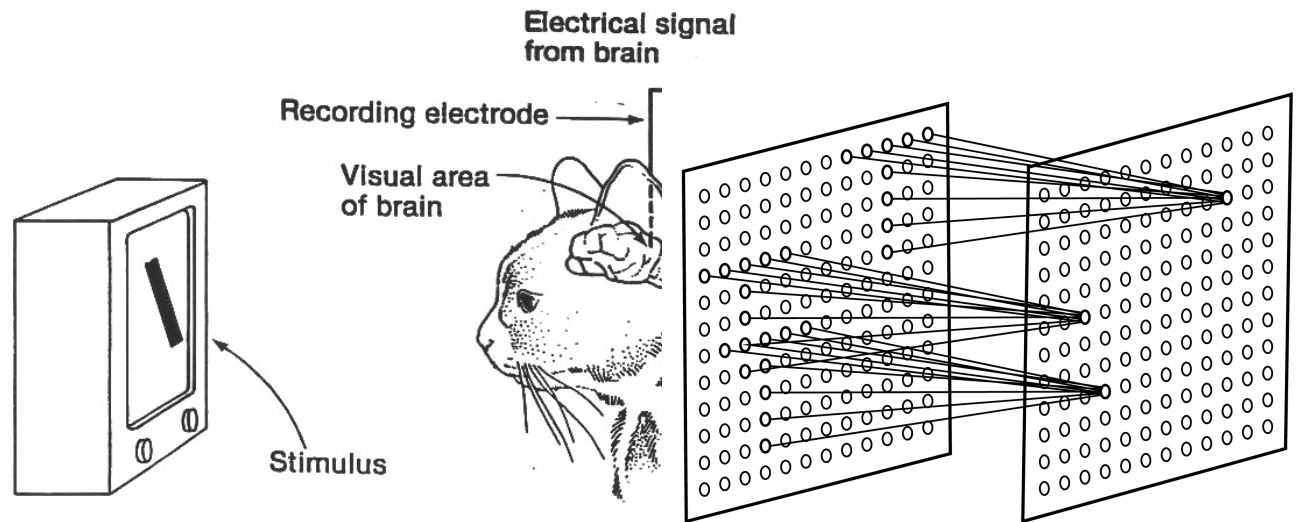
$$\begin{aligned}
 f(\rho_1(g)\blacktriangle) &= \rho_2(g) \color{red}{f(\blacktriangle)} \\
 &\quad \color{red}{\parallel} \\
 f(\rho_1(g)\triangle) &= \rho_2(g) \color{red}{f(\triangle)}
 \end{aligned}$$

Early Geometric Architectures



1959

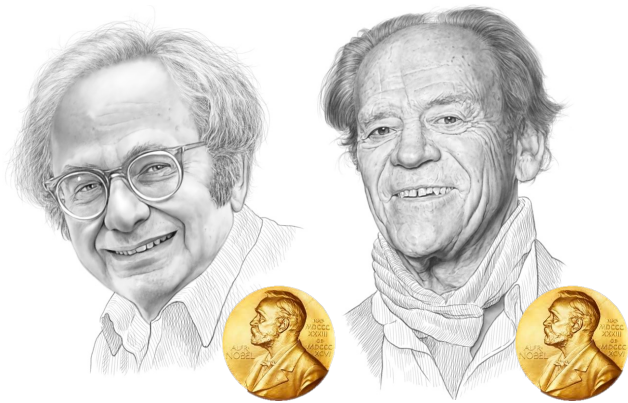
Early Geometric Architectures



K. Fukushima

1959 1980

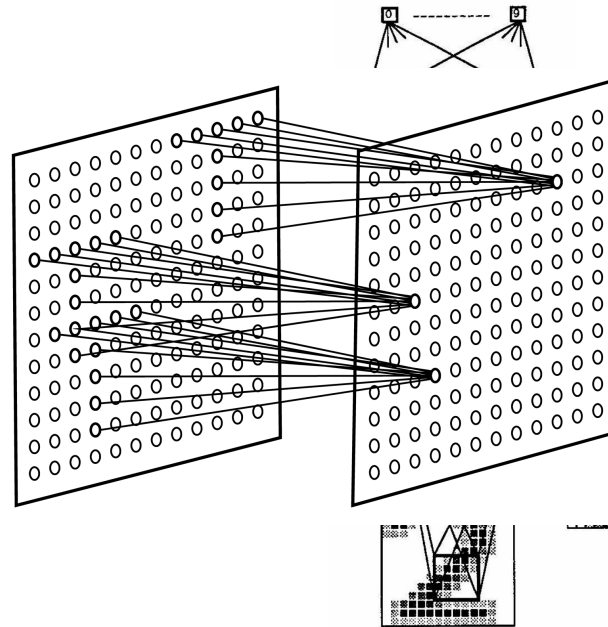
Early Geometric Architectures



D. Hubel

T. Wiesel

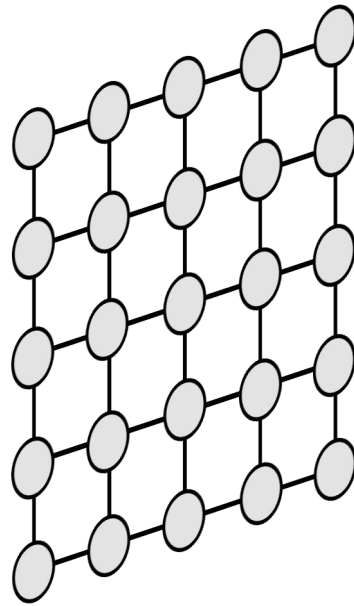
1959



K. Fukushima

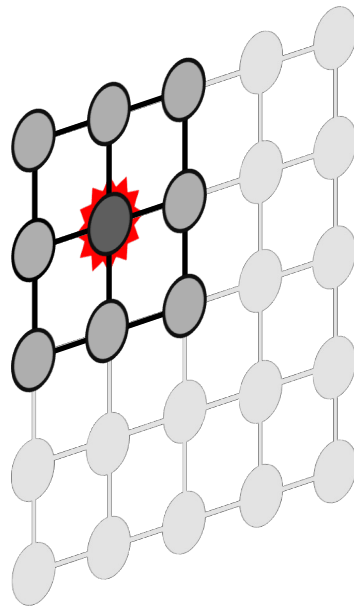
1980

Convolutional Neural Networks



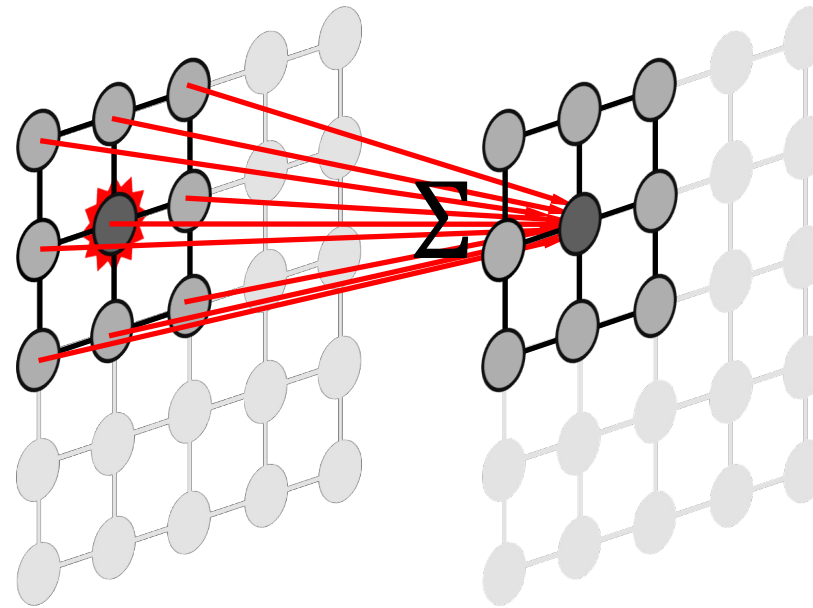
LeCun et al. 1989

Convolutional Neural Networks



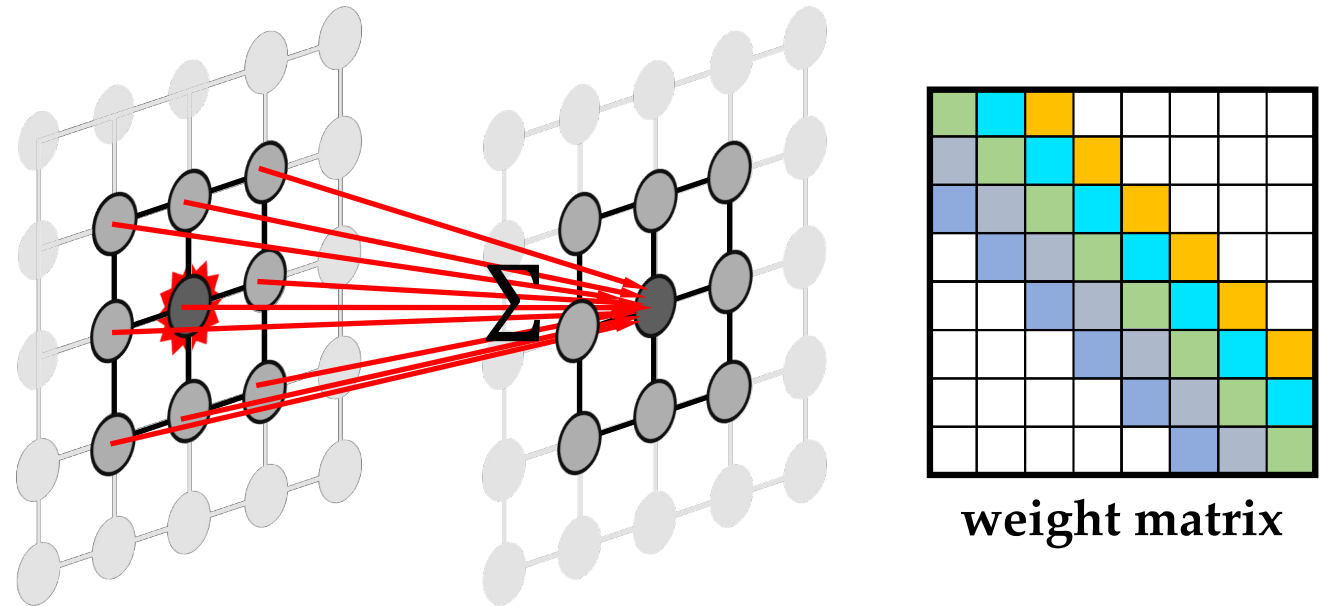
LeCun et al. 1989

Convolutional Neural Networks



Locality + Shared parameters

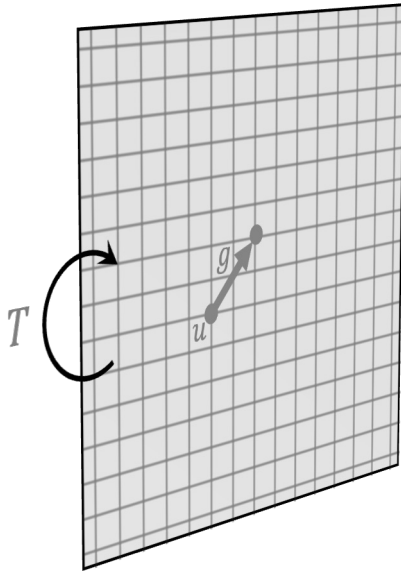
Convolutional Neural Networks



Locality + Shared parameters

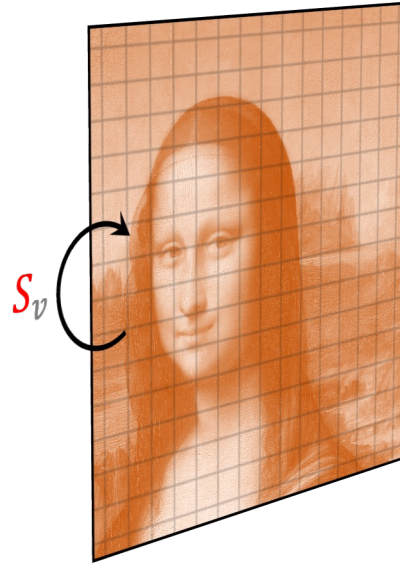
Convolutional Neural Networks

Plane \mathbb{R}^2



Translation group $T(2)$

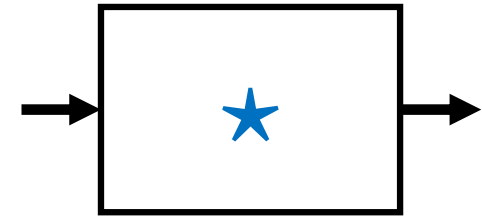
Images $\mathcal{X}(\mathbb{R}^2)$



Shift operator S

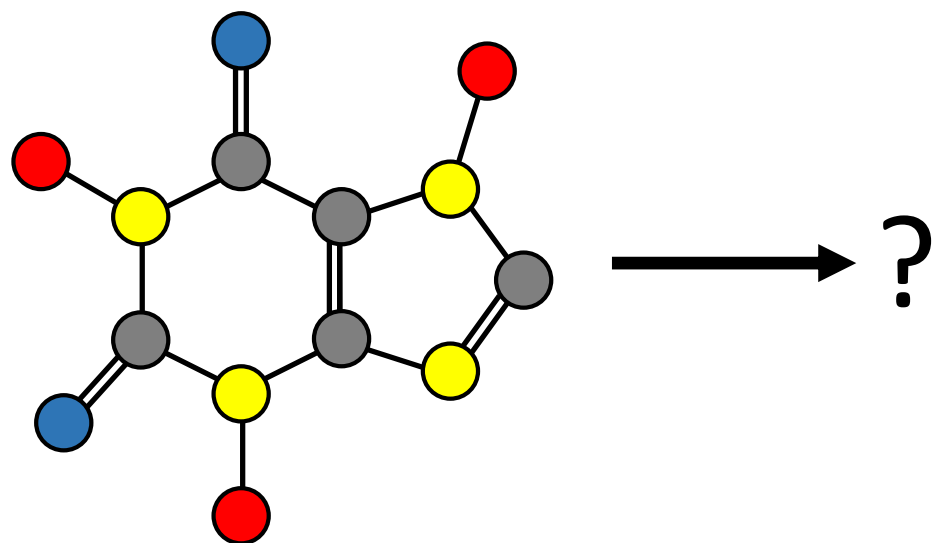
$$S_v x(u) = x(u - v)$$

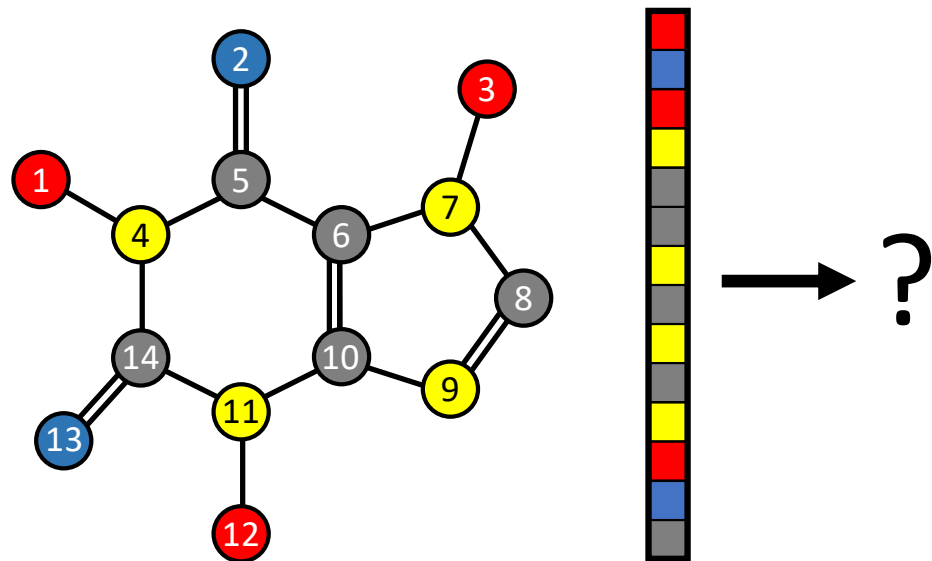
Functions $\mathcal{F}(\mathcal{X}(\mathbb{R}^2))$

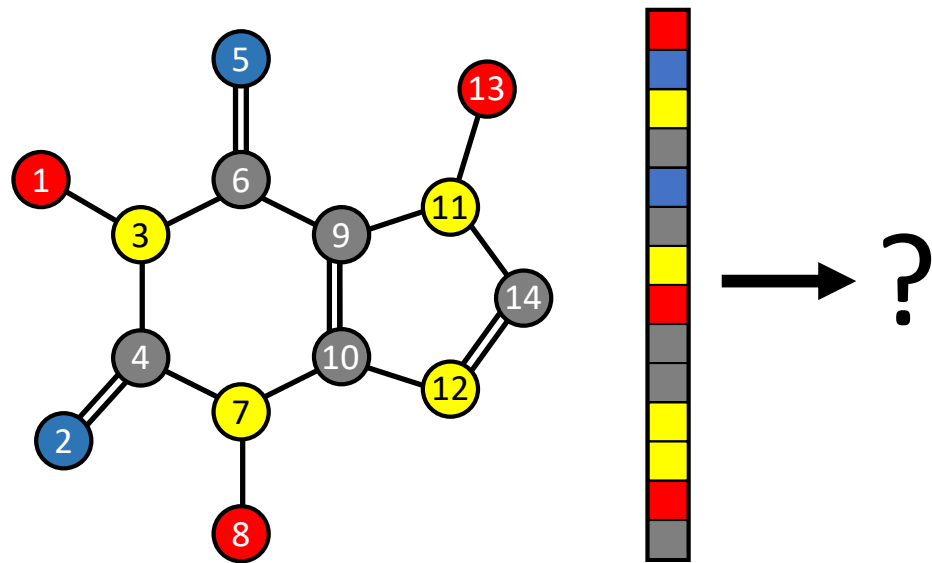


Convolution

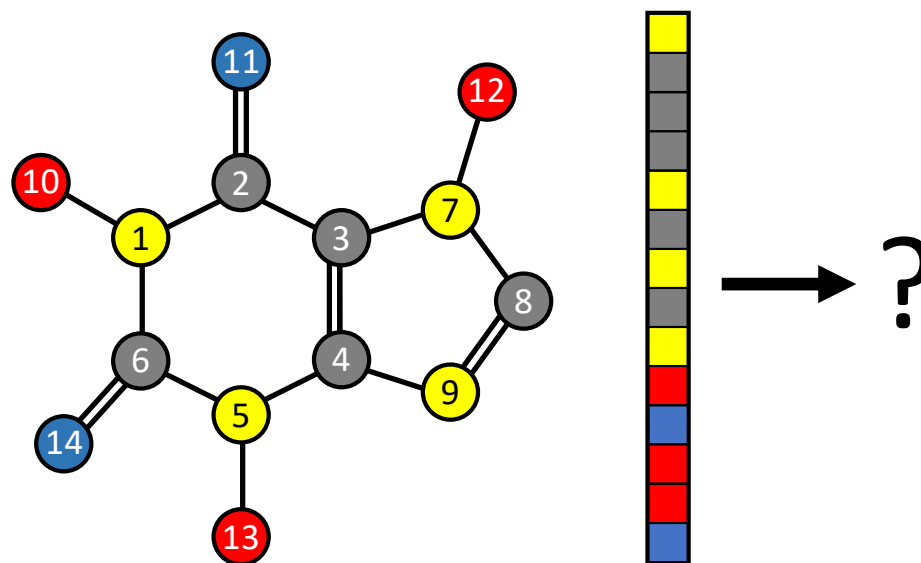
$$(Sx \star y) = S(x \star y)$$





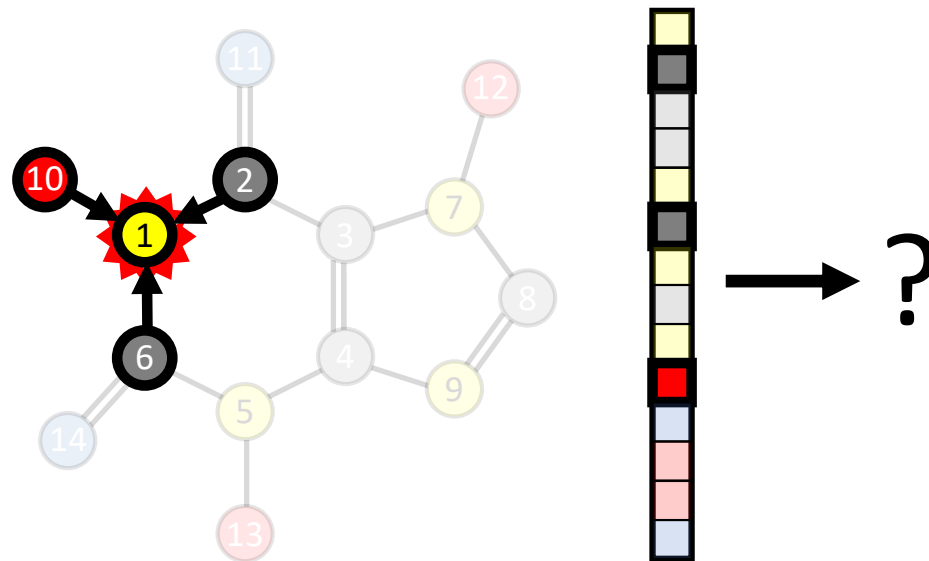


Permutation Invariance



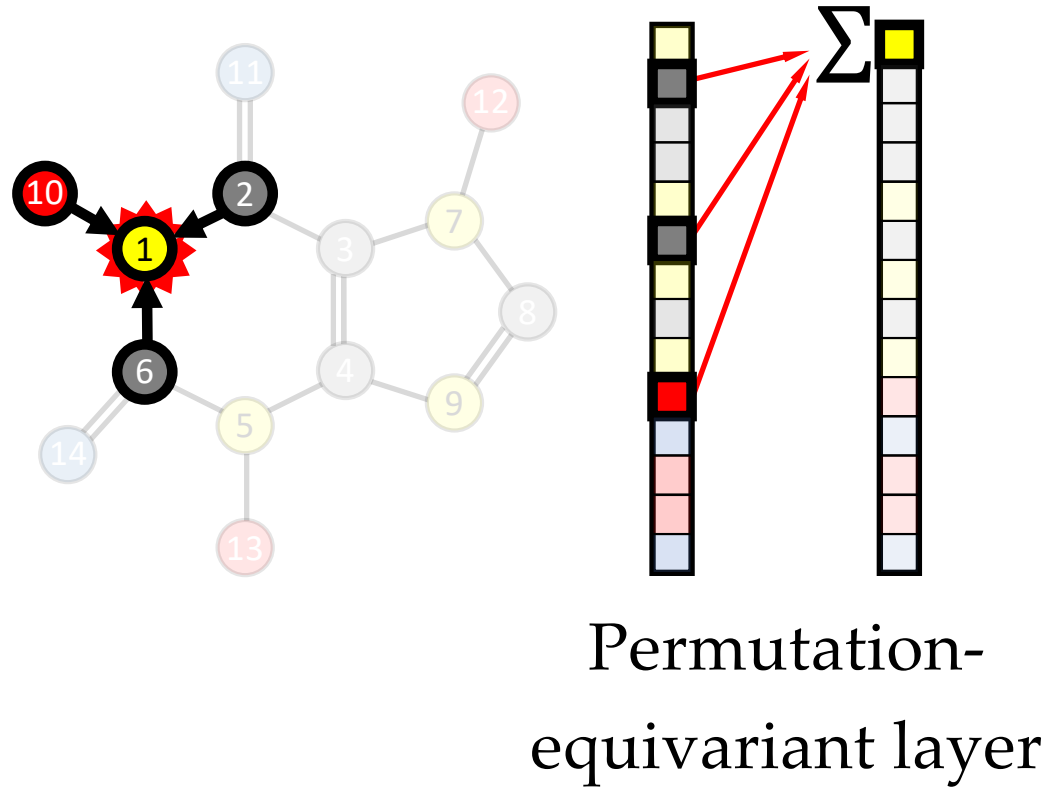
“properties of a molecule do not change if we reorder the atoms”

Graph Neural Networks

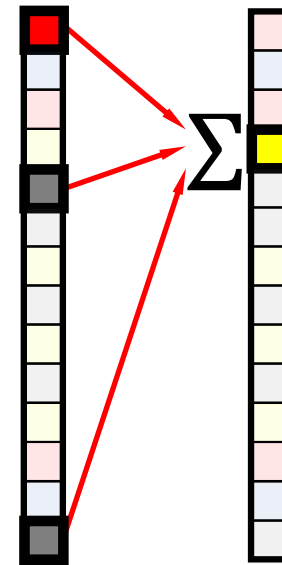
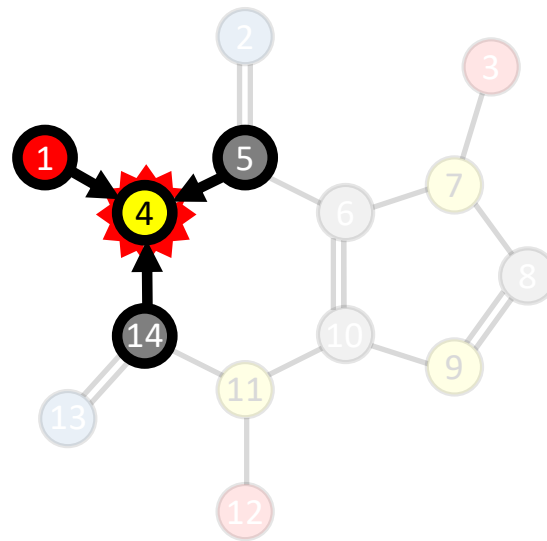


Locality + Shared parameters

Graph Neural Networks

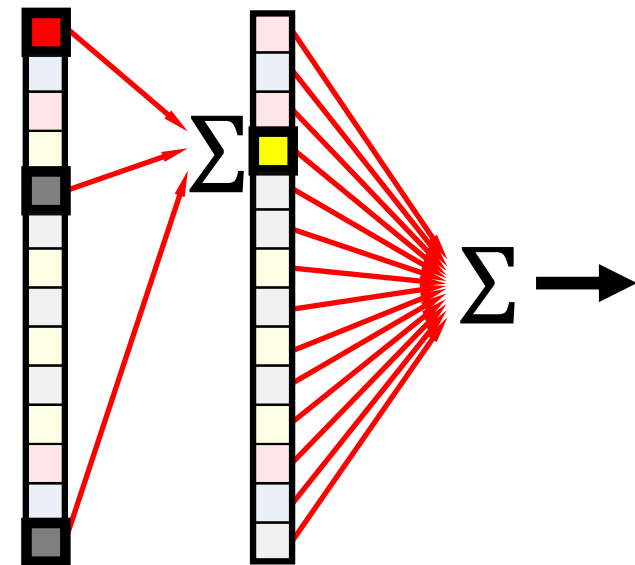
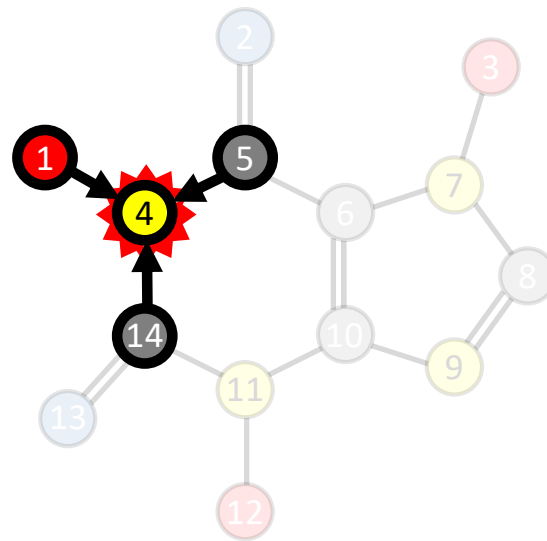


Graph Neural Networks



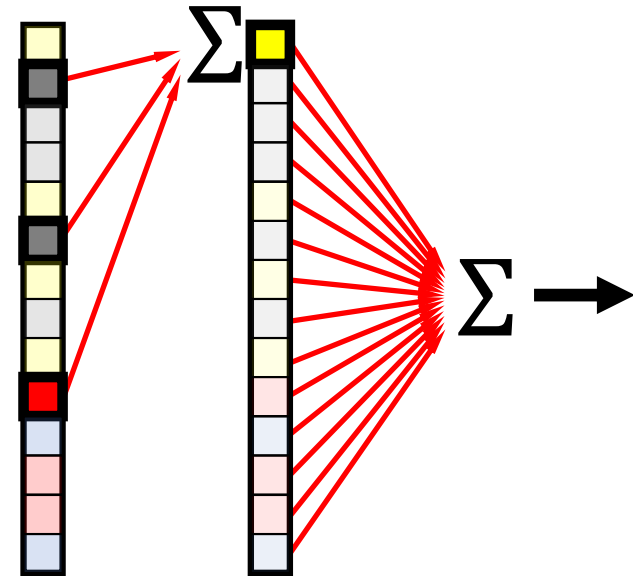
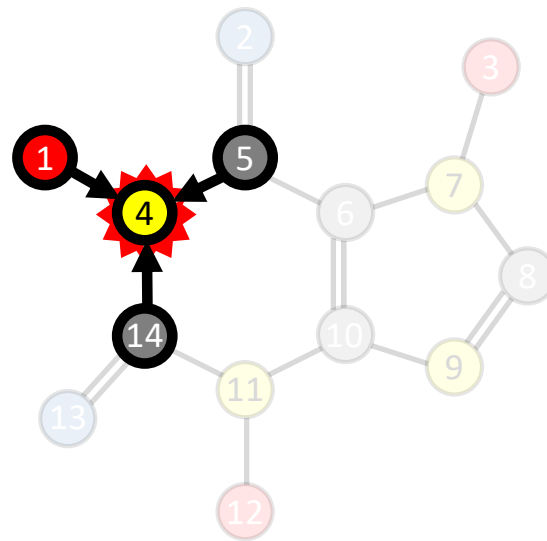
Permutation-
equivariant layer

Graph Neural Networks



Permutation-
invariant readout

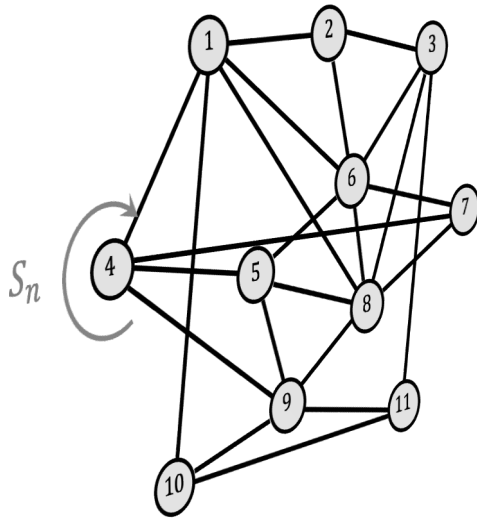
Graph Neural Networks



Permutation-
invariant readout

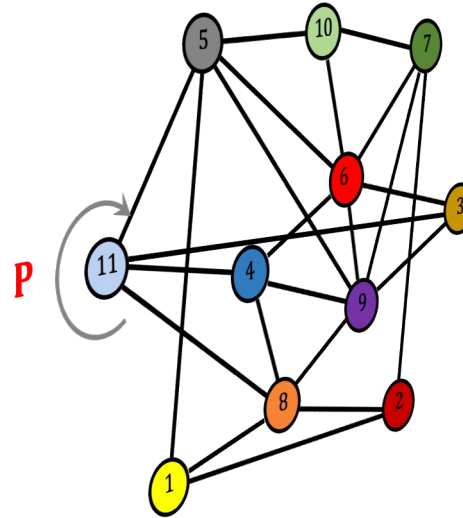
Graph Neural Networks

Graph $G = (V, E)$



Permutation group S_n

Node features $\mathcal{X}(G)$



Permutation matrix P

$$PX = (x_{\pi^{-1}(i),j})$$

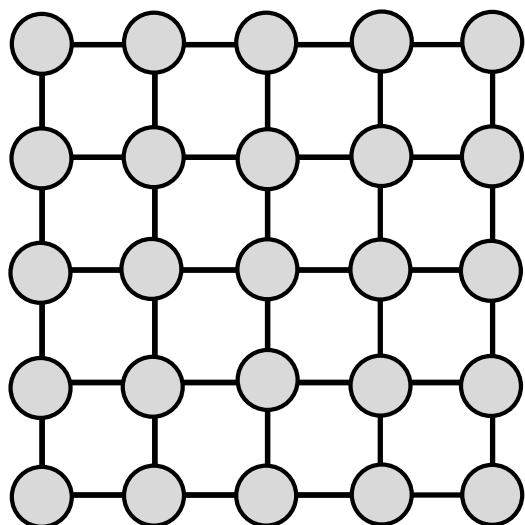
Functions $\mathcal{F}(\mathcal{X}(G))$



Message passing

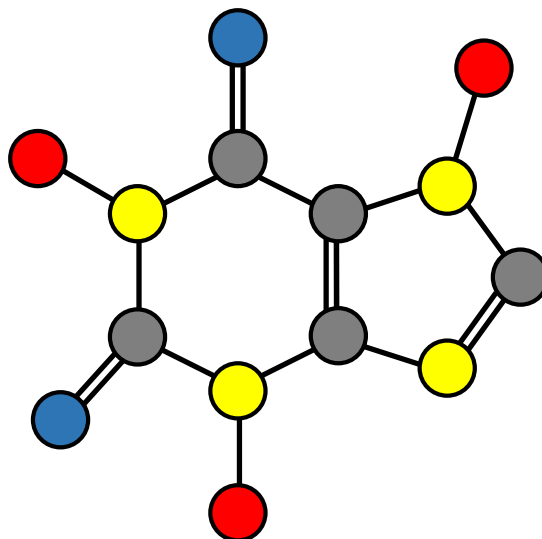
$$F(PX, PAP^T) = PF(X, A)$$

Grids



Translation

Graphs



Permutation

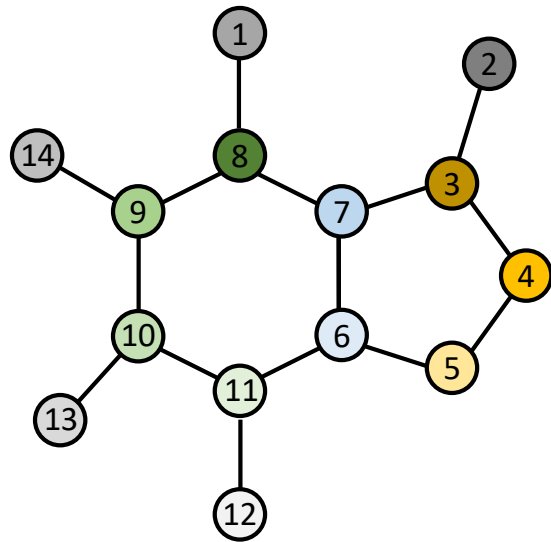
Meshes



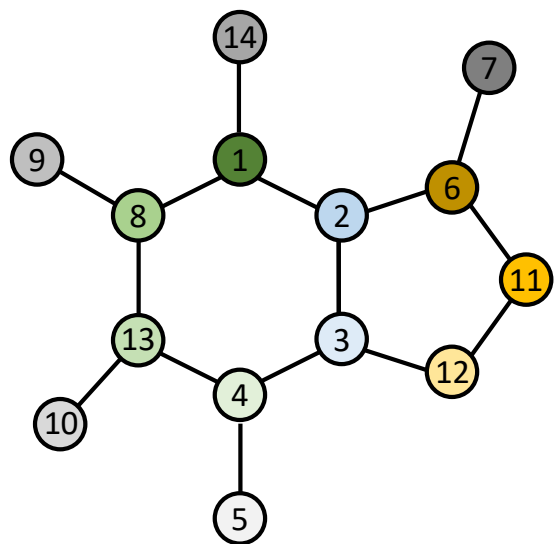
Local Rotation



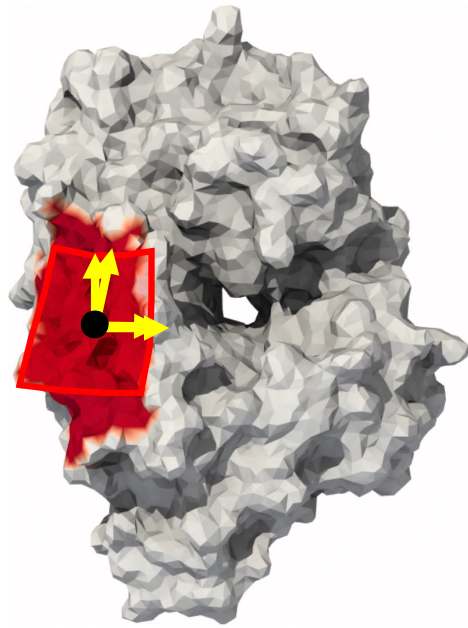
$$+ T(2) = \text{CNN}$$



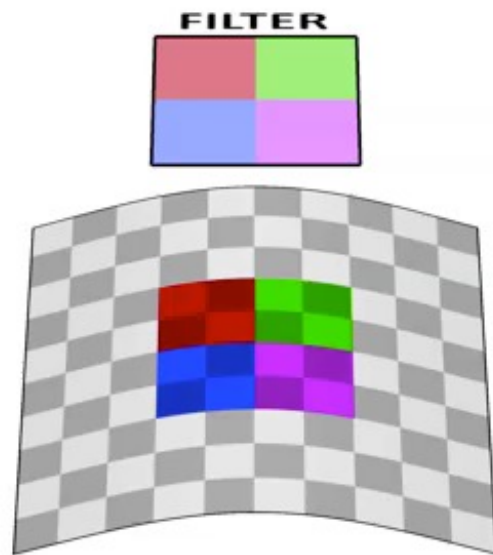
$$+ S_n = \text{GNN}$$



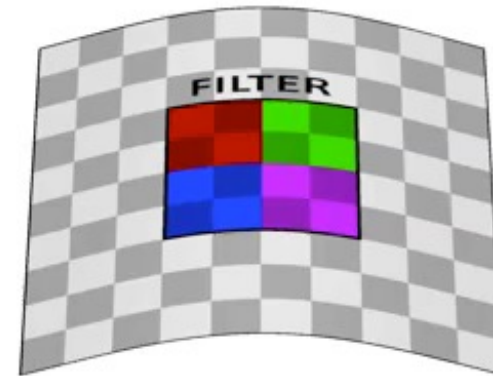
$$+ S_n = \text{GNN}$$



+ $SO(2)$ = MeshCNN



**Euclidean (extrinsic)
convolution**



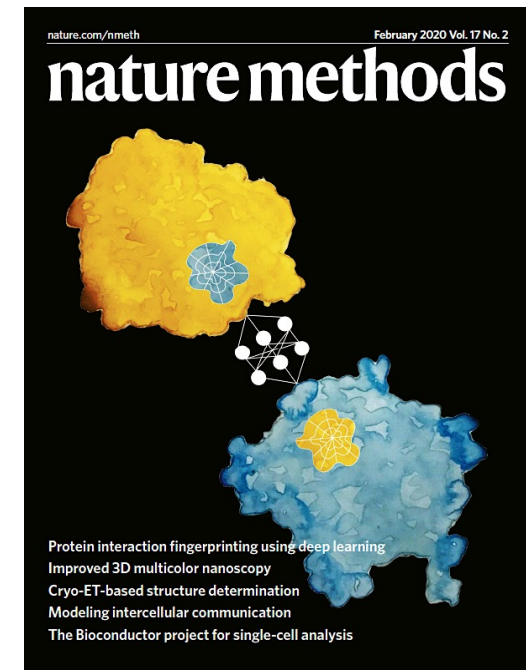
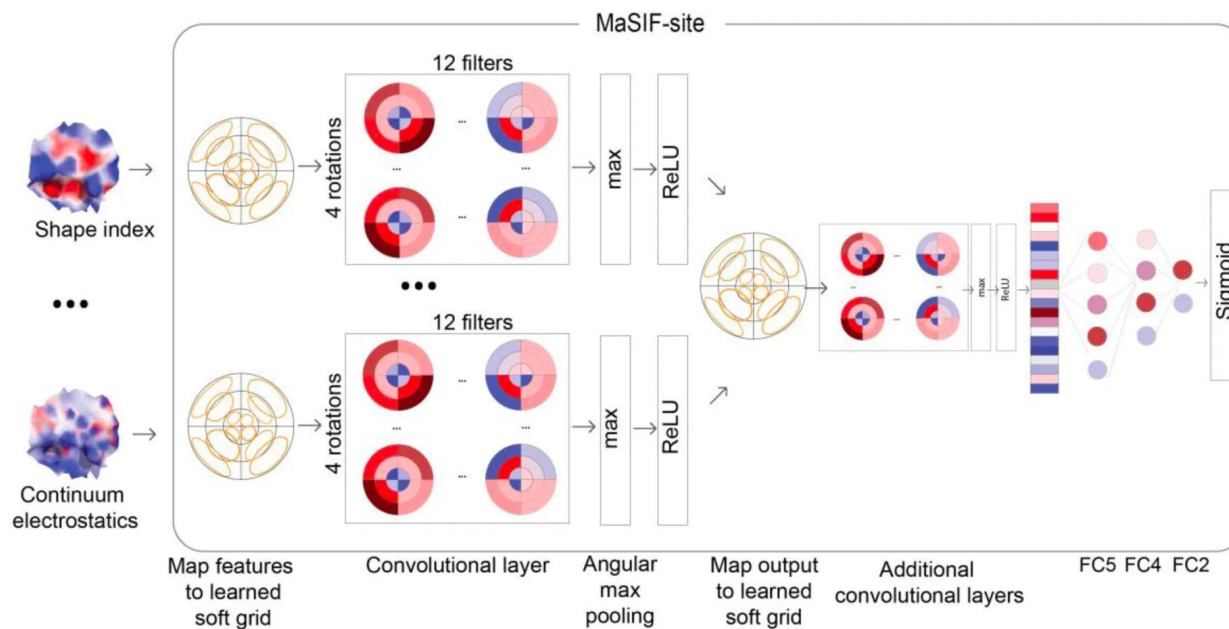
**Geometric (intrinsic)
convolution**



Snap Acquires Ariel AI To Enhance AR Features



MaSIF: Geometric ML for Protein Function Prediction & Design



Article

De novo design of protein interactions via learned surface fingerprints

<https://doi.org/10.1038/s41586-023-05993-x>

Received: 16 June 2022

Accepted: 21 March 2023

Published online: 26 April 2023

Open access

Pablo Gaiñza^{1,2,3,4,5,6}, Sarah Wehrli^{1,2,3}, Alexandra Van Hall-Beauvais^{1,2,3}, Anthony Andreas Schreck^{1,2,3}, Zander Harteveld^{1,2}, Stephen Buckley^{1,2}, Dongchun Ni¹, Frey Sverrisson^{1,3}, Casper Govers^{1,2}, Priscilla Turelli¹, Charlène Raciol¹, Alexandra Teslenko¹, Martin Pacesa^{1,2}, Stéphane Rosset^{1,2}, Sandrine George Jane Marsden^{1,2}, Aaron Petruzzella¹, Kefang Liu¹, Zepeng Xu¹, Yan Chai¹, Pu George F. Gao¹, Elisa Orlicchio¹, Beat Fierz^{1,2}, Didier Trono¹, Henning Stahlhut¹, Michael Bronstein^{2,3,4} & Bruno E. Correia^{1,2,3,4,5}

Physical interactions between proteins are essential for most biological governing life¹. However, the molecular determinants of such interactions are challenging to understand, even as genomic, proteomic and structural data expand. This knowledge gap has been a major obstacle for the comprehensive design of cellular protein–protein interaction networks and for the development of protein binders that are crucial for synthetic biology and translational applications. Here we use a geometric deep-learning framework operating on protein surfaces to generate fingerprints to describe geometric and chemical features that drive protein–protein interactions²⁰. We hypothesized that these fingerprints capture the key aspects of molecular recognition that represent a new paradigm for the computational design of novel protein interactions. As a proof of principle, we computationally designed several de novo protein binders to engage targets: SARS-CoV-2 spike, PD-1, PD-L1 and CTLA-4. Several designs were experimentally optimized, whereas others were generated purely in silico, achieving nanomolar affinity with structural and mutational characterization and accurate predictions. Overall, our surface-centric approach captures chemical determinants of molecular recognition, enabling an approach to the de novo design of protein interactions and, more broadly, of artificial functions.

Designing novel protein–protein interactions (PPIs) remains a fundamental challenge in computational protein design, with broad basic and translational applications in biology. The challenge consists of generating amino acid sequences that engage a target site and form a quaternary complex with a given protein. This represents a stringent test of our understanding of the physicochemical determinants that drive biomolecular interactions¹. Robust computational methods to design de novo PPIs could be used to rapidly engineer protein-based therapeutics such as antibodies and protein inhibitors or vaccines among others, and are therefore of considerable interest for biomedical and translational applications^{2–4}.

Despite recent advances in rational PPI design^{5–8} and prediction⁹, designing novel protein binders against specific targets is very challenging, particularly when no structural elements from pre-existing

binders are known. Current state-of-the-art methods^{10–12}, such as hotspot-centric approaches¹³ and machine learning^{14–17}, rely on placing disembodied residues at the interface and then optimizing their presentation. Intrinsic limitations of these approaches relate to the lack of energetic signatures provided by scoring functions and the lack of structural context, which is compounded in flat interface pockets. These methods also face the challenge of identifying protein scaffolds to precisely display the generate residues. To circumvent these limitations, new approaches to design de novo binders to various surface types^{18–20}. A long-standing model of molecular recognition²¹ posits that PPIs form between protein molecular surfaces with complementary shapes^{22–24}. The complementarity



Designing protein–ligand neosurfaces with a scalable deep learning tool

DOI: 10.1038/s41586-023-05993-x

Anthony Marchand^{1,2}, Stephen Buckley^{1,2}, Arne Schneuing^{1,2}, Martin Pacesa¹, Maddalena Elia¹, Pablo Gaiñza^{1,2}, Evgenia Elizarova¹, Rebecca M. Neeser^{1,2}, Pao-Wan Lee¹, Luc Raymond¹, Yangyang Miao¹, Leo Scheller¹, Sandrine Georgeon¹, Joseph Schmidt¹, Philippe Schwaller¹, Sebastian J. Maerki¹, Michael Bronstein^{2,3} & Bruno E. Correia^{1,2,3,4,5}

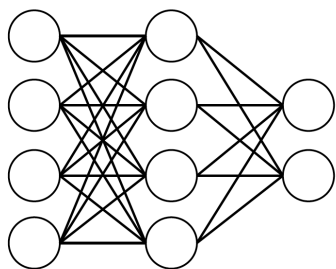
Molecular recognition events between proteins drive biological processes in living systems¹. However, higher levels of mechanistic regulation have emerged, in which protein–protein interactions are conditioned to small molecules^{2–4}. Despite recent advances, computational tools for the design of new chemically induced protein interactions have remained a challenging task for the field⁵. Here we present a computational strategy for the design of proteins that target neosurfaces, that is, surfaces arising from protein–ligand complexes. To develop this strategy, we leveraged a geometric deep learning approach based on learned molecular surface representations⁶ and experimentally validated binders against three drug-bound protein complexes: Bcl-2–venetoclax, DB3–progesterone and PD1–actinonin. All binders demonstrated high affinities and accurate specificities, as assessed by mutational and structural characterization. Remarkably, surface fingerprints previously trained only on proteins could be applied to neosurfaces induced by interactions with small molecules, providing a powerful demonstration of generalizability that is uncommon in other deep learning approaches. We anticipate that such designed chemically induced protein interactions will have the potential to expand the sensing repertoire and the assembly of new synthetic pathways in engineered cells for innovative drug-controlled cell-based therapies⁷.

PPIs have essential roles in healthy cell function and in numerous diseases^{1,8}. For this reason, PPIs have been developed over the years as tools for the design of new drugs⁹. The governing principle of protein–protein interactions is the complementarity of their surfaces, which is compounded in flat interface pockets. These methods also face the challenge of identifying protein scaffolds to precisely display the generate residues. To circumvent these limitations, new approaches to design de novo binders to various surface types^{18–20}. A long-standing model of molecular recognition²¹ posits that PPIs form between protein molecular surfaces with complementary shapes^{22–24}. The complementarity

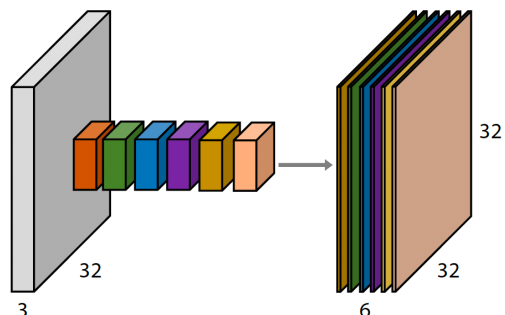
In synthetic biology, molecular components that rely on small-molecule-induced neosurfaces have been used to engineer chemically responsive systems with precise spatiotemporal control of cellular activities¹⁵. Small-molecule triggers have been used to both induce and disrupt PPIs, thereby functioning as ON or OFF switches for engineered cellular functions^{16,17}. There are several practical advantages to using small molecules as triggers, including their simple administration, biocompatibility, safety, and high affinity and specificity to their target proteins. Protein-based switches controlled by small molecules have already been used to regulate transcription¹⁸, protein degradation^{19,20} and protein localization^{21,22}, among many other applications. In addition to their use in basic research, engineering molecular switches are increasingly used to control protein-based and cellular therapeutics, the activity of which may need to be regulated to mitigate potentially dangerous side effects^{23,24}. Although several chemically disruptible heterodimer (OFF-switch) systems have been proposed^{25,26}, computationally designed chemically induced dimerization (CID, ON-switch) systems remain challenging owing to the complexity of modelling neosurfaces. Previous attempts to design CID systems primarily relied on experimental methods^{27,28–30}, and,

engineering, Institute of Bioengineering, École Polytechnique Fédérale de Lausanne, Lausanne, Switzerland. ²Laboratory of Chemical Artificial Intelligence and Engineering, École Polytechnique Fédérale de Lausanne, Lausanne, Switzerland. ³Laboratory of Biological Network Characterization, Institute of Microbiology, Chinese Academy of Sciences, Beijing, China. ⁴Laboratory of Virology and Genetics, School of Life Sciences, École Polytechnique Fédérale de Lausanne, Lausanne, Switzerland. ⁵Swiss Institute for Experimental Cancer Research, School of Life Sciences, École Polytechnique Fédérale de Lausanne, Lausanne, Switzerland. ⁶University of Oxford, Oxford, UK. ⁷Present address: Monte Rosa Therapeutics, Basel, Switzerland. *These authors contributed equally: Anthony Marchand, Stephen Buckley, Arne Schneuing.

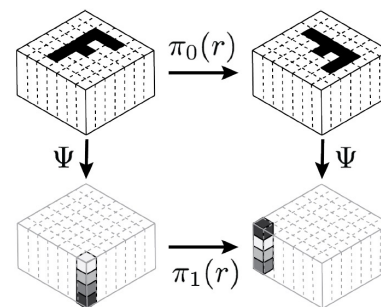
arch 2023



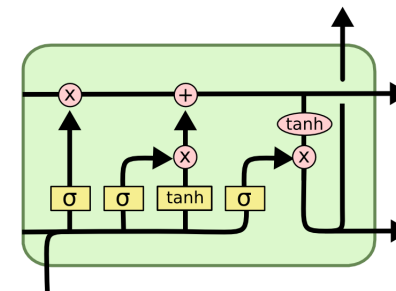
Perceptrons
Function regularity



CNNs
Translation



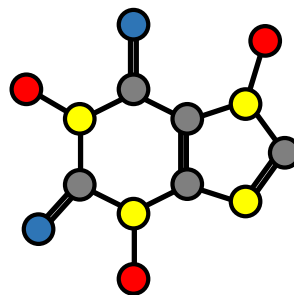
Group-CNNs
Translation+Rotation,
Global groups



LSTMs
Time warping



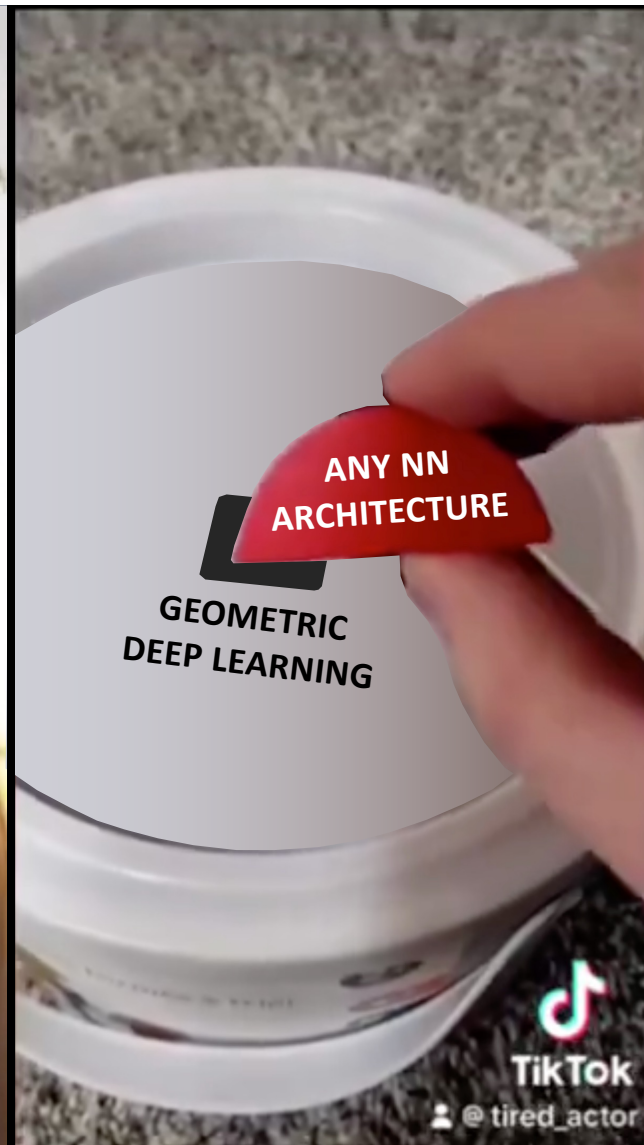
DeepSets / Transformers
Permutation

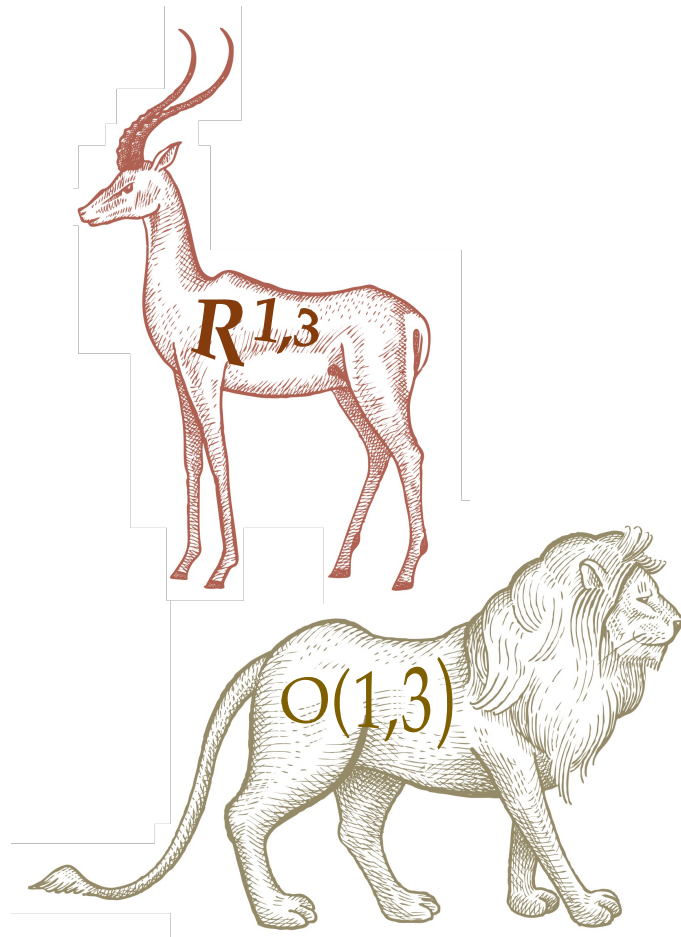


GNNs
Permutation

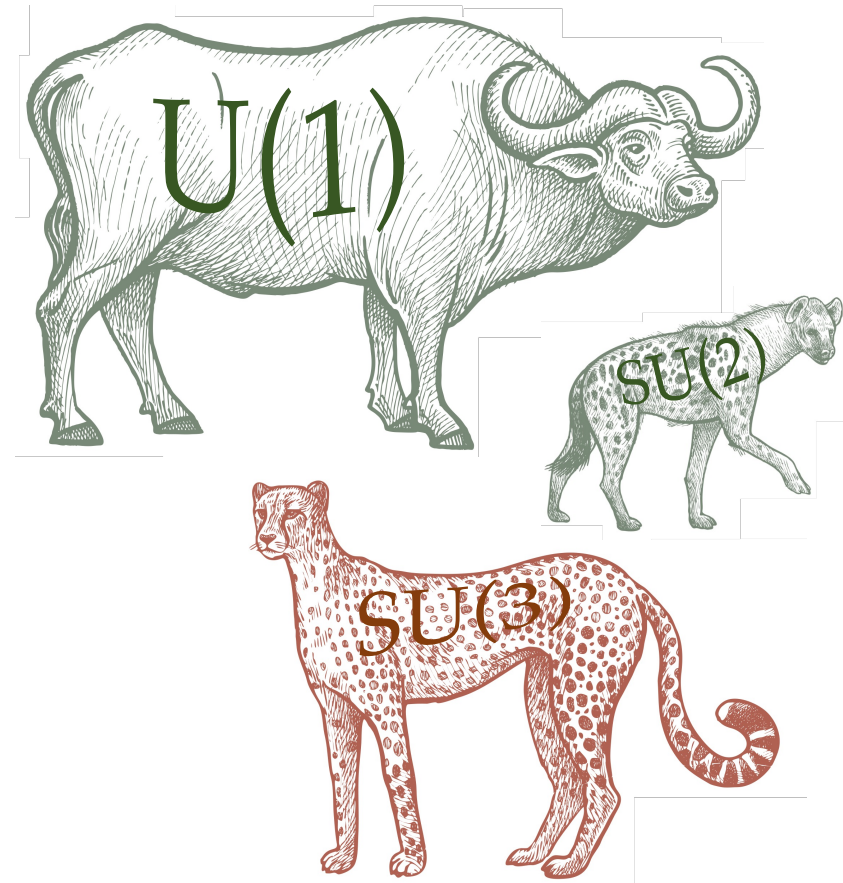


Intrinsic CNNs
Isometry / Gauge choice



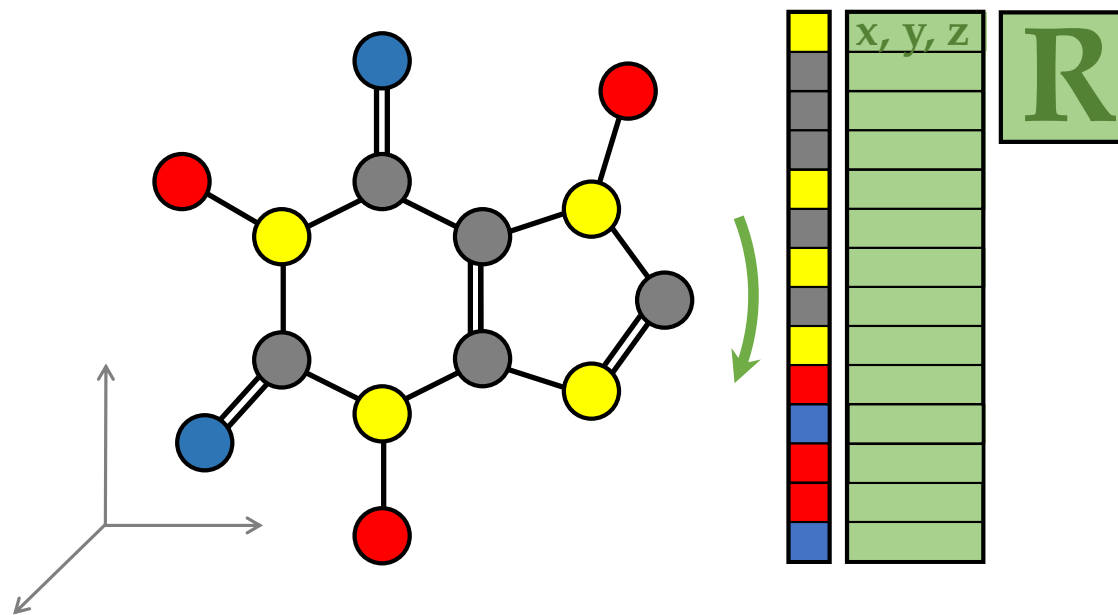


External symmetry



Internal symmetry

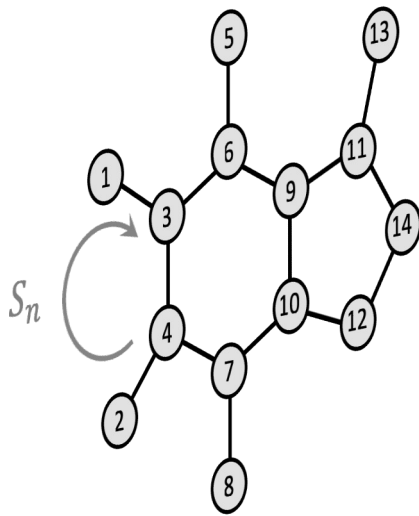
$SO(3)$ -invariance



“properties of a molecule do not change if we rotate it”

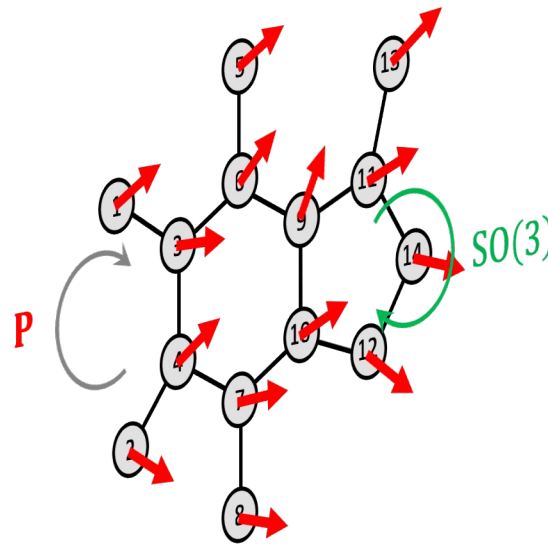
Geometric (“Equivariant”) Graph Neural Networks

Geometric Graph G



Permutation group S_n
“domain symmetry”

Node features $\chi(G)$



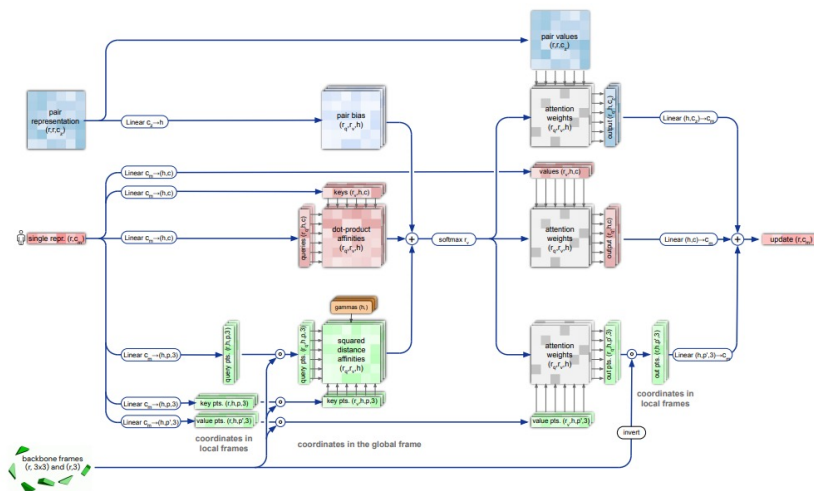
Permutation matrix \mathbf{P}
Rotation \mathbf{R}
“data symmetry”

Functions $\mathcal{F}(\chi(G))$



Geometric message passing
 $\mathbf{F}(\mathbf{P}\mathbf{X}\mathbf{R}, \mathbf{P}\mathbf{A}\mathbf{P}^\top) = \mathbf{P}\mathbf{F}(\mathbf{X}, \mathbf{A})\mathbf{R}$

Revolution in Structural Biology



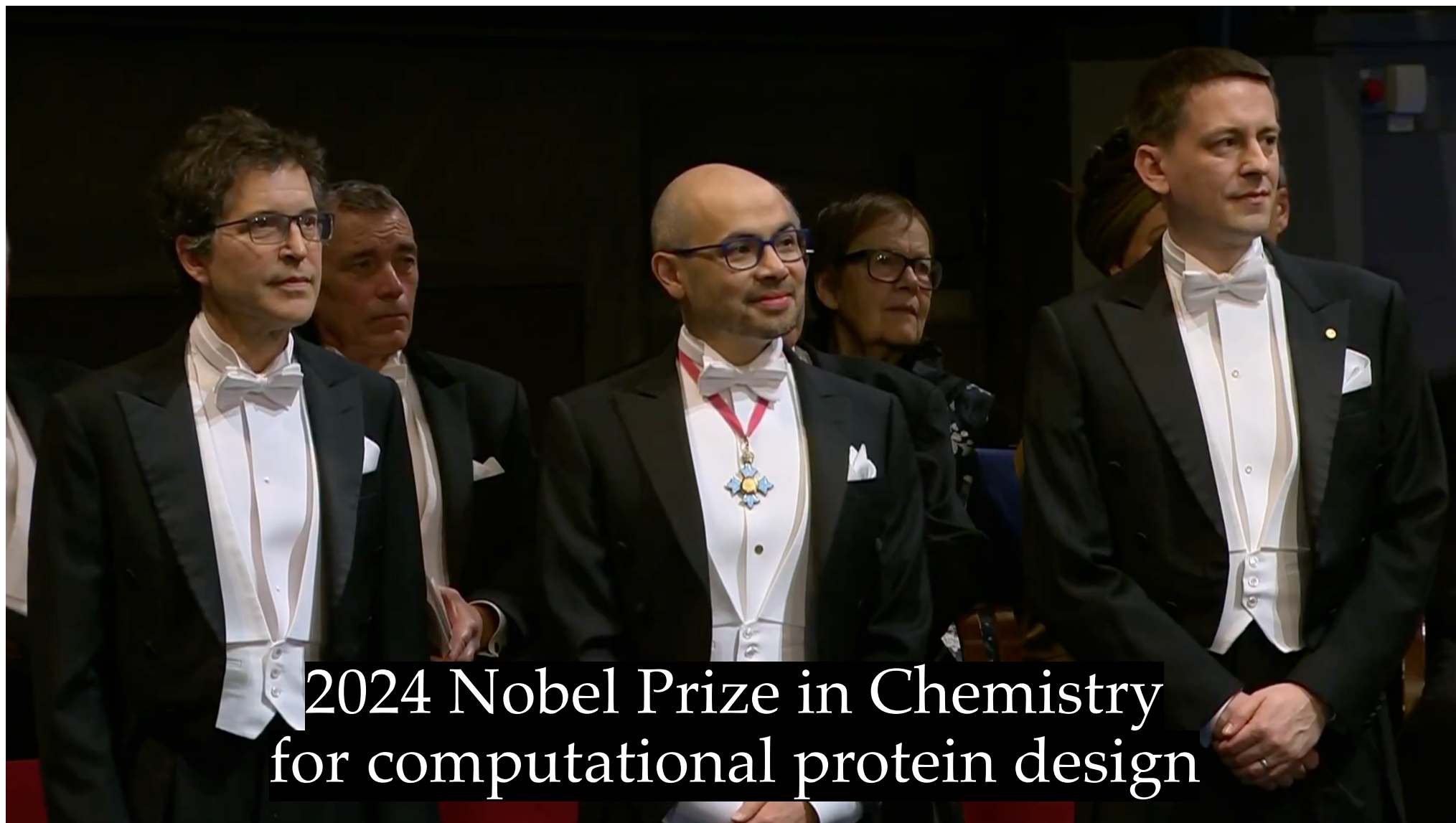
Jumper et al. 2021

AlphaFold 2
“Invariant point
attention”



Baek et al. 2021

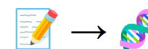
RosettaFold
SE(3)-equivariant
Transformer



2024 Nobel Prize in Chemistry
for computational protein design

AND THEY LIVED

HAPPILY EVER AFTER



The Bitter Lesson: Equivariance is dead...long live equivariance!

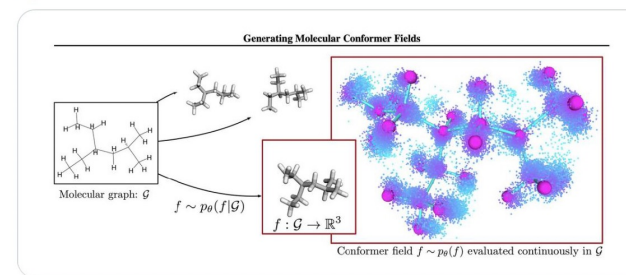
► **Equivariance is the idea of giving a model the inductive biases to natively handle rotations, translations and (sometimes) reflections. It has been at the core of Geometric Deep Learning and biomolecular modelling research since AlphaFold 2. However, recent works by top labs have questioned the existing mantra.**

- **The first shots were fired by Apple**, with a paper that obtained SOTA results on predicting the 3D structures of small molecules using a non-equivariant diffusion model with a transformer encoder.
- Remarkably, the authors showed that using the domain-agnostic model did not deleteriously impact generalization and was consistently able to outperform specialist models (assuming sufficient scale was used).
- **Next was AlphaFold 3, which infamously dropped all the equivariance** and frames constraints from the previous model in favour of another diffusion process coupled with augmentations and, of course, scale.
- Regardless, the greatly improved training efficiency of equivariant models means the practice is likely to stay for a while (at least for academic groups working on large systems such as proteins).



"We [...] empirically show that explicitly enforcing roto-translation equivariance is not a strong requirement for generalization."

"Furthermore, we also show that approaches that do not explicitly enforce roto-translation equivariance (like ours) can match or outperform approaches that do."



stateof.ai 2024

Swallowing the Bitter Pill: Simplified Scalable Conformer Generation

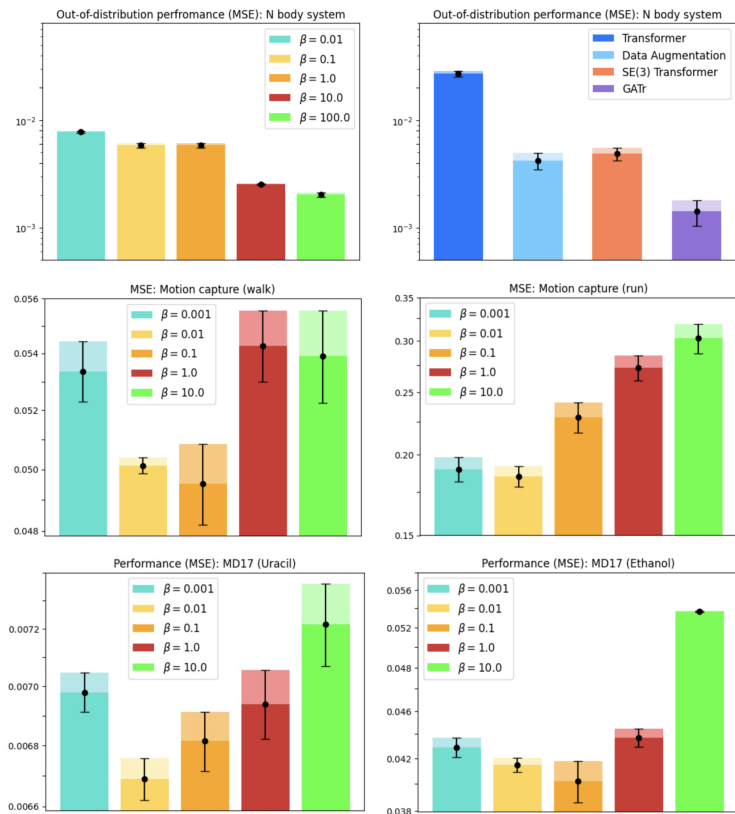
Yuyang Wang¹ Ahmed A. Elhag^{1,2} Navdeep Jaitly¹ Joshua M. Susskind¹ Miguel Ángel Bautista¹

Abstract

We present a novel way to predict molecular conformers through a simple formulation that sidesteps many of the heuristics of prior works and achieves state of the art results by using the advantages of scale. By training a diffusion generative model directly on 3D atomic positions without making assumptions about the explicit structure of molecules (*e.g.* modeling torsional angles) we are able to radically simplify structure learning, and make it trivial to scale up the model sizes. This model, called Molecular Conformer Fields (MCF), works by parameterizing conformer structures as functions that map elements from a molecular graph directly to their 3D location in space. This formulation allows us to boil down the essence of structure prediction to learning a distribution over functions. Experimental results show that scaling up the model capacity leads to large gains in generalization performance *without enforcing inductive biases* like rotational equivariance. MCF represents an advance in extending diffusion models to handle complex scientific problems in a conceptually simple, scalable and effective manner.

is the vast complexity of the 3D structure space, encompassing factors such as bond lengths and torsional angles. Despite the molecular graph dictating potential 3D conformers through specific constraints, such as bond types and spatial arrangements determined by chiral centers, the conformational space experiences exponential growth with the expansion of the graph size and the number of rotatable bonds (Axelrod & Gomez-Bombarelli, 2022). This complicates brute force and exhaustive approaches, making them virtually unfeasible for even moderately small molecules.

Systematic methods, like OMEGA (Hawkins et al., 2010), offer rapid processing through rule-based generators and curated torsion templates. Despite their efficiency, these models typically fail on complex molecules, as they often overlook global interactions and are tricky to extend to inputs like transition states or open-shell molecules. Classic stochastic methods, like molecular dynamics (MD) and Markov chain Monte Carlo (MCMC), rely on extensively exploring the energy landscape to find low-energy conformers. Such techniques suffer from sampling inefficiency for large molecules and struggle to generate diverse representative conformers (Hawkins, 2017; Wilson et al., 1991; Grebner et al., 2011). In the domain of learning-based approaches, several works have looked at conformer generation problems through the lens of probabilistic modeling, using either





The Hardware Lottery

Sara Hooker

Google Research, Brain Team

Hardware, systems and algorithms research communities have historically had different incentive structures and fluctuating motivation to engage with each other explicitly. This historical treatment is odd given that hardware and software have frequently determined which research ideas succeed (and fail). This essay introduces the term hardware lottery to describe when a

research idea wins because it is suited to the available software and hardware and *not* because the idea is superior to alternative research directions.

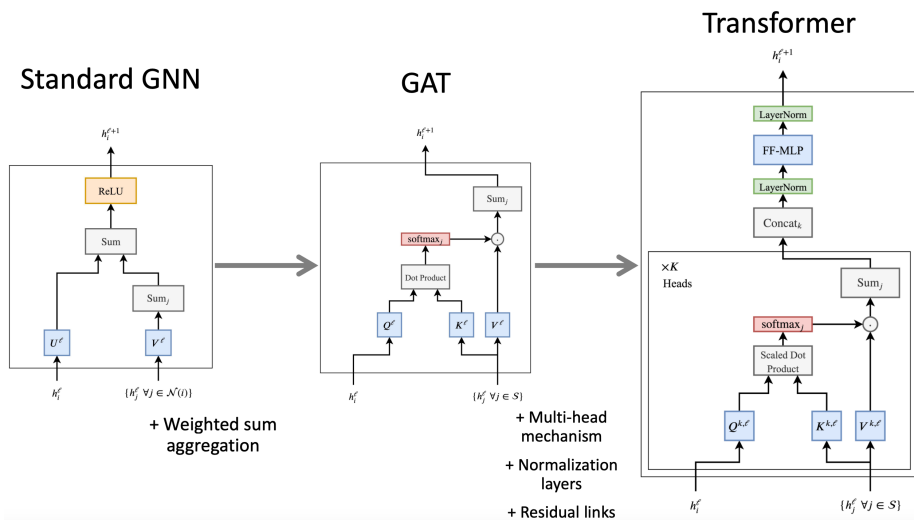
Examples from early computer science history illustrate how hardware lotteries can delay research progress by casting successful ideas as failures. These lessons are particularly salient given the advent of domain specialized hardware which make it increasingly costly to stray off of the beaten path of research ideas. This essay posits that the gains from progress in computing are likely to become even more uneven, with certain research directions moving into the fast-lane while progress on others is further obstructed.

Transformers are Graph Neural Networks

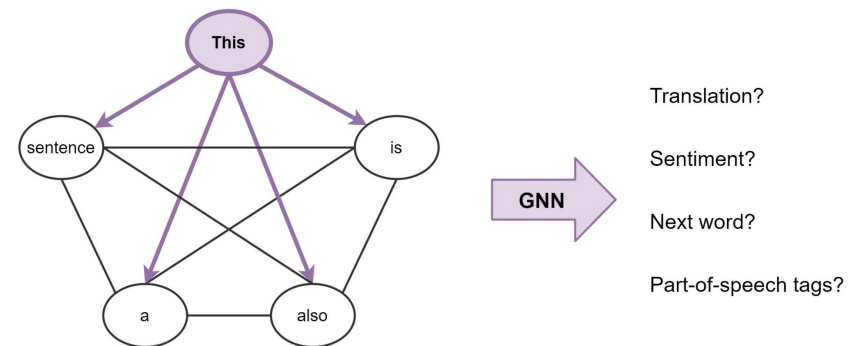
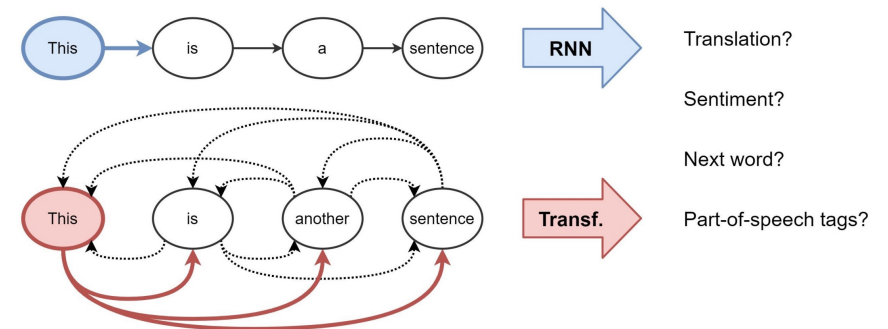
Exploring the connection between Transformer models such as GPT and BERT for Natural Language Processing, and Graph Neural Networks.

Chaitanya K. Joshi

Last updated on Jun 21, 2021 · 12 min read



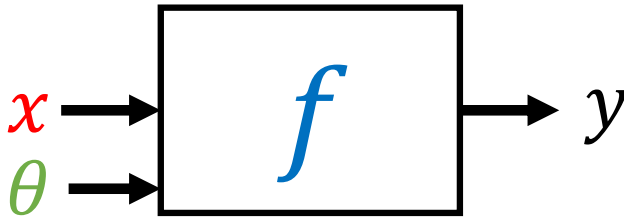
Joshi 2021





“How f interacts with the group G acting on x ?”

$$f(g \cdot x) = f(x)$$



“How f interacts with the group G acting on x ?”

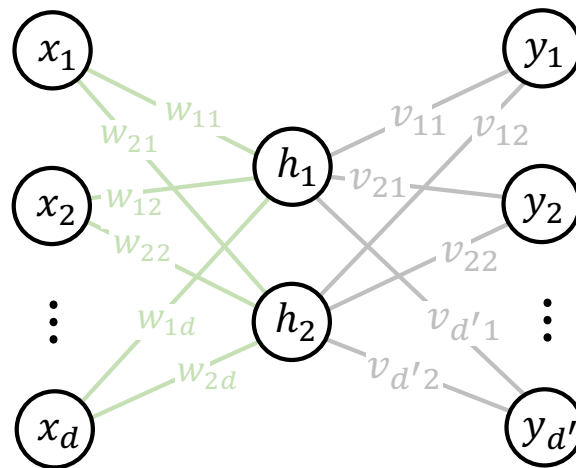
$$f(g \cdot x) = f(x)$$



“How f interacts with the group G acting on x and H acting on θ ?”

$$f(g.x, h.\theta) = f(x, \theta)$$

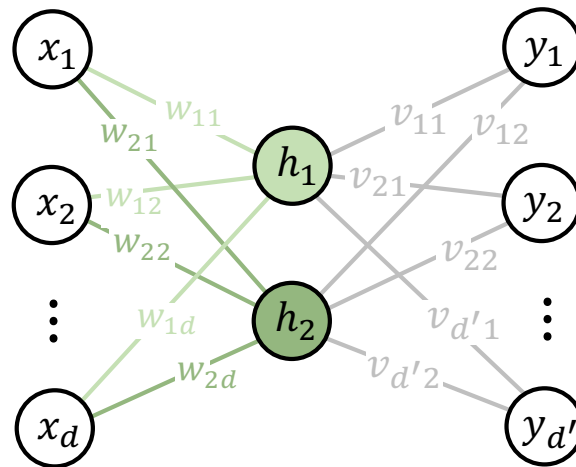
Symmetries of the Weights



$$\mathbf{y} = \mathbf{V} \sigma \left(\mathbf{W} \mathbf{x} \right)$$

The equation shows the output vector \mathbf{y} as a function of the input vector \mathbf{x} . The weight matrix \mathbf{W} is represented by a green grid, and the weight matrix \mathbf{V} is represented by a grey grid. The input vector \mathbf{x} is represented by a red vertical bar, and the output vector \mathbf{y} is represented by a grey vertical bar.

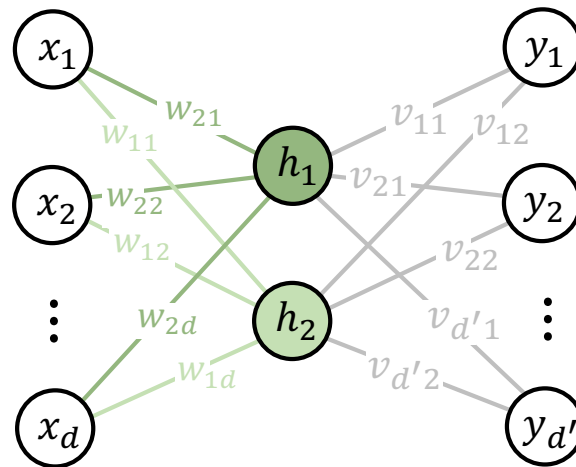
Symmetries of the Weights



$$\mathbf{y} = \mathbf{V} \sigma \left(\mathbf{W} \mathbf{x} \right)$$

The equation shows the relationship between the input vector \mathbf{x} (represented by a red vertical bar), the weight matrix \mathbf{W} (represented by a green grid), the hidden layer output vector \mathbf{z} (represented by a green vertical bar), the activation function σ , and the output vector \mathbf{y} (represented by a gray vertical bar). The weight matrix \mathbf{W} is shown as a grid of green squares, and the input vector \mathbf{x} is shown as a vertical bar of red squares.

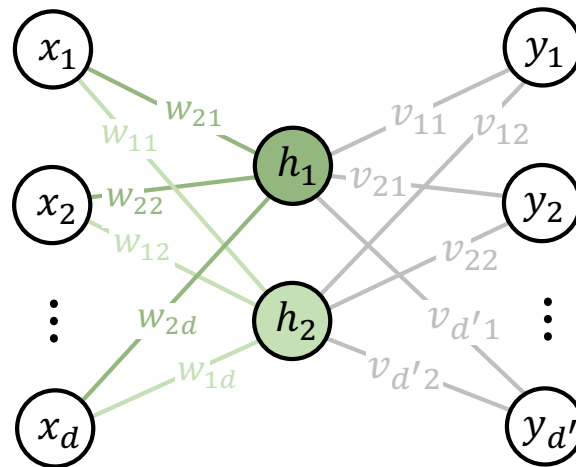
Symmetries of the Weights



$$\mathbf{y} = \mathbf{V} \sigma \left(\mathbf{\Pi} \begin{bmatrix} \text{green grid} \\ \mathbf{w} \end{bmatrix} \begin{bmatrix} \text{red grid} \\ \mathbf{x} \end{bmatrix} \right)$$

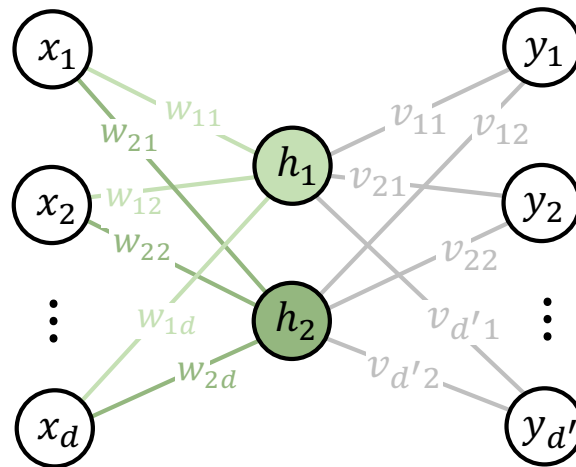
The diagram shows the matrix \mathbf{V} as a 3x3 gray grid, the matrix $\mathbf{\Pi}$ as a 2x4 green grid, and the vector \mathbf{x} as a 4x1 red grid. The vector \mathbf{w} is shown below the green grid.

Symmetries of the Weights



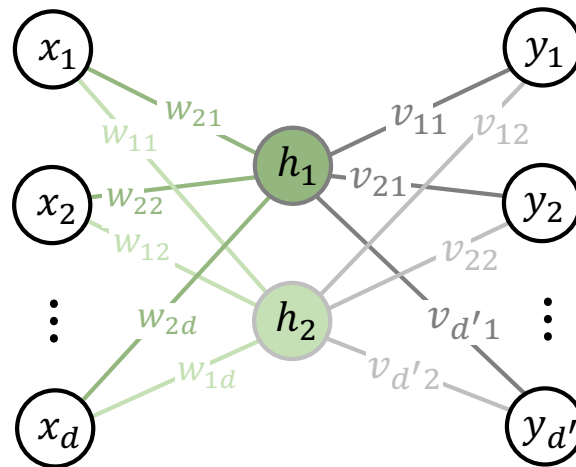
$$\mathbf{y} = \underset{\mathbf{V}}{\begin{bmatrix} \square & \square \\ \square & \square \\ \square & \square \end{bmatrix}} \Pi \sigma \left(\underset{\mathbf{W}}{\begin{bmatrix} \square & \square & \square & \square \\ \square & \square & \square & \square \end{bmatrix}} \underset{\mathbf{x}}{\begin{bmatrix} \square \\ \square \\ \square \\ \square \end{bmatrix}} \right)$$

Symmetries of the Weights



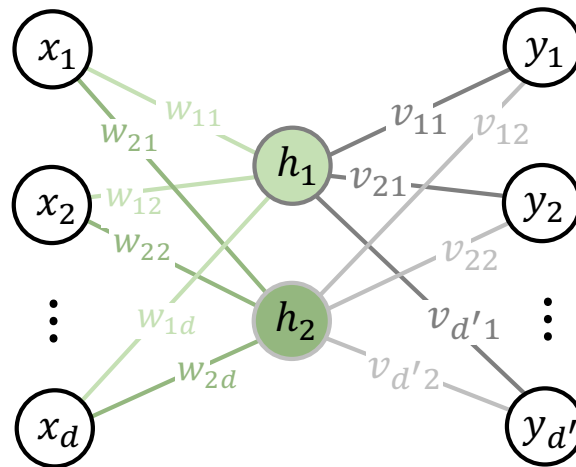
$$\mathbf{y} = \underset{\mathbf{V}}{\begin{bmatrix} \square & \square \\ \square & \square \\ \square & \square \end{bmatrix}} \Pi \sigma \left(\underset{\mathbf{W}}{\begin{bmatrix} \square & \square & \square & \square \\ \square & \square & \square & \square \end{bmatrix}} \underset{\mathbf{x}}{\begin{bmatrix} \square \\ \square \\ \square \\ \square \end{bmatrix}} \right)$$

Symmetries of the Weights



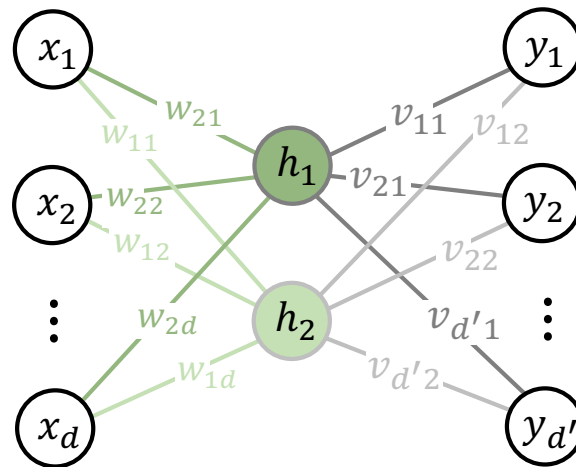
$$\mathbf{y} = \underset{\mathbf{V}}{\begin{bmatrix} \text{grey} & \text{grey} \\ \text{grey} & \text{grey} \\ \text{grey} & \text{grey} \end{bmatrix}} \Pi \sigma \left(\underset{\mathbf{W}}{\begin{bmatrix} \text{green} & \text{green} & \text{green} & \text{green} \\ \text{green} & \text{green} & \text{green} & \text{green} \end{bmatrix}} \underset{\mathbf{X}}{\begin{bmatrix} \text{red} \\ \text{red} \\ \text{red} \\ \text{red} \end{bmatrix}} \right)$$

Symmetries of the Weights



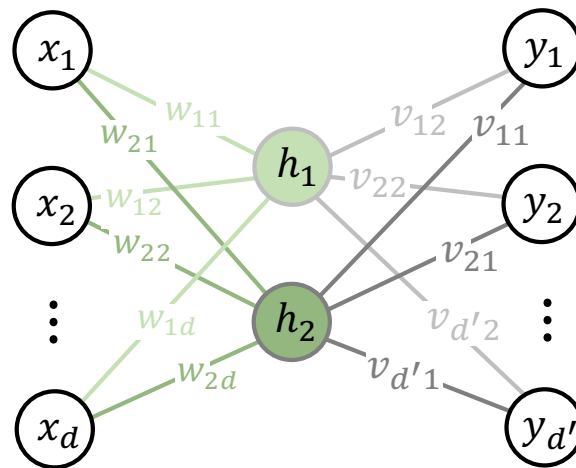
$$\mathbf{y} = \underset{\mathbf{V}}{\begin{bmatrix} \text{gray} & \text{gray} \\ \text{gray} & \text{gray} \\ \text{gray} & \text{gray} \end{bmatrix}} \Pi \sigma \left(\underset{\mathbf{W}}{\begin{bmatrix} \text{green} & \text{green} & \text{green} & \text{green} \\ \text{green} & \text{green} & \text{green} & \text{green} \end{bmatrix}} \underset{\mathbf{x}}{\begin{bmatrix} \text{red} \\ \text{red} \\ \text{red} \\ \text{red} \end{bmatrix}} \right)$$

Symmetries of the Weights



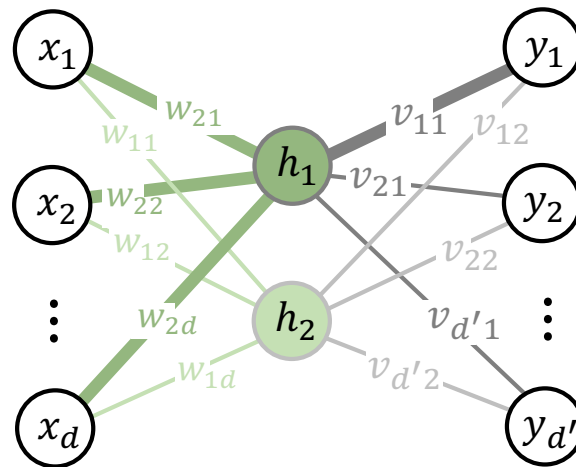
$$\mathbf{y} = \underset{\mathbf{V}}{\begin{bmatrix} \square & \square \\ \square & \square \\ \square & \square \end{bmatrix}} \mathbf{\Pi}^T \mathbf{\Pi} \sigma \left(\underset{\mathbf{W}}{\begin{bmatrix} \square & \square & \square & \square \\ \square & \square & \square & \square \end{bmatrix}} \underset{\mathbf{X}}{\begin{bmatrix} \square \\ \square \\ \square \\ \square \end{bmatrix}} \right)$$

Symmetries of the Weights



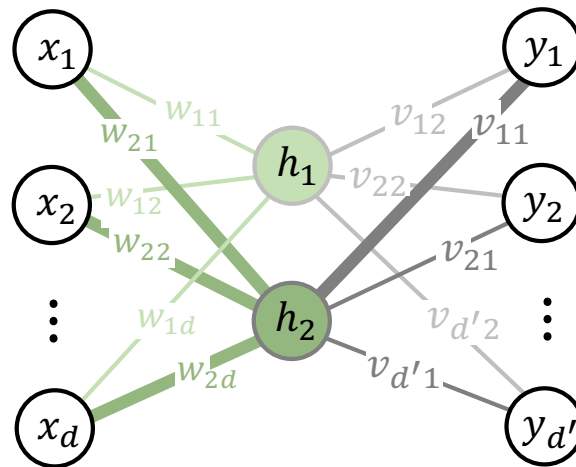
$$\mathbf{y} = \underset{\mathbf{V}}{\begin{bmatrix} \square & \square \\ \square & \square \\ \square & \square \end{bmatrix}} \mathbf{\Pi}^T \mathbf{\Pi} \sigma \left(\underset{\mathbf{W}}{\begin{bmatrix} \square & \square & \square & \square \\ \square & \square & \square & \square \end{bmatrix}} \underset{\mathbf{X}}{\begin{bmatrix} \square \\ \square \\ \square \\ \square \end{bmatrix}} \right)$$

Symmetries of the Weights



$$\mathbf{y} = \underset{\mathbf{V}}{\begin{bmatrix} \square & \square & \square \\ \square & \square & \square \\ \square & \square & \square \end{bmatrix}} \mathbf{\Pi}^T \mathbf{\Pi} \sigma \left(\underset{\mathbf{W}}{\begin{bmatrix} \square & \square & \square & \square \\ \square & \square & \square & \square \end{bmatrix}} \underset{\mathbf{x}}{\begin{bmatrix} \square \\ \square \\ \square \\ \square \end{bmatrix}} \right)$$

Symmetries of the Weights



$$\mathbf{y} = \underset{\mathbf{V}}{\begin{bmatrix} \square & \square \\ \square & \square \\ \square & \square \end{bmatrix}} \mathbf{\Pi}^T \mathbf{\Pi} \sigma \left(\underset{\mathbf{W}}{\begin{bmatrix} \square & \square & \square & \square \\ \square & \square & \square & \square \end{bmatrix}} \underset{\mathbf{X}}{\begin{bmatrix} \square \\ \square \\ \square \\ \square \end{bmatrix}} \right)$$

Symmetries of the Weights

- L -layer neural network with weights $\boldsymbol{\theta} = (\mathbf{W}_1, \mathbf{b}_1, \dots, \mathbf{W}_L, \mathbf{b}_L)$
- Parameter space symmetry $G = S_{d_1} \times \dots \times S_{d_L}$

$$\mathbf{W}'_1 = \boldsymbol{\Pi}_1^T \mathbf{W}_1$$

$$\mathbf{b}'_1 = \boldsymbol{\Pi}_1^T \mathbf{b}_1$$

$$\mathbf{W}'_l = \boldsymbol{\Pi}_l^T \mathbf{W}_l \boldsymbol{\Pi}_{l-1}$$

$$\mathbf{b}'_l = \boldsymbol{\Pi}_l^T \mathbf{b}_l$$

$$\vdots$$

$$\vdots$$

$$\mathbf{W}'_L = \mathbf{W}_L \boldsymbol{\Pi}_{L-1}$$

$$\mathbf{b}'_L = \mathbf{b}_L$$

such that $f(\cdot, g\boldsymbol{\theta}) = f(\cdot, \boldsymbol{\theta})$

Symmetries in the Gradient Space

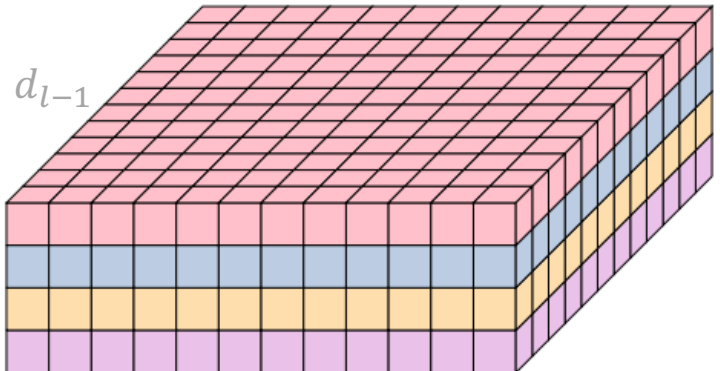
$$\mathcal{L}_{\mathcal{B}} = \frac{1}{|\mathcal{B}|} \sum_{(\mathbf{x}, \mathbf{y}) \in \mathcal{B}} \underbrace{\ell(f(\mathbf{x}, \boldsymbol{\theta}), \mathbf{y})}_{\mathcal{L}_{(\mathbf{x}, \mathbf{y})}}$$

$$\nabla_{\mathbf{b}_l} \mathcal{L}_{(\mathbf{x}, \mathbf{y})} = \mathbf{g}_l \quad \text{where} \quad \mathbf{g}_l = \frac{\partial \ell(f(\mathbf{x}, \boldsymbol{\theta}), \mathbf{y})}{\partial \mathbf{u}_l}$$

$$\nabla_{\mathbf{w}_l} \mathcal{L}_{(\mathbf{x}, \mathbf{y})} = \mathbf{g}_l \mathbf{a}_{l-1}^T$$

Symmetries in the Gradient Space

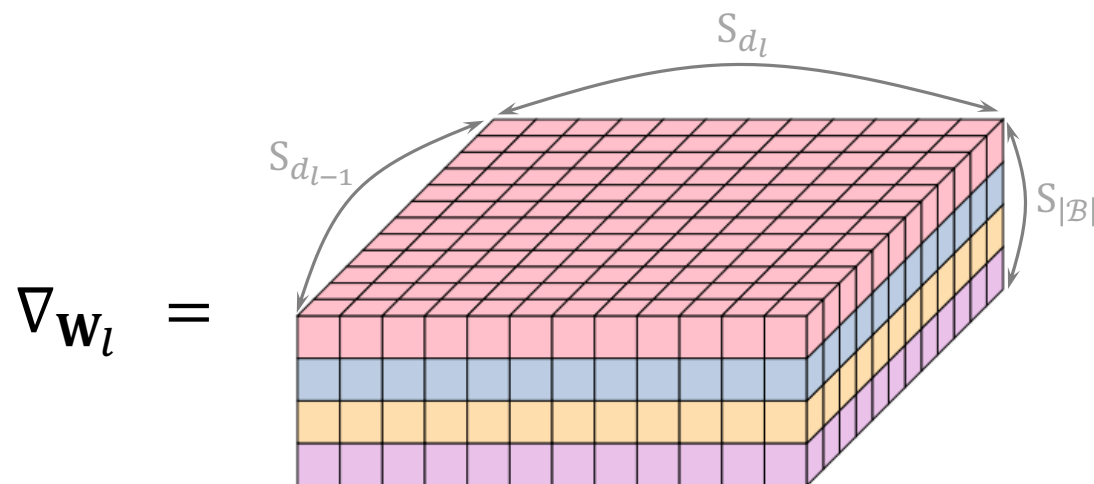
$$\mathcal{L}_{\mathcal{B}} = \frac{1}{|\mathcal{B}|} \sum_{(\mathbf{x}, \mathbf{y}) \in \mathcal{B}} \ell(f(\mathbf{x}, \boldsymbol{\theta}), \mathbf{y})$$

$$\nabla_{\mathbf{w}_l} =$$


A 3D grid representing the gradient space. The grid has dimensions d_{l-1} (width), d_l (depth), and $|\mathcal{B}|$ (height). The grid is divided into four horizontal layers of different colors: pink (top), blue, yellow, and purple (bottom). The pink layer is the largest, followed by blue, yellow, and purple.

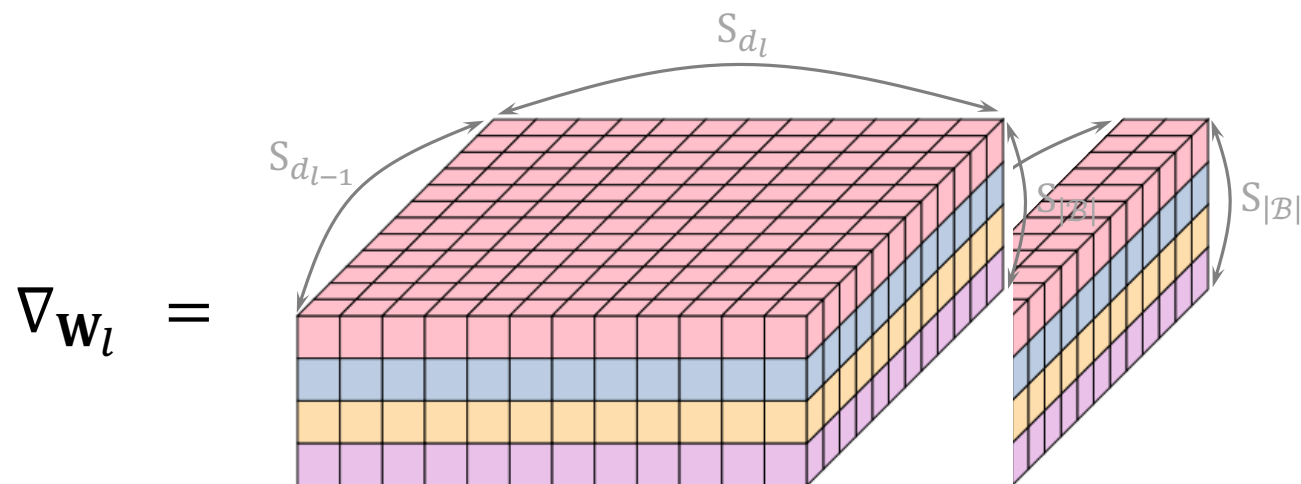
Symmetries in the Gradient Space

$$\mathcal{L}_{\mathcal{B}} = \frac{1}{|\mathcal{B}|} \sum_{(\mathbf{x}, \mathbf{y}) \in \mathcal{B}} \ell(f(\mathbf{x}, \boldsymbol{\theta}), \mathbf{y})$$



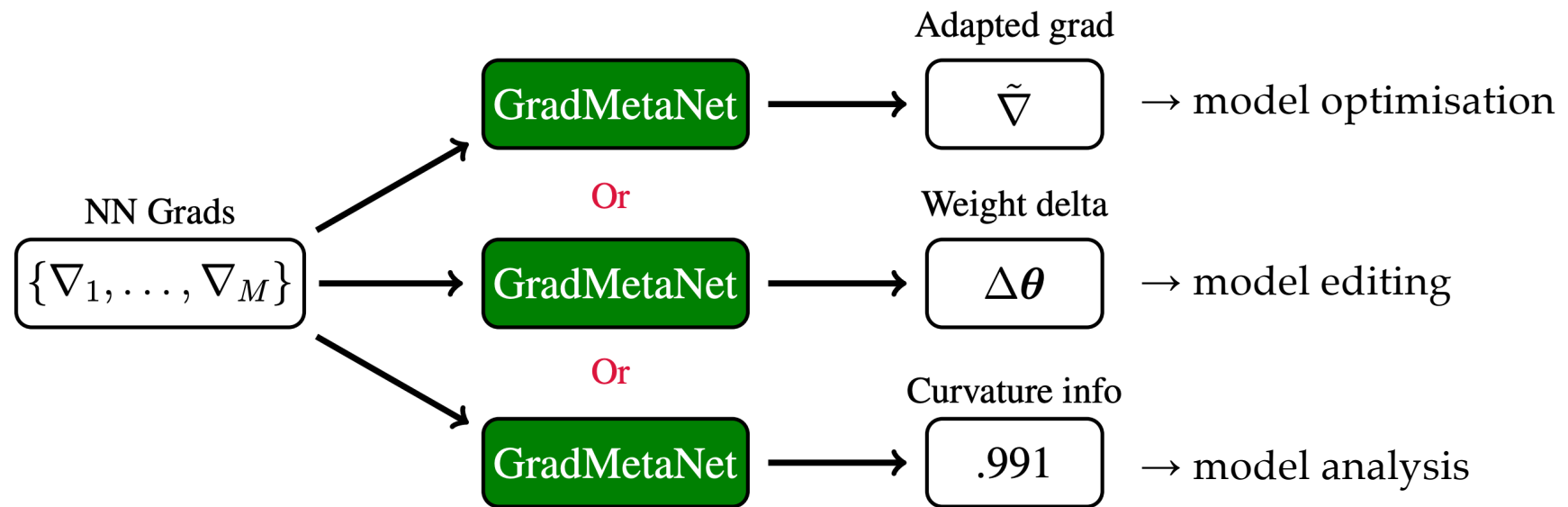
Symmetries in the Gradient Space

$$\mathcal{L}_{\mathcal{B}} = \frac{1}{|\mathcal{B}|} \sum_{(\mathbf{x}, \mathbf{y}) \in \mathcal{B}} \ell(f(\mathbf{x}, \boldsymbol{\theta}), \mathbf{y})$$

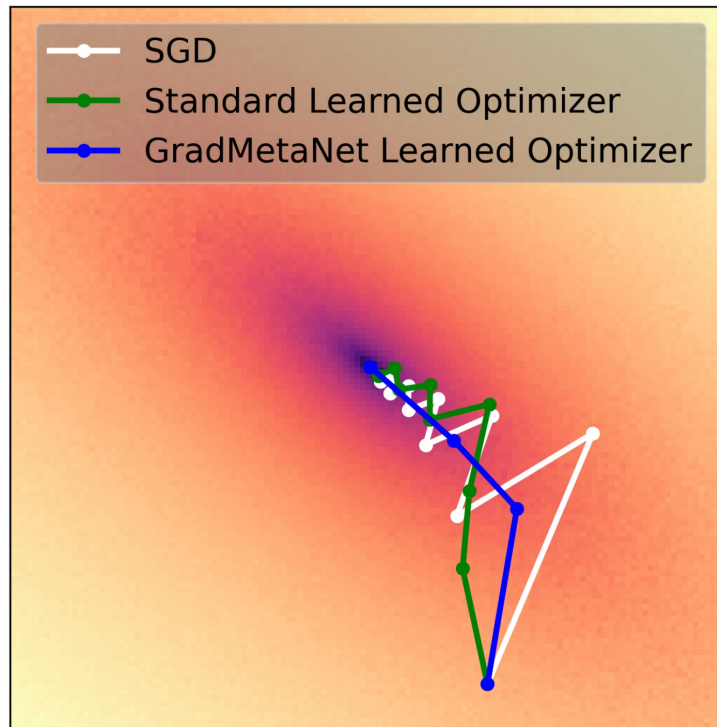


$$G_b = S_{|\mathcal{B}|} \times S_{d_1} \times \cdots \times S_{d_L}$$

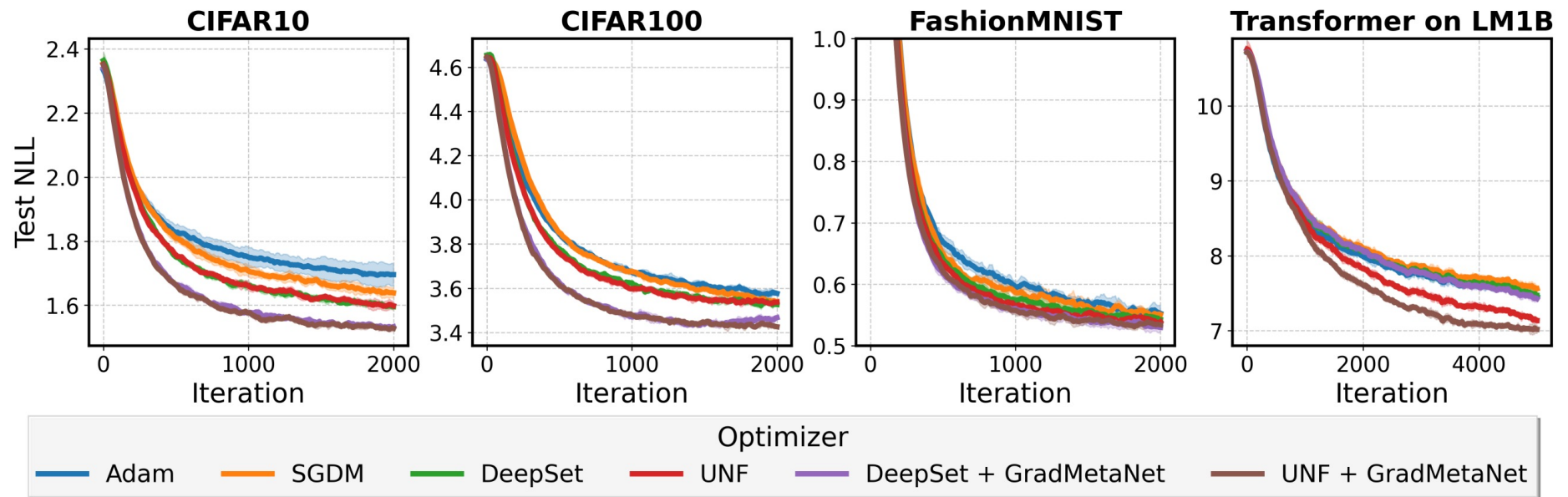
GradMetaNet



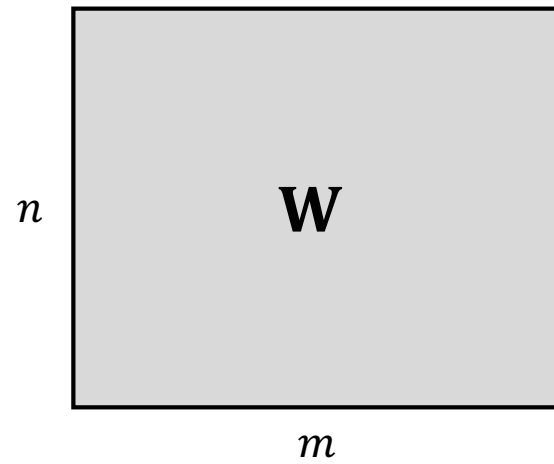
GradMetaNet: Learning Optimisation



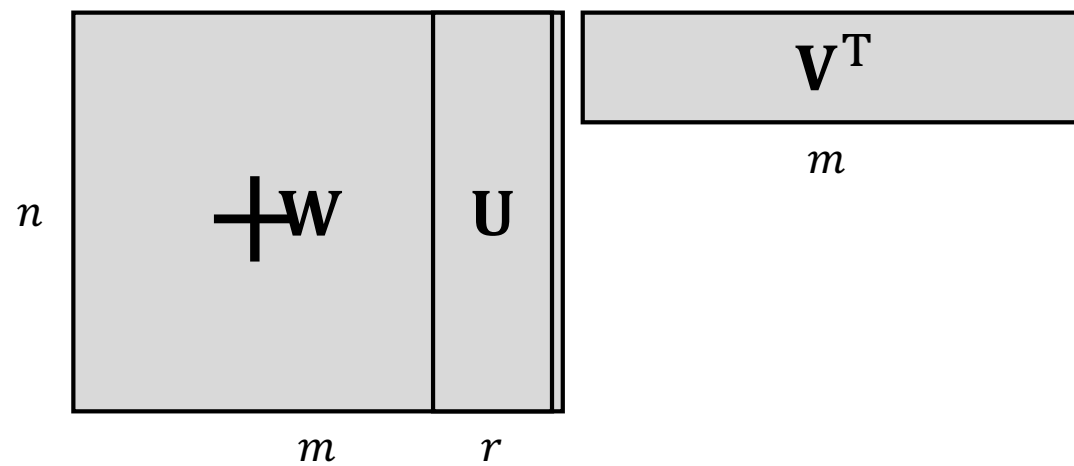
GradMetaNet: Learning Optimisation



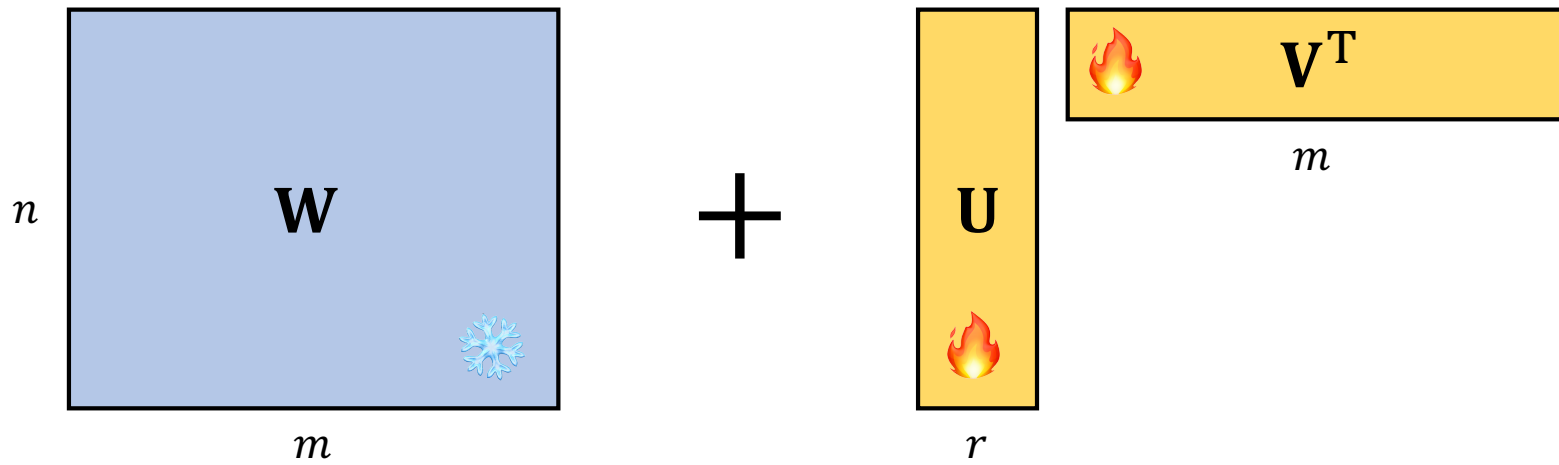
Low-Rank Adaptors (LoRA)



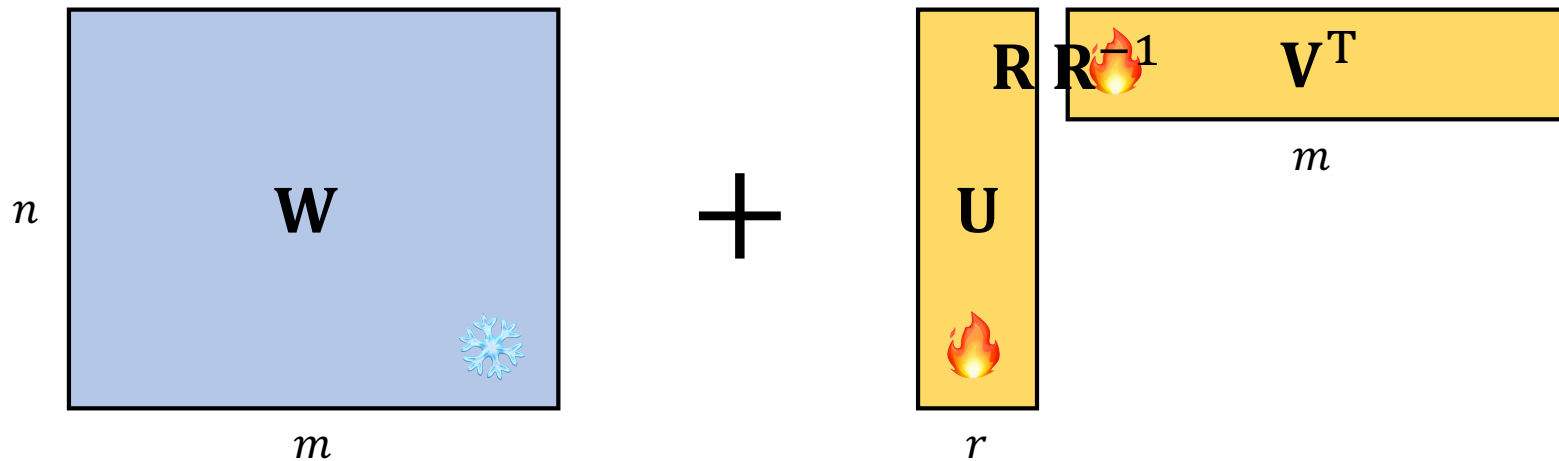
Low-Rank Adaptors (LoRA)



Low-Rank Adaptors (LoRA)

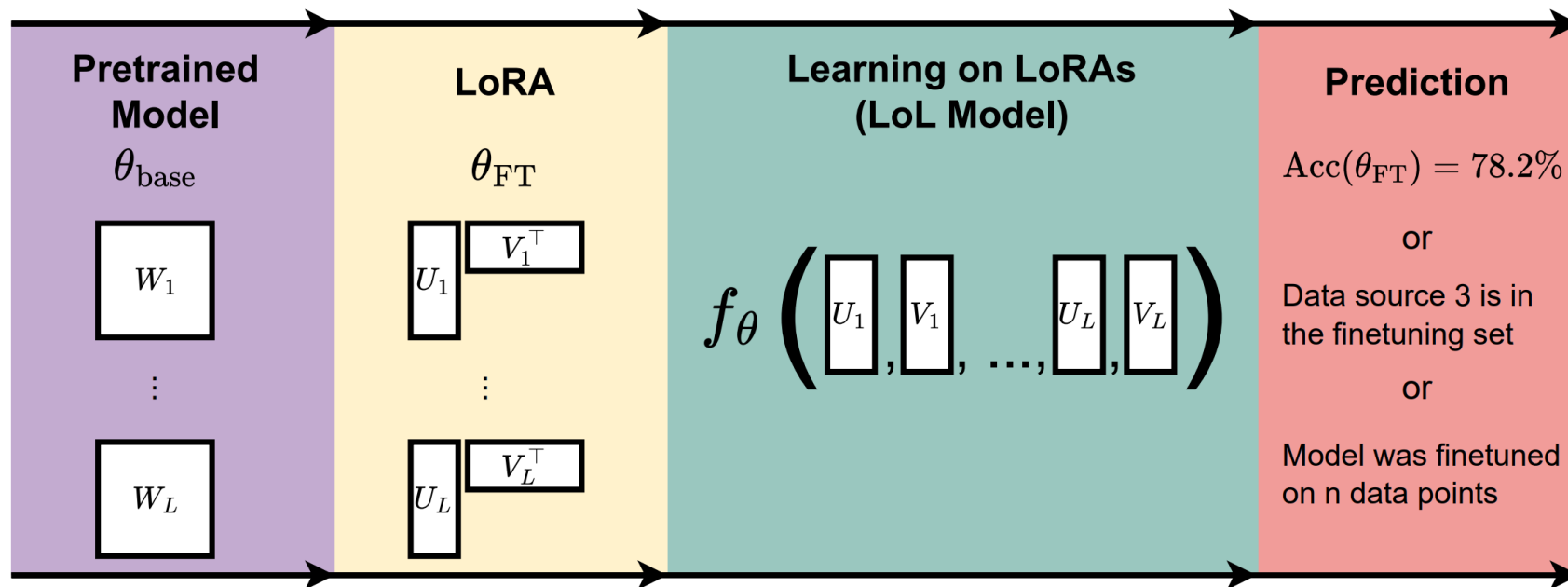


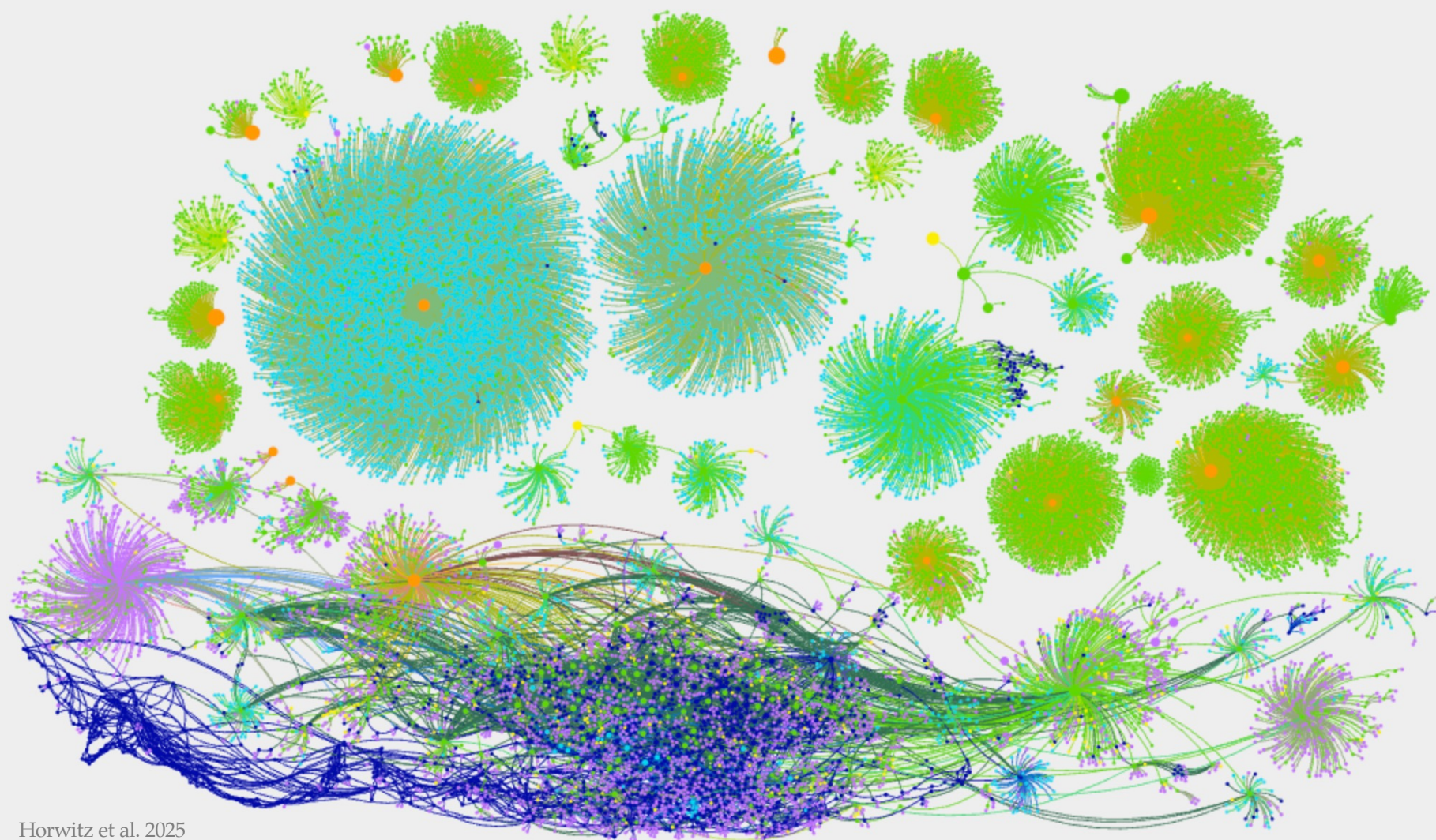
Low-Rank Adaptors (LoRA)



LoRA (\mathbf{U}, \mathbf{V}) defined up to $GL(r)$

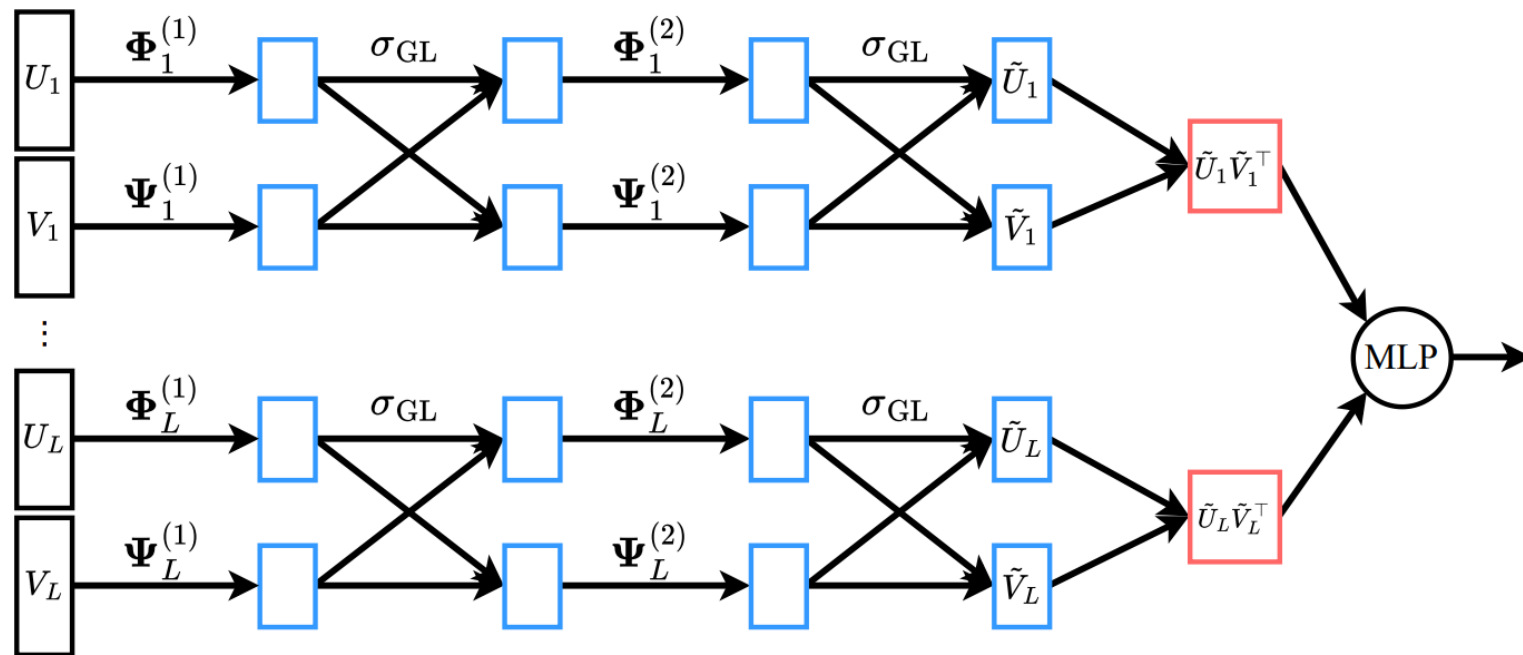
Learning on LoRAs (LOL)





Horwitz et al. 2025

Learning on LoRAs (LOL)



Learning on LoRAs (LOL)

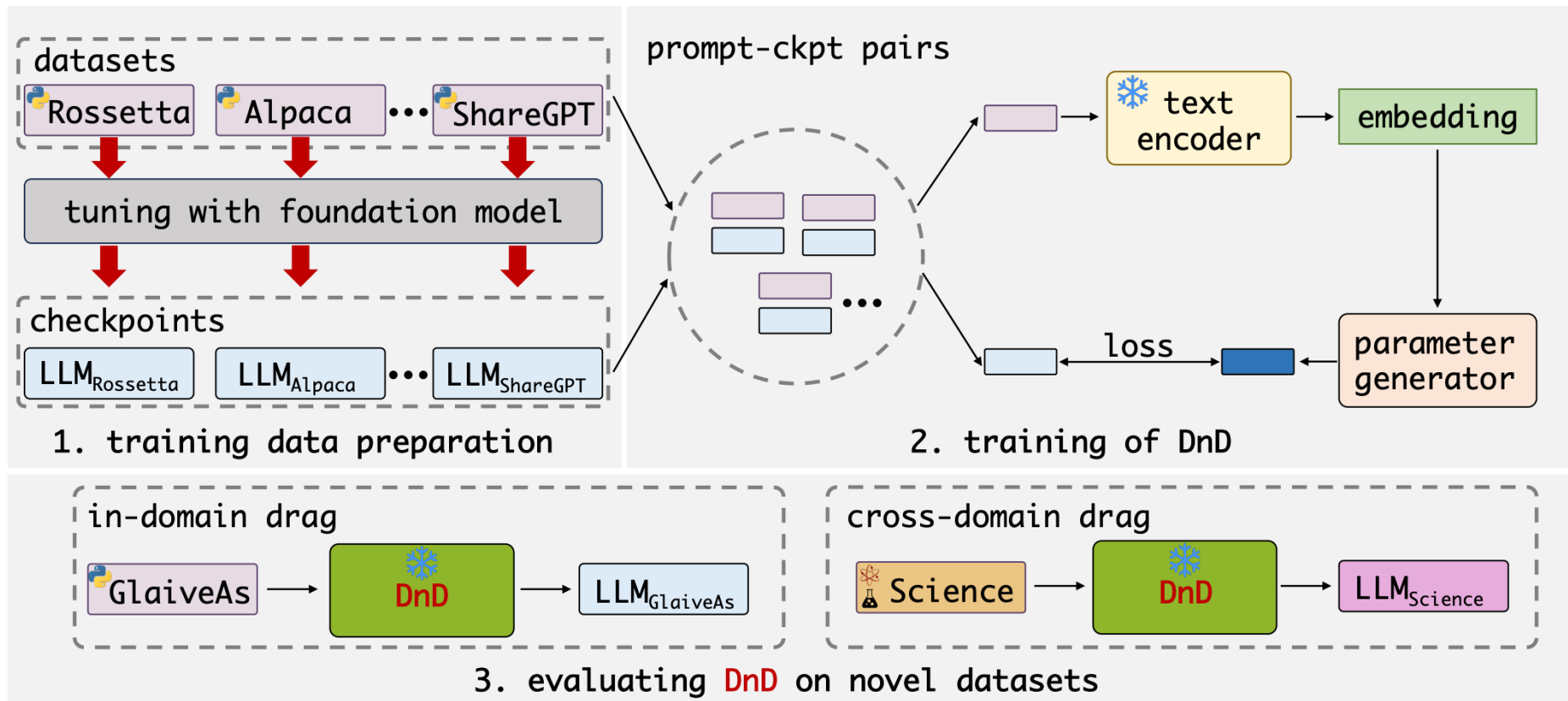
LoL Model	GL-Inv.	O-Inv.	Expressive	Preprocess Time	Forward Time
Naïve architectures					
MLP($[U, V]$)	✗	✗	✓	$O((m+n)r)$	$O((m+n)r)$
Transformer($[U, V]$)	✗	✗	✓	$O((m+n)r)$	$O((m+n)r)$
MLP(UV^\top)	✓	✓	✓	$O(mnr)$	$O(mn)^2$
Efficient symmetry-aware architectures					
MLP(O-Align($[U, V]$))	✗	✓	✓	$O((m+n)r^2)$	$O((m+n)r)$
MLP($\sigma(UV^\top)$)	✓	✓	✗	$O((m+n)r^2)$	$O((m+n)r)$
GL-net	✓	✓	✓	$O((m+n)r)$	$O((m+n)r)$

Learning on LoRAs (LOL)

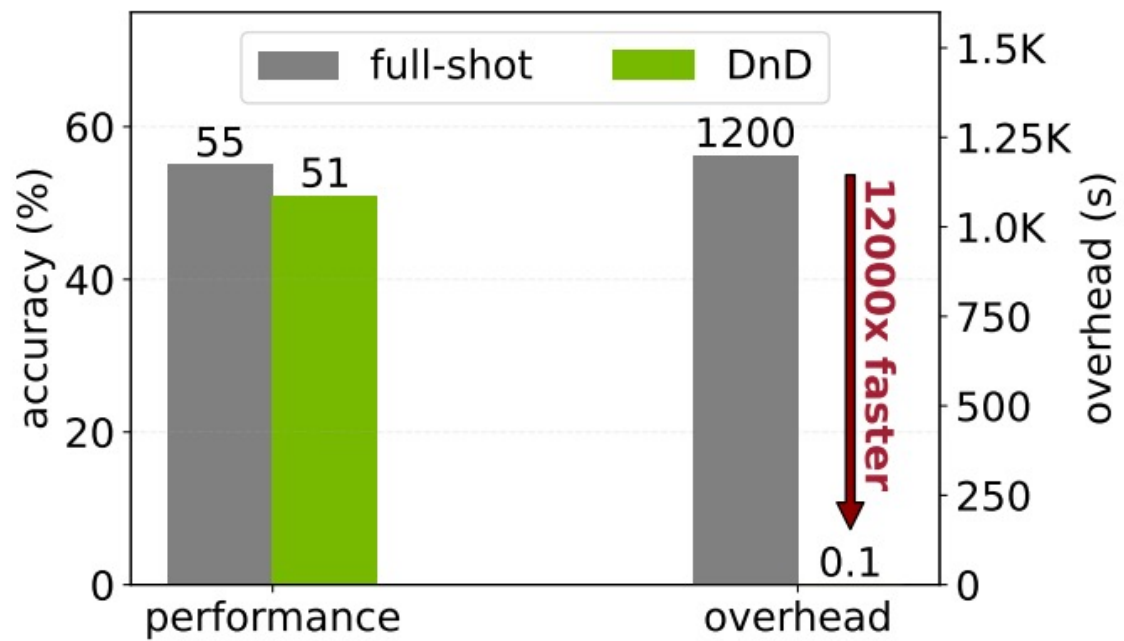
		CelebA Attributes		Imagenette Classes	
LoL Model		Test Loss (\downarrow)	Test Acc (\uparrow)	Test Loss (\downarrow)	Test Acc (\uparrow)
Naive Models	MLP($[U, V]$)	.554 \pm .000	72.4 \pm 0.0	.709 \pm .004	49.6 \pm 1.3
	Transformer($[U, V]$)	.586 \pm .014	73.2 \pm 0.9	.695 \pm .001	50.0 \pm 1.3
	MLP(UV^\top)	.267 \pm .007	89.1 \pm 0.4	.264 \pm .011	88.9 \pm 0.6
Efficient Invariant	MLP(O-Align($[U, V]$))	.333 \pm .008	87.2 \pm 0.5	.278 \pm .008	87.8 \pm 0.3
	MLP($\sigma(UV^\top)$)	.509 \pm .013	77.3 \pm 1.3	.638 \pm .013	65.6 \pm 0.6
	GL-net	.232 \pm .007	91.3 \pm 0.1	.244 \pm .005	90.4 \pm 0.3

Using LoL models to predict *CelebA* attributes (left) and *Imagenette* classes (right) of the finetuning data of diffusion models, given only the LoRA weights.

Drag-and-Drop LLMs



Drag-and-Drop LLMs



THE STORY CONTINUES
IN THE WEIGHT SPACE



ICLR
International Conference On
Learning Representations

First Workshop on Weight Space Learning

<https://weight-space-learning.github.io/>

Invited Speaker



Stella X. Yu

University of Michigan



Michael Mahoney

UC Berkeley, ICSI



Boris Knyazev

Samsung AI Lab (SAIT)



Naomi Saphra

Harvard University



Ludwig Schmit

Stanford University / Anthropic

Organization



Konstantin
Schürholt



Giorgos
Bouritsas



Eliahu
Horwitz



Derek
Lim



Yoav
Gelberg



Bo
Zhao



Allan
Zhou



Damian
Borth



Stefanie
Jegelka

Steering



Michael
Bronstein



Gal
Chechik



Stella
X. Yu



Haggai
Maron



Yedid
Hoshen



Thank you!